Russian Original Vol. 41, No. 2, August, 1976

February, 1977

File

SATEAZ 41(2) 687-792 (1976)

SOVIET ATOMIC ENERGY

АТОМНАЯ ЭНЕРГИЯ
(ATOMNAYA ÉNERGIYA)

TRANSLATED FROM RUSSIAN

CONSULTANTS BUREAU, NEW YORK

SOVIET ATOMIC ENERGY

Soviet Atomic Energy is a cover-to-cover translation of *Atomnaya Énergiya*, a publication of the Academy of Sciences of the USSR.

An agreement with the Copyright Agency of the USSR (VAAP) makes available both advance copies of the Russian journal and original glossy photographs and artwork. This serves to decrease the necessary time lag between publication of the original and publication of the translation and helps to improve the quality of the latter. The translation began with the first issue of the Russian journal.

Consultants Bureau journals appear about six months after the publication of the original Russian issue. For bibliographic accuracy, the English issue published by Consultants Bureau carries the same number and date as the original Russian from which it was translated. For example, a Russian issue published in December will appear in a Consultants Bureau English translation about the following June, but the translation issue will carry the December date. When ordering any volume or particular issue of a Consultants Bureau journal, please specify the date and, where applicable, the volume and issue numbers of the original Russian. The material you will receive will be a translation of that Russian volume or issue.

Subscription
$107.50 per volume (6 Issues)
2 volumes per year

Single Issue: $50
Single Article: $7.50

Prices somewhat higher outside the United States.

CONSULTANTS BUREAU, NEW YORK AND LONDON

227 West 17th Street
New York, New York 10011

Published monthly. Second-class postage paid at Jamaica, New York 11431.

Soviet Atomic Energy is abstracted or indexed in *Applied Mechanics Reviews, Chemical Abstracts, Engineering Index, INSPEC—Physics Abstracts and Electrical and Electronics Abstracts, Current Contents,* and *Nuclear Science Abstracts.*

SOVIET ATOMIC ENERGY

A translation of *Atomnaya Énergiya*

February, 1977

Volume 41, Number 2 August, 1976

CONTENTS

CONTENTS

(continued)

CONTENTS

(continued)

The Russian press date (podpisano k pechati) of this issue was 7/26/1976. Publication therefore did not occur prior to this date, but must be assumed to have taken place reasonably soon thereafter.

ARTICLES

EXPERIENCE IN THE OPERATION OF CHANNELS WITH SINGLE-PASS STEAM GENERATION IN THE REACTOR AT THE FIRST NUCLEAR POWER STATION

V. V. Dolgov, V. Ya. Kozlov,
M. E. Minashin, V. D. Petrov,
V. B. Tregubov, and V. N. Sharapov

UDC 621,039.524.2.034.44

By employing various methods of intensifying heat exchange [1-3], we are able to advance the limit of crisis boiling in the channels almost to the point where the water is completely evaporated in flow. A transition to a lower level of heat exchange under these conditions does not lead to catastrophic results. The so-called temperature "jumps" at the cooling surface during such transitions assume a smooth character and extend the full length of the channel. The maximum temperature rise does not exceed the design value for dry saturated steam with a flow Gx (where G is the two-phase flow and x is the critical steam content). Intensifying elements in the transition zone, and their location in regions of reduced thermal load coupled with overall design modifications can ensure long-term fault-free operation of the cooling surface.

Tubular fuel elements type BAÉS (Beloyarsk Nuclear Power Station) at the world's first nuclear power station (Beloyarsk) have intensifying elements in the form of circumferential corrugations projecting within the tube itself [4, 5]. These intensifiers allow even the first stage to achieve reliable heat absorption from the fuel elements with a heat content by weight of 60-70% at the output (under analogous conditions, but with a smooth tube, the crisis point was reached at a steam content of 25-30%). Tests were then carried out with full evaporation and reheat, without an intermediate separator, i.e., on the single-pass steam generator principle. Reassuring results were obtained.

The present article describes the experimental fuel channels with fuel elements and heat-exchange intensifiers, the channel connection scheme in the reactor loop, and the test conditions, together with some of the test results.

Scheme of Experimental Loop and Measurement. Tests carried out on fuel elements with heat-exchange intensifiers were carried out on a loop of the PV-2 reactor [6] at the Beloyarsk Nuclear Power Station in the same loop that had been used for the boiling crisis experiments [7]. Two experimental fuel channels were connected in series in the loop (Fig. 1). The new element in the loop is a mixing-type condenser built in the form

TABLE 1. Average Parameters of Test Conditions

Parameters	Number of experimental reactor channels		
	1	2	3
Total power of four fuel elements, kW	140±7	145±7	172±9
Flow rate of water, kg/h	305±10	300±10	312±10
Heat flow in center of output fuel element calculated, kW/m^2	700±70	650±60	1120±100
Steam content by wt. in the input flow to the channel, %	30—40	35—45	30—40
Temperature at the output, °C	342±4	350±5	400±10
Steam pressure at the output, atm	123±3	123±3	123±3

Translated from Atomnaya Énergiya, Vol. 41, No. 2, pp. 75-81, August, 1976. Original article submitted April 5, 1976.

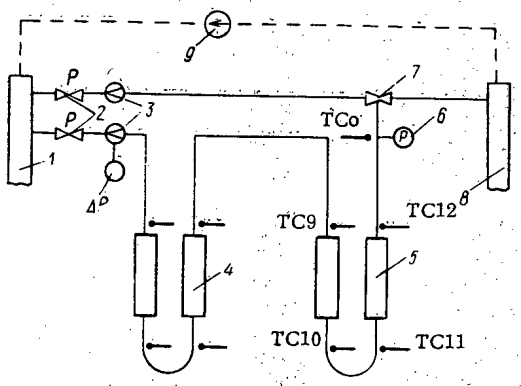

Fig. 1

Fig. 1. Connection scheme of experimental channels in loop: 1) pump reservoir; 2) regulating valve; 3) flowmeter diaphragm; 4) boiling channel; 5) full evaporation channel; 6) manometer channel; 7) mixing-type condenser; 8) manifold; 9) circulating pump.

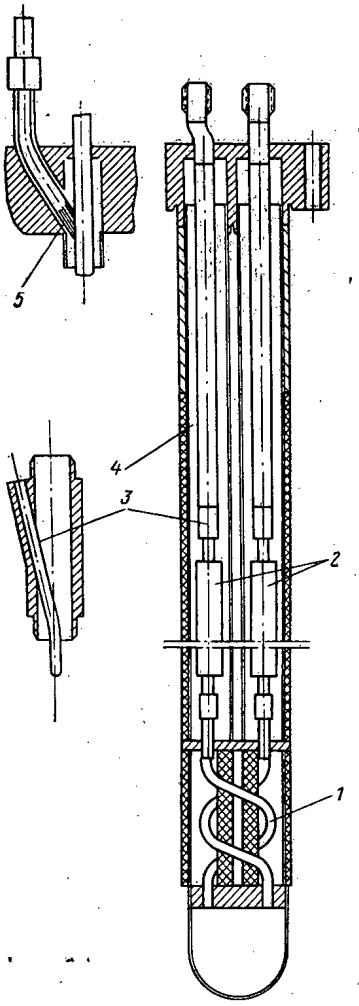

Fig. 2

Fig. 2. Experimental channel: 1) elongation compensator; 2) fuel element; 3) thermocouple housing; 4) hermetically sealed case; 5) output thermocouple.

of a jet pump. The operating medium in this condenser is cooling water, and the injected medium is steam (a mixture of steam and water). The coolant is circulated round the loop by the circulating pump. The broken line in Fig. 1 represents the remaining coolant equipment of the loop with its pipes and metering equipment, feed pump, and gas compensator reservoir. This equipment provides the regulation and maintains the predetermined water parameters in the pump reservoir. During the tests, particular attention was directed to maintaining a stable flow of coolant in the experimental loop. For this reason, boiling was not permitted in the other channels between the pump reservoir and manifold. The cooling water was carried to the condenser through a reserve system. The water flows in the main and reserve systems were regulated by valves. Regulation of relatively small flow rates at high pressure drops across the valve was carried out by valves taking the form of pairs of plungers with two counteracting plates, having a depth of undercut along the forming plunger that varies in a linear manner.

The flow rate of the coolant was varied by means of a unit comprising a metering diaphragm, differential manometer type DM-6, and a secondary instrument type DSR-1 of accuracy class 2.5 with a 100% scale. The coolant temperature was measured by means of a calibration thermocouple type KhA, made from cable type KTMS with an outside diameter of 1.5 mm. The thermocouple was mounted in a housing made of tube with an outside diameter of 4 mm and a wall thickness of 0.5 mm. Contact between the thermocouple and the housing past which the coolant flows was created by hard solder. These thermocouples were installed at the output of each of the four fuel elements (see Fig. 1) and also at the output TCo, 4 m from the output section of the fuel elements in the coolant flow.

The secondary instrument for these thermocouples was an automatic potentiometer type KSP-4, of accuracy class 0.25 at 20 mV, equipped with a switch. The coolant pressure was measured at the output of the channel with the aid of a unit consisting of a type MÉD transducer with a type DSR secondary instrument of

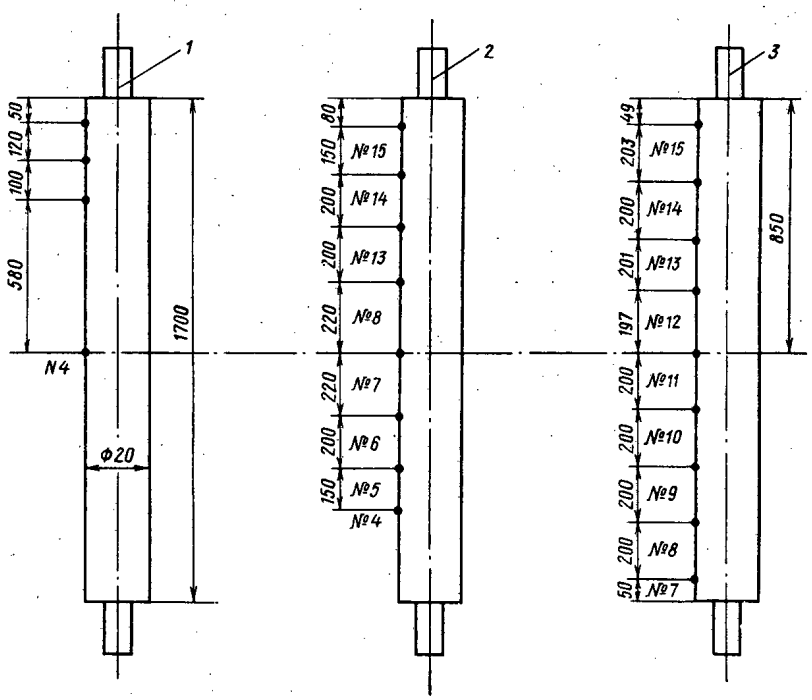

Fig. 3. Location of thermocouples at the output fuel elements in channels 1, 2, and 3.

accuracy class 2.5 on range 160 kgf/cm^2. A standard manometer was connected in parallel. To measure the temperature of the outer case of the fuel element, surface thermocouples were used with two secondary instruments type ÉPP-0.9 equipped with switches. The scales of these instruments were 200-400 and 300-500°C. A portable potentiometer was connected to the first of these instruments to compensate the excess emf when measuring temperatures above 400°C.

Construction of Channel and Fuel Element. The design of the experimental channel is illustrated in Fig. 2. Each of the experimental channels had a pair of fuel elements mounted one after the other within the flow of coolant. Both fuel elements of the channel had heat-exchange intensifiers in the form of annular corrugations projecting into the flow of coolant. To compensate for the difference in temperature of the lower part of the extended branches, a condenser coil was installed. Pockets for the thermocouples were welded in the tube above and below the thermocouples. The fuel elements in the experimental channels were separated from the reactor medium by cores, which also reduced the flow of heat between fuel elements and heat exchange with the graphite lining. The leads to the thermocouples were led out through a hermetically sealed union. Otherwise, the channel resembled a standard reactor fuel channel.

The radial dimensions of the experimental fuel elements were identical with those of the Beloyarsk Nuclear Power Station (Fig. 3). The steam was superheated in the second channel in a quarter of the coolant flow to the fuel element. The superheating regime was tested in three channels altogether.

To reduce the transient zone, and via this, the temperature of the fuel element in which superheated steam is first obtained (channel 1), the heat generator was profiled, ensuring that the heat flow in the output parts was reduced and the corrugation pitch needed to intensify the heat transfer to the steam was reduced accordingly. The annular corrugations projected 0.5 to 1 mm into the flow, 0.5 mm in the fuel elements of channels 2 and 3, while the fuel and corrugation pitch were distributed uniformly.

The maximum permissible operating temperatures of the outer covers of all fuel elements in channels 1 and 2 was 480°C. Therefore, the greatest steam superheat above the saturation temperature t_s did not exceed 30-40°C. All the preconnected channels had similar fuel elements (see Fig. 1).

A fuel element with an operating temperature of up to 600°C was installed in the output arm of channel 3, enabling the steam superheat to be increased to 90-100°C above t_s at greater thermal loads.

The surface thermocouples for measuring the fuel element temperatures were manufactured using type KTMS cable of 1.5-mm outside diameter, taking the form of calibrated type KhA thermocouples. The hot

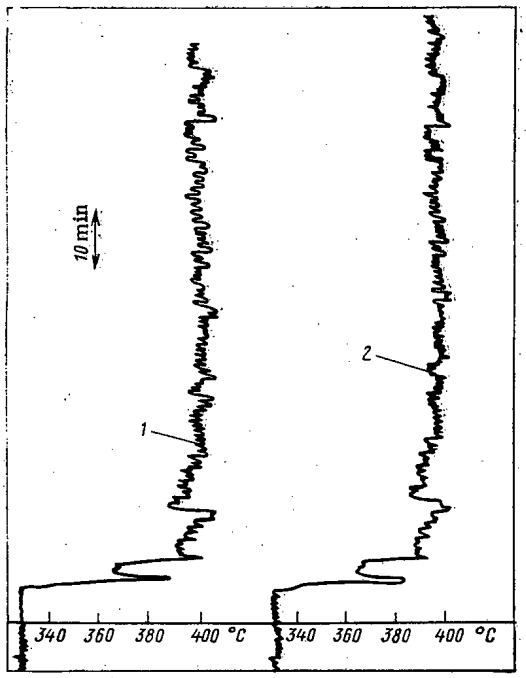

Fig. 4

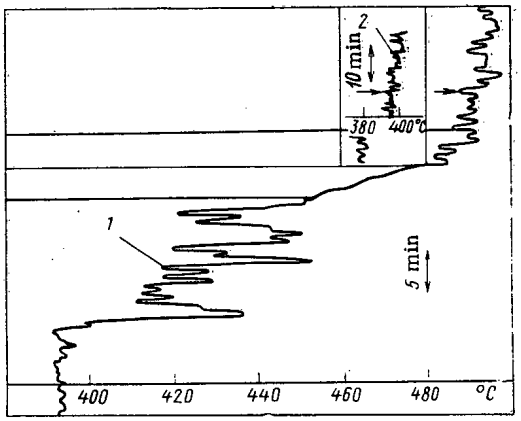

Fig. 5

Fig. 4. Steam temperatures at distances of 1) 150 m and 2) 4.5 m from the output of the fuel element.

Fig. 5. Temperature of fuel element and steam in channel 3: 1) fuel element at point 9, motion of transition zone; 2) steam at output from fuel element.

junctions of these thermocouples were formed by welding the cable sheath with thermoelectrodes, the welding quality being reliably controlled by x-ray examination. The contact between the thermocouple and the casing of the fuel element was created by means of spring clips made out of type R-18 alloy. To improve this thermal contact, the thermocouple was first soldered to the clip with hard solder and a local contact formed under the cylindrical surface with the outer case of the fuel element. The thermocouples were marked with numbers (see Fig. 3).

Stages of Testing the Channels. The tests on the channels to obtain superheated steam by means of a single-pass scheme were started on a reactor at the Beloyarsk Nuclear Power Station in November 1973 (see Table 1). Channel 1 was intended for checking the method of carrying out tests of this nature. The system used for monitoring and maintaining the heat engineering parameters and the nature of their variation under transient conditions were verified. At this stage, the feed water for the loop (steam power station condensate) was subjected to further purification in ion exchange filters. The first channel operated under conditions with steam superheated by 10 to 30°C above its saturation temperature for about 1150 h and for about 2050 h with an 80 to 90% steam content at the output. In June 1974, channel 1 was withdrawn without damage from the reactor in accordance with the program. The temperature of the fuel element did not vary significantly during the course of these tests.

When the tests were carried out on channel 2, instead of being withdrawn, the channel remained installed over a longer period of time, the condensate being employed directly as feedwater for the loop, without any additional purification. The hardness of the feedwater was 2 to 3 μg · equiv./kg, pH = 6.5 to 8.2, dry residue 1.1 to 1.3 mg/kg. Exchange of water in the loop occured as a consequence of making up for natural leakage. The hardness of the water in the loop circuit was 3 to 14 μg · equiv./kg, pH = 5.7 to 6.9, dry residue 1.2 to 2.8 mg/kg. Channel 2 was tested in the reactor for about 15 months, of which about 125 days were under superheated steam conditions. Up to this time, the thermocouples on the casing of the output fuel element showed virtually no change of reading. Channel 2 was withdrawn from the reactor without damage. It was then replaced by channel 3.

The main purpose of the experiments with channel 3 was to study the nature of the temperature regime in a fuel element with relatively large heat flows, especially in the transition zone, while achieving a significant steam superheat.

Some Features of the Variations in Heat Engineering Parameters. Before the start of the experiments, the power of each pair of channels was calibrated with respect to the power of the reactor. This calibration was carried out at an increased flow rate of water through the channels to prevent boiling.

Before each series of experiments, it was also necessary to regulate the flow rates during the first rise in power of the experimental channels. With the power of the channels standing at approximately 50% of maximum, preliminary regulation of the flow rate and temperature of the water in the loop was carried out. As the power rose, these parameters were readjusted. The parameters was stabilized under conditions with a steam content of 80 to 90% (by calculation) at the output. The reactor power was then raised in small steps until superheated steam appeared at the output of the last fuel element in sequence (thermocouple 12, Fig. 1). The need for such regulation during the first approach to superheat arises out of specific features of the experimental loop circuit. It was carried out so that successive approaches to superheat could be accomplished simply by increasing the power of the channels (reactor) without regulating the flow rate and temperature of the water.

Two forms of regime instability were brought to light during the experiments. The first instability was due to fluctuations of flow in the experimental channels. Steam or a steam—water mixture was released from the channel into the receiver manifold (see Fig. 1) where water underheated to t_s was fed in parallel with the channel. The process of compensation in the collector was accompanied by pressure pulses, which gave rise to fluctuations of flow rate in the channel from 10 to 15 sec. The flow rate of the water in the experimental channel was stabilized by a condenser of the mixing type in the form of a water injector (see Fig. 1).

The second regime instability in the experimental channels was due to fluctuations of reactor power, basically within the dead zone of the reactor power regulator (~1% rated). It was observed that the cause of these fluctuations was a periodic variation in the temperature of the water in the primary loop of the reactor following the steam generator, with a period of ~75 sec and an amplitude of ±0.5°C. A reduction in the dead zone of the power regulator leads to a reduction in the amplitude of these temperature fluctuations, as would be expected.

The thermocouple equipment for measuring the steam temperature near the output from the fuel element drew attention to the correspondence of the reading of this thermocouple to the mean temperature of the steam. In particular, it is presumed that this thermocouple is able to indicate the temperature of the superheated steam at steam contents $x < 100\%$. To eliminate this uncertainty, one thermocouple of similar design had been mounted at a distance of ~4.5 m from the fuel element output.

Fig. 4 gives the temperatures from the indications of thermocouples at the approach of superheat in channel 3. By comparing the initial portions of the graphs (before superheat is reached), we can see that the second thermocouple starts to register the change in coolant temperature earlier than the first. This gives us a basis to suppose that the indications of the thermocouples mounted directly at the output from the fuel element are not higher than the average temperature of the coolant.

There is some increase in the steam temperature oscillations in channel 3 compared with channel 1, due to the higher steam superheat. The approach to superheat and the increase in superheat that accompanies the propagation of the transition zone changes the heat transfer coefficient α towards the flow of coolant. When there are power fluctuations, the motion of the transition zone is accompanied by fluctuations in the temperature of the fuel element. As an example, Fig. 5 shows the temperature of the fuel element at point 9* of channel 3 (see Fig. 3) when the transition zone passes through it. Depending on the increase in enthalpy in this section, the temperature fluctuates initially at low amplitude, as in the interval of uncontrolled variation of power, the high heat transfer coefficient is maintained; then, in the interval of power variation within which α varies significantly, the amplitude increases with increase in mean temperature and, finally, with the transition to the cooling of dry steam, the amplitude again falls at the highest mean temperature. The amplitude of the fluctuations in the temperature of the fuel elements naturally depends on the heat flow in the given section, the uncontrolled interval of power variation, and coefficient α. These quantities can be chosen in such a manner that the required capacity of the fuel element is ensured.

A Calculated Assessment of the Parameters of the Transition Zone from Experimental Data. As the distribution of the coolant along the length of the fuel element is close to being cosinusoidal, we are able to determine several of the parameters of the output fuel element of channel 3. For calculation, we use the equation

*Here and subsequently, we refer to the location of thermocouples.

$$\Delta N = 0.5N\left(1 - \frac{\sin \pi z/H_{eq}}{\sin (\pi/2)(H/H_{eq})}\right), \quad (1)$$

where ΔN is the power of that section of the fuel element from coordinate z to the output, kW; N is the total power of the fuel element kW; H is the active length of the fuel element, m; H_{eq} is the equivalent height of the active zone, m; z is the coordinate along the axis of the fuel element with its origin within the core of the element.

As is shown in Fig. 5, when the temperature of the steam at the output is ~400° at point 9 (see Fig. 3), the heat transfer to the coolant is stabilized and has the character of heat transfer to steam. The parameters of the regime of Fig. 5 are close to the mean (see Table 1). The calculation is carried out for these mean conditions.

When calculating the coordinates in which the mean enthalpy in the flow of dry saturated steam i" is attained, we use the equation of balance for determining ΔN:

$$\Delta N = \frac{(i_{ss} - i'')G}{860} = \frac{(728 - 640)\,312}{860} \approx 32 \text{ kW}$$

where i_{ss} is the enthalpy of saturated steam, kcal/kg; G is the flow rate of coolant, kg/h.

From Eq. (1), we determine coordinate z = −180 mm, at which the enthalpy equals i". From measurements of the temperature of the fuel element, the transition zone lies between points 8 and 9, the distance between which is 200 mm (see Fig. 3). The steam content, determined by the use of Eq. (1), equals ~87 and ~93% at points 8 and 9, respectively.

As we can see from Fig. 5, the temperature of the superheated steam at the output fluctuates over the range 5 to 8°C. These variations of the superheated steam are due to fluctuation of the power of the fuel elements, which comprise 1 to 1.5% of the given power level. The power fluctuations of the fuel element lead to a displacement of the transition zone along the length of the fuel element. Defining the steam superheat from the formula $\Delta i_{ss} = 860\Delta N/G$, where ΔN is found from Eq. (1), the variations of superheat with respect to z can be found by differentiating Δi_{ss} with respect to z. From this, we obtain an approximate expression for the displacement of the transition zone boundary in relation to the variation of enthalpy in the given section:

$$\delta z \approx \frac{H_{eq} \sin (\pi/2)(H/H_{eq})}{430\pi} \frac{G\delta(\Delta i_{ss})}{N \cos(\pi z/H_{eq})}. \quad (2)$$

For the end of the transition zone (point 9), $\delta z = 58$ mm.

The calculated estimate and an analysis of experimental data enables us to determine the order of the temperature gradient along the length of the fuel element. In the region of heat transfer to steam, the gradient is equal to 0.1 to 0.2°C/mm, while in the transition zone, it equals 0.5 to 1.0°C/mm (see Fig. 5). The gradient in the radial direction in the carrier tube of the fuel element is two orders of magnitude higher under steady-state conditions. This high temperature gradient along the fuel element over part of the transition zone is caused by the high intensity (power) of the output fuel element and the low heat-transfer coefficient to steam due to the low mass rate. The high intensity in the transition zone is a clear consequence of power fluctuations of the reactor, even those lying within the dead zone of the power regulator.

The power fluctuations enable us to determine the width of the transition zone: It is 100 to 150 mm in the calculated regime. Such a relatively wide transition zone gives us reason to refer to a "degenerate" crisis of heat transfer in tubes with intensifier elements.

CONCLUSIONS

The reactor tests of fuel elements with heat-exchange intensifiers, operating with full evaporation of the water, with superheated steam, and without the use of an intermediate separator, shows that it is possible in principle to design a single-pass steam generator in reactors with tubular fuel elements.

The operations for regulating the parameters in the steady-state regimes have been worked out, and the nature of variations in the heat-engineering parameters under transient conditions has been studied.

During the tests (125 days for channel 2) no significant variations in the temperatures of the fuel elements were observed, which directly confirmed the absence of any marked deposition due to boiling on the heat exchange surfaces (even when using relatively poor quality water).

It has been established that the fluctuations in reactor power within the dead zone of the power regulator give rise to instabilities in the temperature regime of the fuel elements. Under these circumstances, the temperature fluctuations in the transition zone of heat transfer are significant. To reduce these fluctuations in fuel element temperature in the transition zone, we should reduce the dead zone of the power regulator, use fuel elements of lower power for the part of the evaporation channel containing the heat-transfer transition zone, and increase the heat transfer to steam by increasing the mass flow in the fuel elements within the transition zone. Just these measures alone can reduce the amplitude of the fluctuations of fuel element temperature to a safe level.

In our opinion, bearing in mind all the limitations of the experiments, the results achieved are of interest for assessing the prospects of single-pass steam generators in power reactors. The absence of traditional equipment in the form of drum separators and circulating pumps, which are difficult and expensive to manufacture, to a large extent simplifies the nuclear steam-generating plant, and reduces its cost.

LITERATURE CITED

1. V. I. Subbotin et al., Teploénergetika, No. 9, 24 (1974).
2. S. Mizshak, Progress Rep. No. 1, USA, EC, Rep. DP-380 (1959).
3. V. P. Babarin et al., Heat Transfer, Hydrodynamics and the Thermophysical Properties of Matter [in Russian], Nauka, Moscow (1968), p. 45.
4. É. K. Kalinin et al., Intensification of Heat Exchange in Channels [in Russian], Mashinostroenie, Moscow (1972).
5. V. K. Migai, Inzh.-Fiz. Zh., 22, No. 2, 248 (1972).
6. V. V. Dolgov et al., At. Énerg., 9, No. 1, 10 (1960).
7. B. A. Zenkevich et al., At. Énerg., 27, No. 5, 391 (1969).

ZONE REGULATION OF THE POWER OF A POWER REACTOR

I. Ya. Emel'yanov, E. V. Filipchuk,
A. G. Filippov, V. V. Shevchenko,
P. T. Potapenko, and V. T. Neboyan

UDC 621.039.562

The traditional system for regulating the power of a nuclear reactor contains a single regulator, incorporating a number of ionization chambers to serve as detectors, while the executive organ comprises several regulating (control) rods, together with a system for synchronizing their positions.

The tendency toward ensuring high economic indices in large modern nuclear power stations necessitates operating the reactor under conditions in which the fuel and moderator charges approach their limiting permissible values, and this contradicts the requirement of reactor safety. The distribution of the power over the whole volume of the active zone is extremely sensitive toward local perturbations (recharging of the fuel elements, introduction of tools, sensors, etc., into the active zone and their subsequent extraction), and because of the small reserve factors in relation to the limiting loads, this may provoke an emergency situation. It is thus very important to provide modern reactors with a reliable system for regulating the power distribution.

The authors have carried out a careful analysis of various existing structural arrangements of regulation systems [1-4], which may nominally be divided into those consisting of several identical zone regulators (without any artificial links between them), those containing an additional integrated power regulator as well as the foregoing independent zone regulators, and those containing artificial links between the regulators.

Choice of the Number of Zones and Sensors. In designing a system of zone regulation it is important to remember that the most vital function of this system is the regulation of the integrated power; the quality of

Translated from Atomnaya Énergiya, Vol. 41, No. 2, pp. 81-84, August, 1976. Original article submitted October 23, 1975.

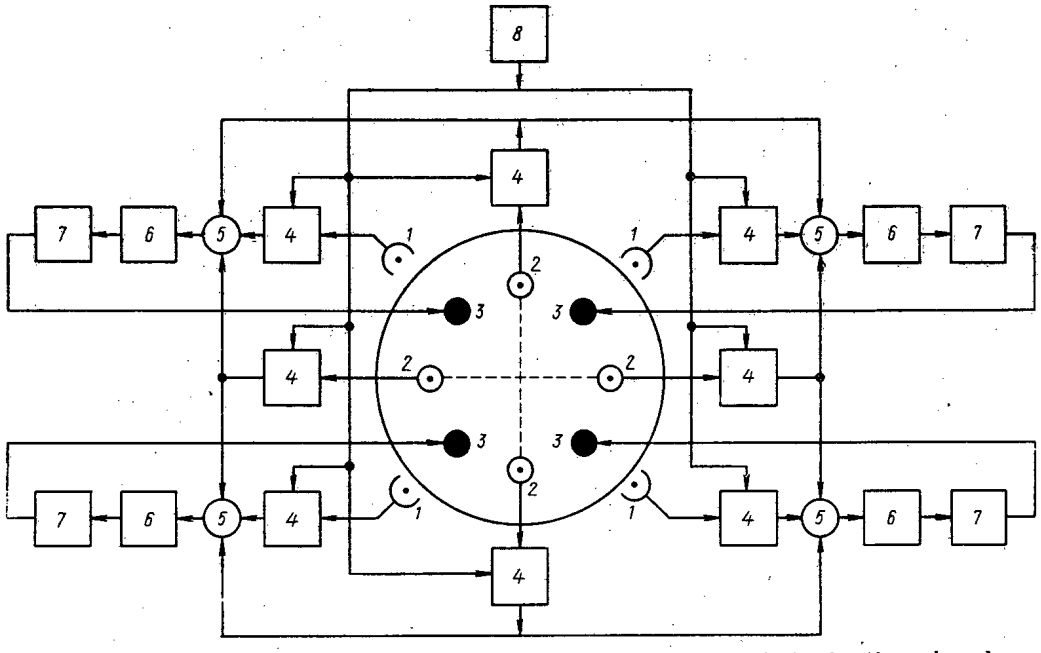

Fig. 1. Structural arrangement of a zone regulation system: 1) ionization chamber; 2) intrareactor sensor; 3) regulating (control) rod; 4) error signal amplifier; 5) adder; 6) drive control circuit; 7) drive; 8) power regulator.

this operation should be no worse than that of traditional regulation systems. The new system should be in no way inferior to the old as regards reliability. The conditions of nuclear safety should still be maintained.

These requirements are satisfied most completely by systems of the first type. The problem is eased by the fact that at the present time nuclear technology possesses a good supply of low-inertia intrareactor devices for monitoring the neutron flux.

The choice of the type, number, and disposition of the sensors, regulating rods, and zone regulators, together with the analysis and synthesis of a multiply linked system of regulation, constitute key aspects in the method of designing a zone regulation system.

The minimum number of regulation zones is determined by the number of unstable harmonics [5], and the maximum by the number of control rods in the reactor. Most power reactors have a fairly stable power distribution and a large number of control rods. The number of regulation zones and rods is also restricted by the maximum feasible rate of introducing additional reactivity by means of the automatic rod system; this necessitates reducing the velocity of the servo drives on increasing the number of zones. If several rods were used in the zone a system of rod synchronization would be required for each local regulator.

Thus the number of regulation zones must be chosen after allowing for the number of rods necessitated by the automatic regulation of the integrated power (four to seven). One regulating rod should be used in each local regulator.

More complicated is the question of choosing the number and disposition of the sensors for the local regulators. Since the sensors are intended to measure the power of the zone served by the corresponding

TABLE 1. Dependence of the Error on the Number of Sensors for the Case of Splitting into Four Zones

No. of sensors	Error, %		No. of sensors	Error, %	
	mean	maximum		mean	maximum
1	35	90	5	1	2
2	12	17	6	1	1
3	3	6	50	$\ll 1$	$\ll 1$
4	1,5	3			

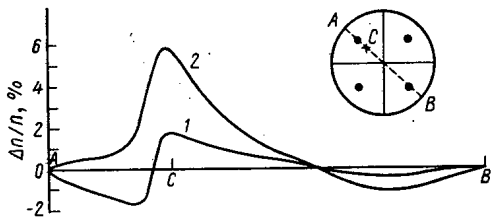

Fig. 2

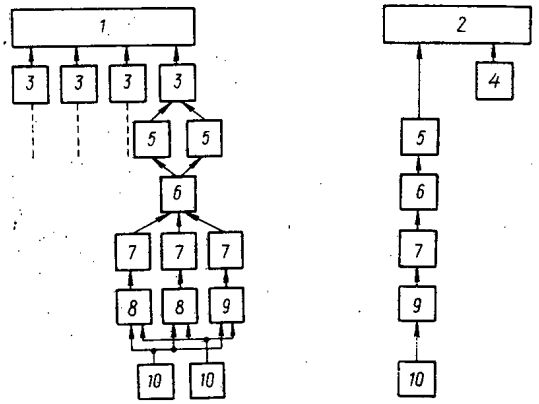

Fig. 3

Fig. 2. Deviation of the static neutron flux distribution during the processing of a perturbation by: 1) the zone regulation system and 2) by the traditional integrated-power regulation device.

Fig. 3. Analysis of the reliability of the two regulation systems: 1) zone regulation system; 2) integrated-power regulation system; 3) zone regulators; 4) reserve automatic regulator; 5) drive; 6) drive control circuit; 7) error signal amplifier; 8) intrazone sensor; 9) ionization chamber; 10) power controller.

regulator, their maximum number is equal to the number of fuel channels in each particular zone, the power of the zone being determined by the sum of the powers of each channel recorded by the corresponding sensors.

In trying to limit the number of sensors, it should be remembered that the readings of any particular sensor mainly depend on the position of the nearest rods and do not necessarily correspond to the power of the whole zone.

The following empirical method of determining the number of sensors for the zone regulator may be proposed.

1. For a nominal power distribution, one of the rods in the zone under consideration is moved, and the change is compensated by the movement of the rods in the other zones. The corresponding deviation in the power of the zone is measured by reference to the change in the power of all the fuel channels, or at any rate a large number of them (20 to 50), and also by reference to several (1-10) preselected sensors.

2. The experiments and measurements are repeated for different rods in the zone.

3. The maximum and mean errors in measuring the deviations of zone power by reference to one, two, three, etc., sensors are determined relative to the same deviations determined by reference to all (or a large number of) the fuel channels. A preliminary analysis of the results of such experiments for reactors of the RBMK type is presented in Table 1.

4. Using the resultant relationship, the number of sensors in the zone is determined from the specified static regulation accuracy. It should be remembered that a determination of the zone power by reference to n sensors also reduces the random component of the sensor errors by approximately $\sqrt{n}$ times.

Structural Scheme and Method of Calculation. The regulation system may, for example, incorporate intrareactor β-emission sensors (best of all are those with cobalt and platinum emitters owing to their low inertia) and also small fission chambers. On dividing the reactor into zones in the form of sectors, intrazone sensors and ionization chambers may be used in conjunction with one another. Thus in the structural scheme of a four-channel system of zone regulation (Fig. 1) the power of each zone is measured by sensors both inside and outside the active zone. The intrareactor sensors are placed at the boundaries of neighboring zones and their readings therefore characterize the power of two zones. This arrangement gives a considerable economy in equipment, since for three sensors per quadrant the total number required is eight. The signals from the sensors pass to the error signal amplifiers, in which they are compared with the setting specified by the power controller, and after amplification pass to the drive control circuit.

The chief structural difference between this system and the traditional automatic power regulator is the elimination of the unit synchronizing the positions of the rods from the system, and the individual control of the servo drives by the error amplifiers.

The structure of systems akin to that illustrated in Fig. 1 may to a first approximation be calculated by using a point model of the reactor. Here it is considered that all the zone regulators are connected in parallel to the object of regulation, with the transmission function of a "point" reactor $W_0(S)$. The advantage of this approximate method lies in the fact that it also operates for nonidentical zone regulators. For example, if the regulation system incorporates m zone regulators with transmission functions W_1, W_2, ... W_m, the stability of the multiply coupled system may be estimated from the stability of the equivalent single-circuit system, with the following transmission function in the open state:

$$W_{eq}(S) = W_0(S) \sum_{i=1}^{m} W_i(S).$$

It is easy to see that the method is equally suitable for analyzing linear systems and systems with relay drive control. In the latter case all existing methods of analyzing relay systems are suitable for the equivalent one-circuit arrangement.

In order to study neutron-field control systems, the analog simulation system is extremely effective. The circuits and computing methods for simulating neutron fields in a reactor were presented earlier [4]. This method was used, for example, to construct a network model of the RBMK reactor, including 233 mesh points and 134 operational amplifiers. The model enables us to find the optimum arrangement of the sensors and rods in the regulation zone, and also to analyze the static and dynamic characteristics of the neutron-field regulating systems. As an example we studied a four-channel system of zone regulation with inertia-free intrareactor sensors (as illustrated in Fig. 1). The characteristics of the zone regulator circuit elements were taken as being similar to the elements of existing integrated-power regulation systems. This enabled the zone regulation system to be realized with apparatus which had already recommended itself in practical service. For a static accuracy of the relay zone regulator equal to 0.5% of the nominal flux, and for the officially specified standard rate of introducing reactivity, the time required to develop the perturbing and control actions amounted to 5-7 sec, in conformity with the operating speed of a traditional integrated-power regulator. The efficiency of zone regulation is clearly illustrated in Fig. 2, which shows the deviation of the static neutron flux distribution with respect to the diameter of the active zone AB passing through the control rods after applying a perturbation $\Delta K = 0.015\,\beta$ at the point C (β is the effective proportion of delayed neutrons). We see that for zone regulation the deviation in the distribution is several times smaller than that obtained with the traditional regulation system.

Questions Regarding the Reliability of the Systems. According to the generally accepted method, the reliability of the zone-regulation system may be assessed in relation to that of the traditional integrated-power control system by making a comparative analysis of their relay-contact systems (RCS) [6], which constitute the result of replacing the functional couplings of the elements in the systems under consideration by logical couplings. In the RCS the elements are represented by electrical contacts and the logical couplings between the elements by conductors. For example, the series connection of several elements means that the whole group of elements fails if any one element becomes defective. For parallel connection, the failure of the group of elements is a consequence of the defection of all the elements. The corresponding RCS for the zone regulation system and the traditional system of integrated-power regulation are presented in Fig. 3.

It should be noted that, in analyzing reliability, the zone regulation system may be considered as one particular version of the integrated-power regulation system in which the existing four identical regulation channels in fact signify a triple reserve factor of the system. Thus, even without allowing for the element-by-element reserve provision in each zone regulator, we may say that the zone regulation system is more reliable than the traditional integrated-power regulation system. The parallel connection of two power controllers, and also the "cold" reserve provision of executive drives and rods, increases still further the reliability of the system under consideration.

We may thus note the following advantages of zone power regulation relative to the traditional "synchronous" regulation systems.

1. The system of zone regulation ensures a higher accuracy of integrated-power regulation, since both intra- and extrareactor sensors are used to measure the power.

2. The system under consideration fulfills the additional function of power equalization.

3. Zonal power regulation eliminates the system of automatic control-rod synchronization.

4. The zone regulation system eases the work of the operator during recharging and increases in power. In the steady state the system ensures stabilization of the radial power distribution without the participation of the operator, and hence suppresses azimuthal fluctuations in power distribution.

5. The zone regulation system has a greater structural reliability than the traditional system of integrated-power regulation.

LITERATURE CITED

1. I. Ya. Emel'yanov, Izv. Akad. Nauk SSSR, Énergetika i Transport, No. 3, 97 (1974).
2. A. N. Kosilov, P. T. Potapenko, and E. S. Timokhin, Atomnaya Tekhnika za Rubezhom, No. 7, 17 (1975).
3. E. V. Filipchuk et al., At. Énerg., 35, No. 5, 317 (1975).
4. I. Ya. Emel'yanov et al., At. Énerg., 37, No. 2, 118 (1974).
5. A. Hitchcock, Stability of Nuclear Reactors [Russian translation], Gosatomizdat, Moscow (1963).
6. I. Ya. Emel'yanov, A. I. Klemin, and E. F. Polyakov, At. Énerg., 37, No. 5, 408 (1974).

REDISTRIBUTION AND MOBILITY OF URANIUM DURING THE METAMORPHISM OF VOLCANOGENIC FORMATIONS

V. P. Kovalev, A. D. Nozhkin, A. G. Mironov, and Z. V. Malyasova

UDC 553.53:553.495

Data regarding the redistribution and mobilization of uranium from volcanogenic formations during their metamorphism are of major cognitive and applied significance; they are directly related to the theory of endogenic ore formation and give a clear representation of the genetic relationships of ores with magmatism. These data are usually obtained by comparing the initial and final contents of the elements in rocks experiencing various changes as well as the contents established in transitional states. Apart from comparisons of this kind, analytical data regarding mobile, easily extracted uranium may also be used, and this facilitates estimation of the mobilizational activity of the element in the rocks under consideration.

Intrusive masses have for a long time received special consideration when solving the problem of the relationship between ore formation and magmatism, and only with the establishment of a close spatial relationship between ore formation and volcanogenic accumulations have the latter become more and more widely studied by geochemical workers.

It is found that effusive rocks contain more uranium than intrusive. The uranium deficit in deep magmatic rocks is constantly confirmed on comparing these with effusive petrochemical analogs (only statistically rich samples are compared). The difference in content is so considerable that it may readily be detected on comparing rocks belonging to the same magmatic province and epoch, related by having an identical source but differing environmentally. Adams was the first to notice the important geochemical difference between plutonites and volcanites [1]; he considered that the absolute uranium content of lavas reflected the real content of this element in the magma.

It was later shown that the rocks crystallizing in the interior contained altogether 20-70% of all the uranium incorporated in the vitreous extrusive tertiary rocks of the Western United States [2]. It was found that the recrystallization of melts under near-surface conditions was accompanied by the loss of uranium, while the thorium content remained almost unchanged [3]. The preferential loss of uranium from completely crystallizing melts is responsible for the different Th:U ratios in effusive (2.5-3.5) and intrusive (4.0-6.0) rocks

Translated from Atomnaya Énergiya, Vol. 41, No. 2, pp. 85-91, August, 1976. Original article submitted July 15, 1975.

TABLE 1. Content of Mobile Uranium* in Volcanic Rocks Subjected to Weak Transformations

Region	Characteristic of rocks	No. of samples	Limits of total content, $n \cdot 10^{-4}$ %	Limits of mobile uranium content, $n \cdot 10^{-4}$ %	Extraction,† %
Minusinsk Depression	Effusive and explosive formations				
	Rocks of basic composition	10	0,75—2,4	0,01—0,10	1,2—6,0 / 3,1
	Rocks of acid composition:				
	prophyry, felsites	11	3,0—32,0	0,02—0,43	0,5—6,0 / 2,9
	dehydrated pearlites, spherulites	6	4,8—8,5	0,09—0,66	1,0—12,0 / 5,5
	ignimbrites, sintered tufas	12	6,0—9,9	0,35—0,83	5,0—10,0 / 7,0
Eniseisk Ridge	Rocks of basic composition	6	1,0—2,8	0,10—0,11	3,8—10,0 / 6,0
	Rocks of acid composition	3	3,4—13,0	0,38—2,02	10,0—15,4 / 12,2
Minusinsk Depression	Subvolcanic formations: granite-porphyries	1	9,6	2,46	25,6
Eniseisk Ridge	Quartz porphyries	3	4,6—14,0	1,30—6,40	28,5—45,7

*Extracted from rocks with a 5% solution of $(NH_4)_2CO_3$.
†Numerator, limit; denominator, average value.

[4, 5]. The enrichment of volcanites with uranium is explained by the fact that, during the very rapid solidification of aluminosilicate melts, the whole mass of dissipated uranium and thorium is captured by the quasi-crystalline matrix, while during the slower release of heat in the interior a considerable proportion of the uranium is accumulated in the residual melt solution and is lost in the environmental rocks. The incapacity of uranium to be separated, together with high-temperature emanations, from the melts coming to the earth's surface was also noted in [6].

The conclusion as to the uranium enrichment of the effusive petrochemical analogs of intrusive rocks has not yet been universally accepted. This may be judged from a table [7] giving the world-average values of the Clarke coefficients of uranium and thorium in intrusive and effusive equivalents with different basicities, in which the uranium content and the Th : U ratio are precisely or almost identical. Higher concentrations of uranium in intrusive rocks were indicated in [8]. This latter conclusion is only valid for extreme differentiates; these make only a small contribution to the total volume in a mass of intrusive rocks, as a result of which the weighted-mean values of the uranium content in intrusive complexes will actually be smaller than in the effusive series. The appearance of extreme differentiates in effusive facies is excluded, since in contrast to the intrusive process the volcanic process may be regarded as more dynamic, with the predominant transition of magmatic melts to the surface. Very rarely conditions may occur in which crystallizational differentiation takes place, together with alkali enrichment, in conjunction with a sharp increase in thorium and uranium content.

The foregoing differences in the radiogeochemical characteristics of intrusive and effusive analogs are not unique. While being inferior to extrusive rocks as regards absolute uranium contents, intrusive rocks are capable of passing a considerable proportion of their residual uranium content into the solutions flowing around them. Whereas the deep rocks, including extrusive formations, pass 20-90% of their uranium into aqueous carbonate solutions, fresh effusive and subvolcanic rocks containing a vitreous or weakly decrystallized mass are disinclined to lose uranium. Aluminosilicate glasses obtained as a result of the melting of intrusive and extrusive rocks containing mobile uranium (altogether $n \cdot 10^{-6}$% of uranium is extracted with a 5% solution of ammonium carbonate [9]) also hold their uranium very strongly. This situation is associated with the metastable state of the main mass of the material, which usually contains 70-90% of the total uranium content. The reason for the poor extractability lies not in the sorptional properties of the glasses, but in the appearance of gels preventing diffusion, these being readily formed as a result of the considerable instability of the compounds in the main mass [10].

The appearance of mobile uranium, capable of being extracted from the crystalline material without decomposing the latter in intrusive rocks, is associated with a variety of phenomena and processes: with the

TABLE 2. Uranium Content in Metamorphosed Volcanic Rocks of the Eniseisk Ridge

Form of metamorphism	Facies of metamorphism	Characteristics of rocks and mineral associations	No. of analyses	Limits of uranium content, $n \cdot 10^{-4}$ %	Mean uranium content, $n \cdot 10^{-4}$ %	Extraction, %
Diagenesis, metamorphism of the charge	—	Basic rocks	15	0,5—1,25	0,9	3—5
		Acid rocks	20	1,3—10,0	5,6	10
		Chloride zone				
Regional-contact (plutonometamorphism)	Greenschist	Basic rocks	24	0,5—2,6	1,4	10
		Acid rocks	46	1,8—12,7	6,4	15,4
		Biotite zone				
		Metabasites (carb.+chl.+ab.)	20	0,1—3,9	1,3	10
		Porphyroids (cer.+musc.+ab.+quartz)	25	2,0—18,0	7,5	45
	Epidote amphibolite	Metabasites (carb.+ep.+chl.+act.+ab.)	16	0,1—2,4	0,7	—
	Amphibolite	Orthoamphibolites (ep.+ horbl.+ olig.)	15	Not obs.—1,9	0,4	—
		Muscovite-quartz orthoschists	9	0,4—3,4	0,9	10
Regional	Granulite	Hypersthene-plagioclase gneisses	22	Not obs.—0,9	0,1—0,2	—
Dynamometamorphism	—	Prasinitic schists (leuc.+cer.+carb.+ab.+chl.)	22	1,0—5,5	2,7	15
Hydrothermal metamorphism (propylitization)	—	Quartz porphyries (quartz+ab.+cer.+pyr.)	10	4,2—12,7	7,9	21,4—95,0

Note. act. = actinolite; ab. = albite; carb. = carbonate; leuc. = leucoxene; musc. = muscovite; olig. = oligoclase; pyr. = pyrite; horbl. = hornblende; cer. = cerisite; chl. = chlorite; ep. = epidote.

degree of oxidation of the material in the magmatic melt, with hypergenic and hypogenic processes, and with metamictic decomposition. The mobility of the uranium is determined by the degree of processing of the rocks in late- and postmagmatic processes which are customary in intrusive chambers.

The extractable uranium, a product of autometasomatic and epigenetic activity, is the result of the action of hydrothermal flows draining completely crystalline rocks. The solutions washing the acid igneous rocks are richer in uranium than those draining the basic rocks; hence the amount of mobile uranium is greater in granitoid than in gabbroid formations.

It has already been mentioned that uranium is poorly extracted from effusives and their tufas [9]. It has been found that comparatively fresh ceno- and paleotypic effusives (rocks without any clear traces of hydrothermal processing) only yield a small quantity of uranium to 5% solutions of ammonium carbonate. The low rate of extraction of uranium by 5-10% soda solutions was noted by L. N. Shatkov and G. A. Shatkov, who tested samples of effusives from the environment of a hydrothermal site. Effusives give poor uranium yields even to solutions of strong acids and bases: A 2N solution of NaOH on average extracts only 4-6% of uranium from the Upper Paleozoic effusives of Silesia, while 2N H_2SO_4 extracts 13-19% [11].

The lowest rate of uranium extraction is characteristic of glasses. The yield is probably little higher for devitrified glasses. The results of our own investigations show that the degree of extraction depends on the age of the rocks. Thus the Middle Paleozoic effusives of the Minusinsk Depression yield less uranium than the later samples from the Eniseisk Ridge (Table 1), although in the latter case the superposition of epigenic changes may exert an effect. Since the intratelluric impregnations of volcanic rocks contain an insignificant proportion of gross uranium, they cannot seriously influence the results of the extraction experiments. Not to speak of feldspar phenocrysts, even the biotites of acid lavas are extremely poor in uranium, although hysteromagmatic biotites of intrusive rocks are on rare occasions uranium-enriched. This enrichment is associated with the presence of submicroscopic precipitates of accessory minerals [12], the separation of which is uncharacteristic of not only the biotites of effusives but also the main mass of the latter.

The considerable difference between the principal radiogeochemical characteristics of the two general types of rocks of magmatic origin is doubtless associated with the fundamental differences in the modes of solidification of melts with identical chemical properties. In our own opinion this difference cannot be explained (as it has been for a long time) simply by reference to a geobatial cause. It is more reasonable to distinguish two independent, mutually antagonistic types of magmatism, volcanic and plutonic, which are associated with completely different geoenergetic and geostructural states of the earth's crust and mantle, and do not occur in simple relation to one another.

Thus the difference between the absolute and mobile uranium contents in effusive and intrusive rocks, and the difference between the quantities of overall and mobile uranium in rocks of differing basicities, prove

that each quantity is determined by the composition and conditions of formation of the igneous rocks, i.e., by their petrochemistry and petrology. In other words, the denial of any relationship between the extraction of uranium and petrology, uncritically accepted by certain research workers [13], is refuted by repeated investigations.

Our own accumulated material indicates that the syngenesis, diagenesis, and metamorphism of the charge do not involve any great changes in the original uranium concentrations or the appearance of migrationally mobile forms of this element. Sintered tufas, ignimbrites, felsites with pearlitic divisions, spherulites, devitrites, hydrated glasses, and so forth, retain their original basic content and contain hardly any mobile uranium. All this shows that such syngenetic phenomena as the sintering of volcanoclastics and the hydration and dehydration of natural glasses do not result in the appearance of mobile forms of uranium. Aqueous extracts from pearlites contain only $n \cdot 10^{-6}$ g/liter of U [3]. The carbonate, sodium chloride, and sodium chloride–sulfate thermal waters of Kamchatka contain from 0.04 to 0.1 γ/liter U [6]. This shows that weak solutions fail to extract even part of the uranium in effusives and pyroclasts. A disruption of the original basic uranium content as a result of gas and hydrothermal activity occurs in cenotypic volcanites (the sulfate waters of Kamchatka, for example, contain an average of 1 γ/liter of U), but as a rule the proportion of extracted rocks taken over the whole volume of an effusive – explosive accumulation is comparatively low – altogether 5-10%. The weathering of the rocks under the influence of acid vapors also leads to the release and removal of uranium, but as a result of the small scale of these processes they only make a very small contribution to the appearance of mobile uranium. This also applies to processes involving the terrestrial and underwater weathering of volcanites, although these are sometimes regarded as responsible for a growth in the basic concentrations.

The foregoing facts convincingly demonstrate the incapacity of uranium to be removed from rapidly solidifying melts together with the gases and vapors evolving from lavas, and severely shake our recent confidence in the possibility of the synvolcanic formation of ores. Nevertheless, the syngenesis and diagenesis of volcanic rocks play an important part as processes tending to level out the considerable differences existing between water-free volcanites and, for example, sedimentary rocks of similar composition. As a result of syngenesis and diagenesis, the amount of glass in the principal mass is reduced, the rocks undergo hydration, and minerals containing hydroxide groups are produced. The metamorphism of the volcanites produced in this way may be completed by analogy with the metamorphism of deposits.

The foregoing picture is not characteristic of volcanites experiencing considerable epigenetic changes. In the metavolcanites, the amount of mobile uranium increases substantially, and in many cases exceeds the amount found in intrusive rocks. Regional, local (warp zone), regional-contact (involving the appearance of granite-gneiss complexes), intrinsically contact, and hydrothermal metamorphism is accompanied by the inflow and outflow of uranium and the appearance of uranium in a form capable of migrating. Table 2 presented certain results obtained by Nozhkin and Mironov regarding the Eniseisk Ridge revealing a change in content from facies to facies, together with data facilitating the estimation of the relationship between the metamorphosed effusives and the degree of extraction.

Metamorphism of low and high degrees, and frequently metasomatosis as well, are accompanied by the formation of completely new basic concentrations of uranium and a change in the original Th:U ratios. The intensification of metamorphism reduces the dimensional characteristics of the distribution (the variation coefficients increase); in each specific case this effect is mainly determined by the limits of metamorphic differentiation of the material. The infringement of the dimensional characteristics of the uranium distribution may be directly appreciated from the α tracks and the tracks due to fission fragments of ^{235}U nuclei even in effusives with a not-very-clearly decrystallized basic mass. In metaeffusives with a more decrystallized metastasis there is also a higher content of mobile uranium. In the porphyry precipitates of metavolcanites there is a (3-10 times) increment in the uranium content owing to the development of low-temperature albite and chlorite in the place of the highly basic plagioclase and pyroxene. The increase in the combined distribution is associated with this fact.

There are probably no special reasons for opposing the metamorphism of volcanites to the metamorphism of, for example, sedimentary aluminosilicate rocks, although such a contradistinction is based on the well-known metastability and primary state of dehydration of effusive rocks. During the processes of syn- and diagenesis, and also initial metamorphism, many of the effusive rocks undergo secondary hydration, so that their subsequent metamorphism is accompanied by the appearance of interstitial solutions, while the sharply unstable states of the rock-forming material (characteristic of effusives) constitute one of the invariable conditions for the development of metamorphism. The metamorphism of "dry" glassy rocks probably plays no part in the creation or loss of mobile uranium.

In weakly metamorphosed effusives of acid composition the uranium content usually remains practically unchanged at low temperatures. In metabasaltoids, on the other hand, there is usually a considerable uranium enrichment by comparison with the nonmetamorphosed analogs. This is characteristic for considerable uranium chlorite zone of regional metamorphism and especially for the greenstone (prasinitic albite — chlorite) orthoschists of the zones of dynamometamorphism. The increment in uranium concentration is associated with the development of secondary schistous aluminosilicates (up to 60% of the uranium is concentrated in these) and also titanium hydroxides (up to 25%), which make good uranium sorbents [14].

In the biotitic zone of greenschist metamorphism, however, there is a certain loss of uranium on account of the reduction in the amount of chlorite, leucoxene, and other sorbents, and as a result of the increase in the desorption and release of hygroscopic water, etc. Nevertheless, in the porphyroids and quartz–cerisite–muscovite orthoschists (well-developed among acid effusives) the amount of mobile uranium increases to 40-60% for the same primary uranium level. A microradiographic investigation shows that 50-80% of the uranium of these rocks is accumulated in the cerisite, muscovite, biotite, and also in the hydroxides of the ferrous metals along cracks, grain boundaries, and in interstices.

Under more high-temperature conditions, such as exist, for example, in zones of regional-contact metamorphism, in which orthoamphibolites are formed, there is an effective erosive loss of uranium. The remaining uranium is chiefly concentrated in clinozoisite (2.5 g/ton) and ilmenite (4 g/ton). In the main rock-forming minerals (hornblende and plagioclase), however, the quantity is no greater than 0.1-0.2 g/ton. This is also confirmed by the reduced uranium content in such minerals as magnetite (0.3-0.5), muscovite (0.8), carbonate (0.5), biotite (1.5), and albite (0.5 g/ton). In quartz porphyries encountered in the amphibolite zone under conditions of dynamometamorphism there is a sharp microdifferentiation into essentially quartz and mica aggregates. On the macroscopic scale similar phenomena result in the appearance of micaceous quartzite schists with a far lower uranium content than the original rocks. It is noteworthy that the remaining uranium in these is strongly combined and is concentrated in accessory minerals and micas.

The lowest uranium content (under 0.1-0.2 g/ton) occurs in hypersthene–plagioclase and garnet–hypersthene–plagioclase rocks of the Eniseisk Ridge characterized by granulite facies of basic-rock metamorphism. It is abundantly clear that the low uranium content of these minerals is due to the metamorphic phenomena, initially producing the decarbonatization and later the complete dehydration of the rocks. In this case it is pointless to speak of the amount of mobile uranium.

Thus the tendency for the release of dissipated uranium from volcanic rocks is extremely clear even in the basaltoids, not to speak of the acid rocks. If the uranium content is kept at its previous level in the metamorphosed effusives, a qualitative change appears, in that a greater proportion of mobile uranium is encountered. Both features (in our own view) constitute a sign of the action of metamorphic solutions. The recrystallization of the principal mass of the volcanogenic rocks is accompanied, as metamorphism intensifies, by an increase in the role of the migratory uranium, which offers a basis for its subsequent mobilization and redeposition as a result of the ensuing superposition of hydrothermal processes. The deviation from isochemical metamorphism accompanied by metamorphic differentiation or complicated by the development of metamorphic zonal structure in no way contradicts the conclusions of the present investigation.

Information regarding the contact metamorphism of the almond rocks of the Byskarsk series in the Krasnoselsk granosyenite intrusion (Eastern Sayan) indicates the preservation of the original uranium content. The selective extraction of basic hornstones, at present constituting a plagioclase–biotitic aggregate containing abundant magnetite in the main mass of the material, with plagioclase and hypersthene in the geodes, reveals the presence of considerable quantities of mobile uranium. During the contact metamorphism of the volcanites, uranium is evidently not inclined to leave the rocks, especially those of the basic type. In the apical parts of the massifs, in fact, trapping of uranium and thorium occurs. This is especially clearly expressed in xenolites and residual mountains.

Epigenetic hydrothermal metamorphism also disrupts the initial basic uranium content in volcanites and promotes the appearance of large quantities of mobile uranium in these. Paleotypic volcanogenic strata are often affected no less by hydrothermal epigenetic than by metamorphic alterations. The modification of the basic concentration in hydrothermally altered rocks occurs not simply as a result of the inflow and outflow of uranium but also (at high temperatures) as a result of changes in thorium content. Usually uranium is found in the original basic quantities in rocks which have experienced low-temperature hydrothermal metamorphism. The uranium and thorium concentration increases sharply in the altered rocks surrounding the ore (according to Maksimovskii and Rudnik and to Mel'nikov and Berzina by a factor of 5-10). The low-temperature hydrothermal alteration of effusives and tufas results in a twofold or more increment in uranium content, while the

thorium remains constant [15]. According to our own data, propylitized basalt and basalt–andesite porphyrites experiencing chloritization and pretinization are enriched with uranium by a factor of two or more, and always contain mobile uranium in considerable quantities.

We are here only considering those hydrothermally changed volcanites in which the basic concentration of uranium is initially constant. These rocks correspond to the facies of low-temperature propylites. According to the results of neutron-fission microradiography, the principal mass of the uranium in such rocks belongs to the chlorite (60-70), leucoxene (20-35), and epidote (10-15%) phases. The maximum uranium content is established in leucoxene (5 g/ton) and chlorite (3 g/ton). In epidote the uranium content is 1-3 g/ton. In cerisitized, quartzized (with sulfides and sometimes carbonates and epidote), and acid effusives, even the regions of most intensive processing are hardly distinguishable as regards uranium content from unaltered porphyrites. However, the proportion of mobile uranium in these increases sharply (to 60-90%).

The preparation of the uranium Clarke content for migration and its entry into migratory processes are of considerable interest when searching for ore sources. Naturally chief attention should here be paid to acid and alkaline rocks, in which a great deal of mobile uranium appears. Although no direct proof of the relationship between ores and the uranium extracted from igneous rocks has yet been found, many research workers consider that not only the melts but also the magmatic rocks themselves (including volcanogenic forms) may act as useful sources. The volcanogenic rocks are certainly better as sources of uranium than intrusive and many sedimentary rocks of identical chemical compositions. For the ordinary uranium content of 3-10 g/ton, from 4.5 to 15 kg of metal capable of forming rich ores may be displaced from a prism 1 km high with a base 1 m^2 (subject to 50% extraction) and duly concentrated when a chemical barrier exists. This problem will clearly be made easier if the source comprises rocks similar to the tertiary porphyries of Colorado, containing 0.002-0.014% of uranium. Many consider that the erosive loss of 0.2-0.1 of the uranium in the rocks is a normal phenomenon. It is considered that the formation of ore deposits involves the displacement of a mass of metal exceeding by 150-200 times the weight of the actual ores. This especially applies to effusives which have been subjected to metamorphism under the conditions of the greenschist facies, to local dynamometamorphism or to hydrothermal epigenetic changes, and are characterized by an increased content of mobile uranium. The latter may be particularly easily mobilized by solutions and concentrated in a favorable endogenic situation. It is clearly from this point of view that we may explain the frequently observed large time gap between the accumulation of volcanogenic rocks and the appearance of uranium mineralization.

CONCLUSIONS

1. Effusive and intrusive petrochemical analogs differ considerably as regards their content of ordinary and mobile uranium. This is because of the fundamentally differing conditions of solidification of the chemically identical melts.

2. As products of the rapid supercooling of aluminosilicate melts, effusives mechanically capture all the uranium dissipated within them, and as a result of the metastable state of the main mass fail to transfer this uranium to solutions without the complete chemical decomposition of the material composing them.

3. The initial concentration and distribution of the uranium in volcanogenic rocks are altered when epigenetic processes associated with tectonic magmatism and metamorphism develop on the large scale. As they develop regional, local, contact, and hydrothermal forms of metamorphism lead to the appearance of different amounts of mobile uranium and to a change in the original content. Ultrametamorphism leads to the greatest losses of uranium.

4. The most promising sites as regards the discovery of uranium ore-formation are regions of acid volcanism having widely evident areas of low- and medium-temperature hydrothermal metamorphism, with traces of later tectono-magmatic activization. No less favorable are regions corresponding to the propagation of early volcanogenic accumulations of the same composition which have experienced metamorphism of the greenschist facies and then been subjected to hydrothermal action.

Thus the uranium contained in volcanogenic rocks can only migrate after fundamental recrystallization of the rock-forming material, or after its complete decomposition, which may be effected either in metamorphic processes or alternatively in exogenic processes in which chemical decomposition of the rocks takes place. Effusive — explosive formations usually undergo the greatest metamorphic transformations in the epigenetic stage of their existence (a long time after the extinction of the volcanos), by virtue of the appearance of a superimposed deep tectono-magmatism influencing and basically modifying the volcanogenic strata.

LITERATURE CITED

1. I. Adams, Nuclear Geology, New York (1954).
2. I. Rocholt et al., Econ. Geol., 66, 1061 (1971).
3. L. N. Shatkova and G. A. Shatkov, Geologiya Rudnykh Mestorozhdenii, No. 4, 36 (1973).
4. V. P. Kovalev, Uranium and Thorium in Magmatic and Metamorphic Rocks in the Central Part of the Altae-Sayan Folded Region [in Russian], Nauka, Moscow (1972), p. 164.
5. V. P. Kovalev, Radioactive Elements in Rocks [in Russian], Nauka, Novosibirsk (1975), p. 95.
6. L. L. Leonova and N. I. Udal'tsova, Geochemistry of Uranium and Thorium in the Volcanic Process, the Kurile-Kamchatka Region Being Taken as an Example [in Russian], Nauka, Novosibirsk (1975).
7. A. A. Smyslov, Uranium and Thorium in the Earth's Crust [in Russian], Nedra, Leningrad (1974).
8. I. E. Smorchkov, in: Geology of Hydrothermal Uranium Sites [in Russian], Nauka, Moscow (1966), p. 119.
9. V. P. Kovalev and Z. V. Malyasova, Geokhimiya, No. 7, 855 (1971).
10. G. V. Kukolev, Chemistry of Silicon and Physical Chemistry of Silicates [in Russian], Vysshaya Shkola, Moscow (1966).
11. H. Sylwestrzak, Bull. Institut Geol., Warsaw (259), 21, 5 (1972).
12. O. P. Eliseeva, B. I. Omel'yanenko, and I. E. Smorchkov, Zap. Vsesoyuz. Mineralog. Obshch., 103, 508 (1974).
13. G. Neuerburg, I. Antweiler, and B. Bieler, 20th Intern. Geol. Congress, Abstracts, Mexico (1956), p. 221.
14. N. A. Kulik, S. V. Mel'gunov, and V. M. Gavshin, in: Radioactive Elements in Rocks [in Russian], Nauka, Novosibirsk (1975), p. 229.
15. A. S. Mitropol'skii, V. P. Kovalev, and S. V. Mel'gunov, in: Geochemistry and Conditions of Gold and Rare-Metal Ore Formation [in Russian], Nauka, Novosibirsk (1972), p. 88.

MATHEMATICAL SIMULATION OF PROCESSES IN THE EXTRACTIVE REPROCESSING OF NUCLEAR FUEL

4. SEPARATION OF URANIUM AND PLUTONIUM BY THE METHOD OF DISPLACEMENT RE-EXTRACTION

A. M. Rozen and M. Ya. Zel'venskii

UDC 621.039:59.001.57

Together with the removal of fission-fragment elements from the solution of irradiated fuel elements, the separation of plutonium and neptunium from uranium is the most important task of extractive technology in the reprocessing of nuclear fuel. Soviet specialists have widely used the methods of chemical conversion of plutonium and neptunium into unextractable forms, their re-extraction, and their subsequent refining [1-3]. These methods are reliable but have a number of shortcomings: It is necessary to set up special installations to obtain the reagents; if reducing agents of the iron-salts type are used, the salt composition of the solution becomes worse; if U (IV) is used, it must be stabilized.

Recently, attempts have been made to develop methods for separating U, Pu, and Np which are free from these shortcomings [4, 5]. In particular, one of the schemes used re-extraction with a concentrated uranium solution for complete saturation of the extracting agent with uranium and the displacement of plutonium and neptunium by uranium from the extract into the aqueous phase [5] (this process has come to be known as displacement re-extraction).

The possibility of carrying out displacement processes is due to the chemical characteristics of extraction by means of tri-n-butylphosphate (TBP) and other neutral organophosphorus compounds — the formation

Translated from Atomnaya Énergiya, Vol. 41, No. 2, pp. 91-95, August, 1976. Original article submitted August 6, 1975.

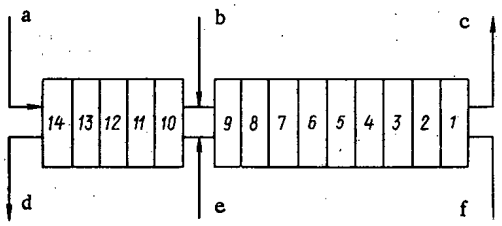

Fig. 1

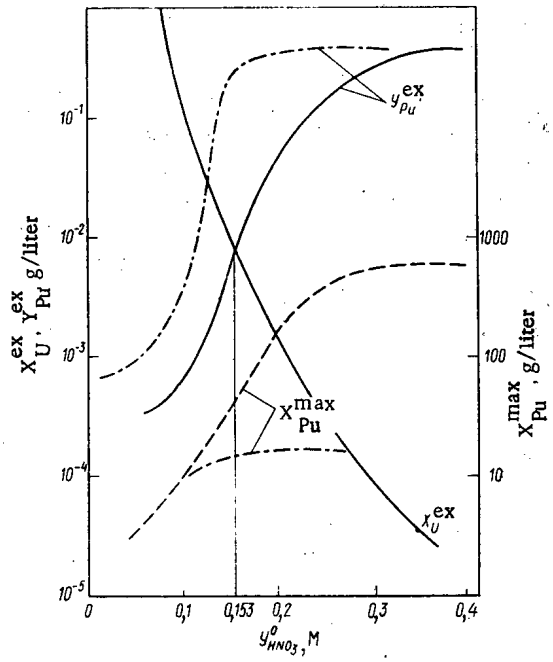

Fig. 2

Fig. 1. Scheme and parameters of the nominal regime of the displacement re-extraction process [5]: a) $V' = 156$ liter/h; 30% TBP; b) $V^0 = 640$ liter/h; $Y^0_U = 78$, $Y^0_{Pu} = 0.47$, $N^0_{Np} = 0.08$ g/liter; c) $V^0 + V' = 796$ liter/h; $Y^{ex}_U = 110$, $Y^{ex}_{Pu} = 10^{-6}$, $Y^{ex}_{Np} = 10^{-7}$ g/liter, $Y^{ex}_{HNO_3} = 0.01$ M; d) $L = L^0 + L' = 232$ liter/h; $X^{ex}_U = 0.01$, $X^{ex}_{Pu} = 1.3$, $X^{ex}_{Np} = 0.22$ g/liter, $X^{ex}_{HNO_3} = 1$ M; e) $L' = 11.6$ liter/h, 10 M HNO_3; f) $L^0 = 220$ liter/h, $X^0_U = 172$ g/liter, $X^0_{HNO_3} = 0.01$ M; 1-14 are the numbers of the stages.

Fig. 2. Variation of the indicators for the separation of uranium and plutonium and the accumulation of plutonium in the aqueous phase as functions of the acidity of the initial organic solution (-.-.-.-.- represents the calculation in which the plutonium is taken to be a macrocomponent).

of complexes of salts of the metals with the extracting agent [6] and the competition between different metals for the free extracting agent [7, 8].

Saturation of the organic phase with uranium is widely used for excluding fission fragments more completely from the organic phase; some quantitative estimates are given in [9], which gives the static characteristics of the Purex process and notes that as the limiting conditions are approached, the uranium zone expands, the degree of purification of the valuable elements is improved, but at the same time there is an increase in their concentration in the discarded solution (the raffinate). In addition, there are problems with the circulation of elements in the cascade and the internal accumulation of plutonium [8, 9].

In the present study we investigate the characteristics of the process of displacement re-extraction; for this purpose, we have used the method of mathematical simulation. The mathematical model and algorithm used for the extraction processes are those described in [10, 11].* For the sake of simplicity, we assumed in the calculations that the plutonium and neptunium are microcomponents (in part of the calculations we took account of the characteristic concentration of plutonium). The equations used for the extraction equilibrium are those given in [12]. The scheme, the notation, and the parameters of the nominal regime of the variant of displacement re-extraction [5] calculated for a productivity of approximately 1 ton of uranium per day are shown in Fig. 1. The fundamental parameters of the process are the plutonium content in the uranium extract (Y^{ex}_{Pu}) and the uranium content in the plutonium re-extract (X^{ex}_U). The first quantity characterizes the degree to which the plutonium has been removed from the uranium, while the second characterizes the degree to which

* In [10] we also show the correctness of the models.

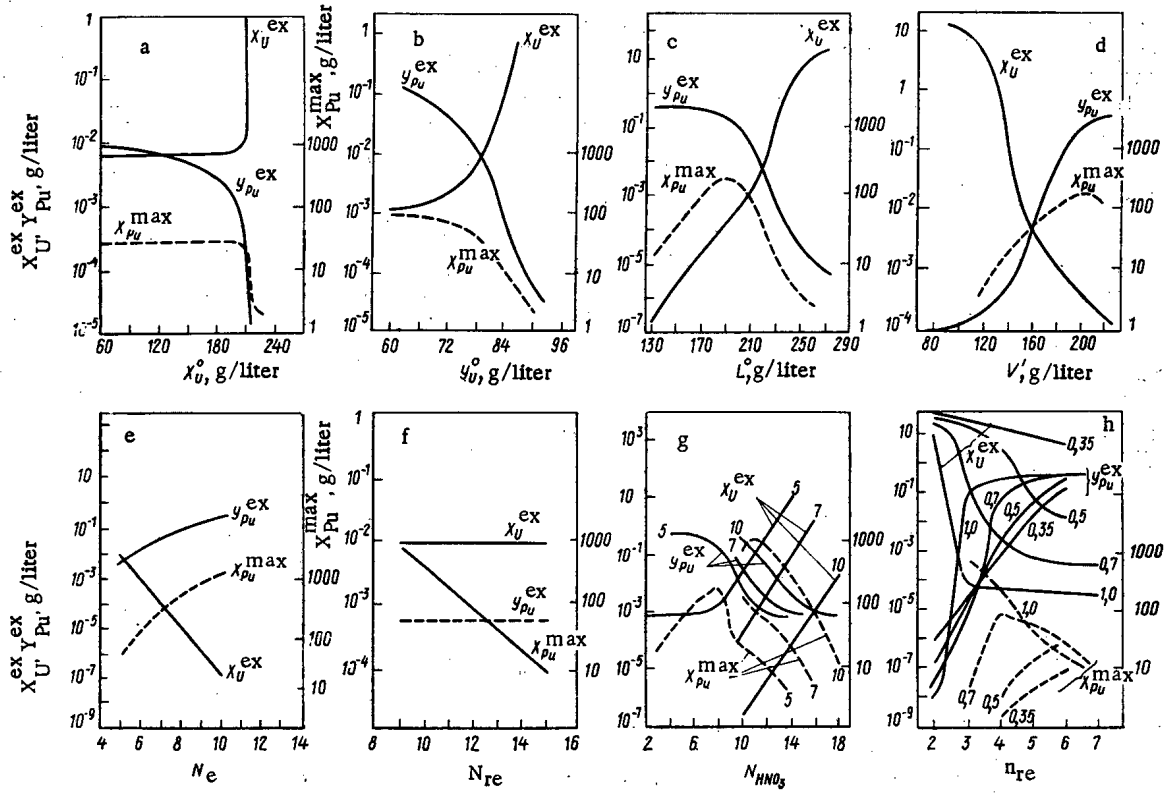

Fig. 3. Variation of the indicators for the separation of uranium and plutonium (————) and the accumulation of plutonium in the aqueous phase (— — —) as functions of the parameters of the regime of displacement re-extraction: a) concentrations of uranium in the re-extracting agent; b) concentrations of uranium in the initial organic solution; c) flow rates of re-extracting agent; d) flow rates of TBP for pre-extraction; e) numbers of stages in the pre-extraction section; f) numbers of stages in the re-extraction section; g) stages of introduction N_H of acid input (flow rates L') (the numbers next to the curves represent N_e); h) ratios of the flow rates $n_{re} = (V^0 + V')/L^0$ (the numbers next to the curves represent $n_e = V'/(L^0 + L')$).

the uranium has been removed from the plutonium. In order to obtain acceptable separation, we must have $Y_{Pu}^{ex} \leq 10^{-6}$ g/liter, but $X_U^{ex} \leq 10^{-2}$ g/liter $\simeq 4 \cdot 10^{-5}$ M.

The purpose of the calculations is to study the characteristics of the process for different kinds of variation of the regime parameters: The composition of the initial organic solution (Y_U^0 and $Y_{HNO_3}^0$), the uranium content in the re-extracting agent (X_U^0), the flow rates of the extracting agent (V') and the re-extracting agent (L^0), the ratio of the flow rates and the number of stages in the re-extraction section (n_{re}) and the pre-extraction section (N_e) for the uranium, and the point of introduction of the flow (L') of the input 10 M HNO_3 (N_{HNO_3}).

As the nominal regime we took the one described in patent [5], supplemented by the value $Y_{HNO_3}^0 = 0.153$ M;* in each regime only one parameter was different from its nominal value. The results of the calculations, in the form of curves showing the variation of Y_{Pu}^{ex} and X_U^{ex} and the plutonium accumulation value X_{Pu}^{ex} as functions of the indicated parameters, are given in Figs. 2 and 3.

The calculations showed that a sharp decrease in the plutonium content of the uranium fraction (the extract) is accompanied by a sharp deterioration of the indicator at the other end of the cascade (an increase of the uranium content in the plutonium re-extract), and conversely. Thus, when there is an increase in the concentration of uranium in the initial organic solution, or in the flow rate of re-extracting agent, or the concentration of uranium in the re-extracting agent, there will be a decrease in the plutonium content of the extract, but there will nevertheless be an increase in the concentration of uranium in the re-extract (see Fig. 3a, b, c). When there is an increase in the acidity of the initial organic solution, or in the flow rate of the extracting

* In patent [5] $Y_{HNO_3}^0$ was not indicated; it was selected by using the variation of Y_{Pu}^{ex} and X_U^{ex} as functions of $Y_{HNO_3}^0$ (see Fig. 2) as the value giving the maximum separation of uranium and plutonium.

agent for the pre-extraction, or in the ratio of flow rates in the organic and aqueous phases, the concentration of plutonium in the extract will increase, while the uranium content of the re-extract will decrease (see Figs. 2, 3d, h). All of the relationships give us a point of intersection of the Y_{Pu}^{ex} and X_U^{ex} curves (i.e., the maximum separation of uranium and plutonium) at a level of 10 mg/liter, which is an acceptable value for the uranium content in the re-extract but too high for the plutonium content in the extract. It is interesting that in the vicinity of the point of intersection all the curves have very sharp slopes, i.e., a small change in the parameters yields a very large change in Y_{Pu}^{ex} and X_U^{ex}. In some cases the derivatives $\partial Y_{Pu}^{ex}/\partial\alpha$ and $\partial X_U^{ex}/\partial\alpha$ (α is a regime parameter) even approach infinity. This shows the high sensitivity of the separation indicators to changes in the regime parameters.*

An increase in the acidity of the initial organic solution by 0.1 M (from 0.1 to 0.2) increases Y_{Pu}^{ex} from $7 \cdot 10^{-4}$ to $4 \cdot 10^{-2}$ g/liter, while X_U^{ex} decreases from $1.4 \cdot 10^{-1}$ to $1.7 \cdot 10^{-3}$ g/liter.

An increase in the uranium concentration in the initial organic solution (78 g/liter) by 5 g/liter increases X_U^{ex} by a factor of 16.5 (from 9.5 mg/liter to 0.16 g/liter) and decreases Y_{Pu}^{ex} by a factor of about 30 (from 7 to 0.24 mg/liter). A further increase of Y_U^0 by 7 g/liter (to 90 g/liter) increases X_U^{ex} by a further factor of 100 (to 16 g/liter) and decrease Y_{Pu}^{ex} by a factor of 7 (to $3.5 \cdot 10^{-5}$ g/liter).

An increase in the uranium content of the re-extracting agent from 60 to 208 g/liter leaves X_U^{ex} practically unchanged (10 mg/liter), while Y_{Pu}^{ex} decreases somewhat (from 10 to 1 mg/liter). If there is a further slight increase in the saturation of the extract with uranium (increasing X_U^0 to 214 g/liter), Y_{Pu}^{ex} drops very sharply (to $2 \cdot 10^{-5}$ g/liter), while X_U^{ex} increases (to 2.8 g/liter). Obviously, when the uranium saturation of the extract rises above 92%, the regime passes to the region beyond the boundary.

When the flow rate of the re-extracting agent increases by 20 liter/h (from 210 to 230 liter/h), there is an increase of X_U^{ex} by a factor of more than 30 (from 3 to 100 mg/liter) and a decrease in Y_{Pu}^{ex} by a factor of 100 (from 50 to 0.5 mg/liter).

When the flow rate of extracting agent for pre-extraction increases by 30 liter/h (from 140 to 170 liter/h), there is an increase in Y_{Pu}^{ex} by a factor of 60 (from 0.5 to 30 mg/liter) and a decrease in X_U^{ex} also by a factor of 60 (from 0.14 to 0.0024 g/liter).

An increase in the ratio of flow rates in the re-extracting section (the calculation was carried out for values from 2.0 to 7.0 at intervals of 1.0) increases Y_{Pu}^{ex} by several orders of magnitude and decreases X_U^{ex} somewhat less sharply. When n_e increases, there is a sharp increase in the slope of the curves $X_U^{ex} = f(n_{re})$ and $Y_{Pu}^{ex} = f(n_{re})$; the point of intersection of these curves is displaced toward the region of lower concentrations and at the same time in the direction of lower values of n_{re} (see Fig. 3h). The point of intersection, lying at a level of 1 mg/liter at $n_{re} \approx 2.6$ and $n_e = 1.0$, corresponds to considerable loads on the extractor: approximately 500 liters/h for the aqueous phase, approximately 1000 liters/h for the organic phase. The calculations for $n_e = 1.2$ showed that the point of intersection will lie at $n_{re} < 2.0$; in order to obtain such a regime, we must raise the load on the apparatus to about 1100 liters/h for the aqueous phase and about 2000 liters/h for the organic phase. At such a flow rate, instead of concentration, we have an unacceptable dilution of the extract and the re-extract. In addition, regimes which simultaneously yield relatively low values of X_U^{ex} and Y_{Pu}^{ex} ($\sim 10^{-4}$-10^{-5} g/liter) are unstable and are characterized by high internal accumulation of plutonium.†

The substantial accumulation of plutonium and the high sensitivity of the process to changes in the regime parameters in this region are due to the fact that when we simultaneously have good removal of uranium from the plutonium and of plutonium from the uranium, the re-extracting and extracting sections of the apparatus must have regimes which are fairly close to the limiting regime [9].

The addition of one stage to the re-extraction section in the nominal regime reduces the plutonium concentration in the extract by a factor of 2 without changing the uranium content in the re-extract or the plutonium accumulation value (see Fig. 3f).

*In the theory of automatic control, sensitivity means the vector $dX(t, \alpha)/d\alpha$, where $X = \|x_i\|$, the vector of the phase coordinates of the system [13]. The quantities $dx/d\alpha$ are its components and are called the sensitivity functions.

†If the distribution of plutonium is calculated as a microcomponent, the amount of plutonium accumulation is too high. Therefore the indicated value of X_{Pu}^{max} should be regarded as merely a guide, giving us only a qualitative picture. As the plutonium concentration increases in the accumulation process, the plutonium becomes a macrocomponent, capable of competing with the uranium for the "free" extracting agent; its accumulation must be reduced. This can be seen from Fig. 2, where the results of the calculation for macroplutonium are shown by a dot—dash curve, but the picture obtained from the calculation for microquantities of plutonium is qualitatively correct.

Thus, if the value of X_U^{ex} = 10 mg/liter is considered acceptable, then the reduction of Y_{Pu}^{ex} (from 10 to 1 mg/liter) requires 12 stages in the re-extraction section. In order to get $Y_{Pu}^{ex} = 10^{-6}$ g/liter, we need a 27-stage extractor (22 stages in the re-extraction section). When the uranium pre-extraction section is enlarged, we reduce the uranium content of the re-extract by a factor of 8 per stage, but this also brings an increase in the loss of plutonium with the extract (by a factor of 2 per stage) and sharply increases the plutonium accumulation (Fig. 3e).

Calculations for an apparatus with different numbers of stages in the pre-extraction section (5, 7, and 10) showed that when the point of introduction of the input acid is displaced in the direction of the re-extract exit, increasing the uranium content in the re-extract by a factor of about 3, we reduce the loss of plutonium with the extract by a factor of about 2 but not below a value of $Y_{Pu}^{ex} \approx 1$ mg/liter (see Fig. 3g).

The neptunium concentration in the uranium extract depends chiefly on the flow rate of the re-extracting agent. When L^0 is decreased, the neptunium content in the exiting organic phase increases, and when L^0 = 120 liters/h, the neptunium content reaches approximately 10 mg/liter (which corresponds to a 14% loss of neptunium with the extract). When the other parameters were varied, the neptunium concentration of the extract did not exceed 10^{-10} g/liter.

Thus, simulation has shown that displacement re-extraction can be used for separating U, Pu, and Np, but this method is highly sensitive to small changes in the regime parameters and is characterized by very high internal accumulation of plutonium. It will probably not be adopted as a complete substitute for reductive re-extraction; it should be regarded as a supplement to chemical methods which will make it possible to decrease the amount of reducing agent used.

The indicators for the separation of uranium and plutonium which are mentioned in [5] were not obtained in any of our calculated regimes. This disagreement cannot be the result of any inaccuracy in our calculations arising out of the fact that the plutonium was regarded as a microcomponent. If we take account of the characteristic concentration of plutonium, its concentration in the uranium fraction is increased, and the separation of U and Pu becomes worse (see Fig. 2). The disagreement between the calculated data and the patent data is probably due to the fact that the patent description omits some important technological operations (for example, an additional plutonium branch).

LITERATURE CITED

1. V. B. Shevchenko (editor), Reprocessing of Fuel from Power Reactors [Russian translation], Atomizdat, Moscow (1972).
2. V. B. Shevchenko (editor), Chemical Technology of Irradiated Nuclear Fuel [in Russian], Atomizdat, Moscow (1971).
3. V. B. Shevchenko et al., Fourth Geneva Conference, Report No. 49/P-435 [in Russian] (1971).
4. J. Ortega and A. Rusheed, Anales de Química, 69, No. 1, 117 (1973).
5. US Patent No. 3,714,324, January 30, 1973; FRG Patent No. 1,929,512, March 5, 1970.
6. G. Best, H. McKay, and P. Woodgate, J. Inorg. and Nucl. Chem, 4, 315 (1957).
7. A. M. Rozen, At. Énerg., 2, No. 5, 445 (1957).
8. A. M. Rozen, At. Énerg., 7, No. 3, 277 (1959).
9. A. M. Rozen et al., Third Geneva Conference, Report No. 346 [in Russian] (1969).
10. A. M. Rozen et al., At. Énerg., 37, No. 3, 187 (1974).
11. A. M. Rozen and M. Ya. Zel'venskii, Teor. Osnovy Khim. Tekhnol., 10, No. 5 (1976).
12. A. M. Rozen and M. Ya. Zel'venskii, Radiokhimiya, 18, No. 5 (1976).
13. E. N. Rozenvasser and R. M. Yusupov, Sensitivity of Automatic Control Systems [in Russian], Énergiya, Moscow (1969).

MATHEMATICAL SIMULATION OF PROCESSES IN THE EXTRACTIVE REPROCESSING OF NUCLEAR FUEL

5. SEPARATION OF URANIUM AND PLUTONIUM BY THE METHOD OF RE-EXTRACTION WITH A WEAK ACID

A. M. Rozen and M. Ya. Zel'venskii

UDC 621.039:59.001.57

While in reductive re-extraction the separation of uranium and plutonium is achieved by bringing the latter into a weakly extractable form [1], and in displacement re-extraction it is achieved by means of high uranium saturation of the organic phase [2, 3], in the process of separation re-extraction with weak nitric acid we make use of the fact that the coefficient of separation of uranium and plutonium depends on the concentration of nitrate ions:

$$\beta_{U/Pu} = \alpha_{U(VI)}/\alpha_{Pu(IV)} = \tilde{K}_{U(VI)}/\tilde{K}_{Pu(IV)}\,[NO_3^-]^2.$$

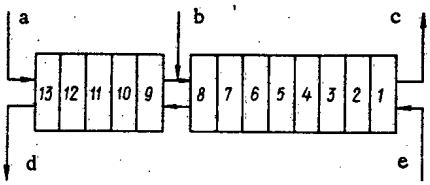

Fig. 1

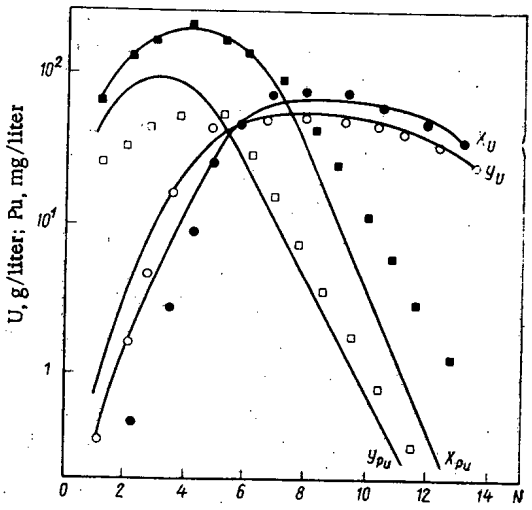

Fig. 2

Fig. 1. Scheme and parameters of the nominal regime of the separation re-extraction of uranium and plutonium with weak HNO_3 [4]; a) $V' = 65$ liters/h, 20% TBP; b) $V^0 = 100$ liters/h, $Y_U^0 = 50$ g/liter, $Y_{Pu}^0 = 30$ mg/liter, $Y_{HNO_3}^0 = 0.14$ M; c) $V = V^0 + V' = 165$ liters/h, $Y_U^{ex} = 31$ g/liter, $Y_{Pu}^{ex} = 0.3$ mg/liter, $Y_{HNO_3} = 0.04$ M; d) $L = 50$ liters/h, $X_U^{ex} = 0.1$ g/liter, $X_{Pu}^{ex} = 61$ mg/liter, $X_{HNO_3} = 0.56$ M; e) $L = 50$ liter/h, $X_{HNO_3}^0 = 0.3$ M; 1-13 are the numbers of the stages.

Fig. 2. Comparison of the results of mathematical simulation of separation re-extraction (——) with the experimental data of [4] on the distribution of uranium and plutonium in the two phases for each phase of the extractor: ●, ■) U, Pu in the aqueous phase; ○, □) U, Pu in the organic phase.

Translated from Atomnaya Énergiya, Vol. 41, No. 2, pp. 95-98, August, 1976. Original article submitted August 6, 1975.

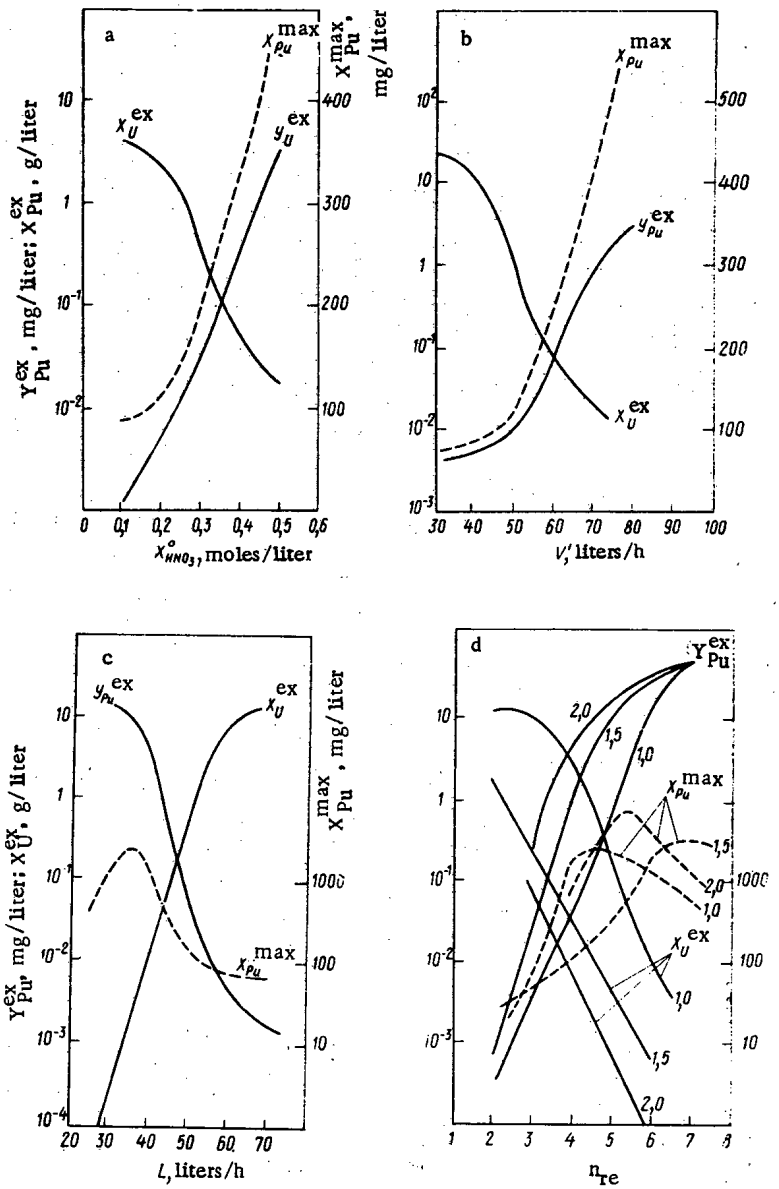

Fig. 3. Variation of the separation indicators (——) and of the concentration of plutonium in the uranium extract and uranium in the plutonium re-extract and the accumulation of plutonium in the aqueous phase (— — — —) as functions of the parameters of the separation re-extraction regime: a) acidity values of the re-extracting agent; b) flow rates of TBP for the pre-extraction of uranium; c) flow rates of re-extracting agent; d) ratio of flow rates $n_{re} = (V^0 + V')/L$ (the figures next to the curves represent $n_e = V'/L$).

Since the constants of extraction of uranium and plutonium differ greatly ($\tilde{K}_{U(VI)} \gg \tilde{K}_{PU(IV)}$), for low acidities ($[NO_3^-] \sim X_{HNO_3}$) the coefficient of separation β will be relatively high. The scheme proposed in [4] is based on the use of 0.3 M HNO_3 as the re-extracting agent (Fig. 1).

In the present article we used the method of mathematical simulation for investigating separation re-extraction; we compare the calculation results with the experimental results, and we compare the two processes of separating uranium and plutonium without using reducing agents.

To do this, we performed calculations for the scheme of [4] and found the characteristics of the process, Y_{Pu}^{ex} and X_U^{ex}, which define, respectively, the degree of removal of plutonium from the uranium extract and the degree of removal of uranium from the plutonium re-extract.

We varied the following parameters of the process: the acidity of the re-extracting agent ($X^0_{HNO_3}$), the flow rates of the extracting agent (V') and the re-extracting agent (L), the ratio of the flow rates ($n_{re} = (V^0 + V')/L$ and $n_e = V'/L$), and the number of stages in each section of the apparatus (N_{re} and N_e). As the nominal regime we took the regime of [4] (its parameters are shown in Fig. 1); for this regime we compare the experimental distribution [4] and the calculated distribution of the uranium and plutonium concentration in the aqueous and organic phases for each stage of the apparatus. As can be seen from Fig. 2, the agreement is good.

In the calculations only one parameter in each regime was different from its nominal value.

The results of the calculations, in the form of curves showing the variation of Y^{ex}_{Pu} and X^{ex}_U as functions of the indicated parameters, are given in Fig. 3, from which it can be seen that, as in the process of displacement re-extraction [3], variation of the acidity of the re-extracting agent and of the flow-rate values produce opposite effects on the indicators of the separation of uranium and plutonium (as the plutonium content in the uranium extract decreases, there is an increase in the uranium content of the plutonium re-extract).

It should be noted that the regime of [4] is sufficiently close to the optimal regime* for an apparatus with eight stages in the re-extraction section and five in the uranium pre-extraction section.

The calculations also showed that the addition of one stage to the uranium pre-extraction section decreases X^{ex}_U by a factor of 3.18 (Y^{ex}_{Pu} remains practically unchanged); the addition of one stage to the re-extraction section reduces Y^{ex}_{Pu} by a factor of 2.68 (without changing X^{ex}_U).

Thus, acceptable separation of uranium and plutonium ($Y^{ex}_{Pu} = 10^{-6}$ g/liter, $X^{ex}_U = 10$ mg/liter) would have been feasible in an apparatus with 16 re-extraction stages and eight extraction stages in the regime proposed in [4].

The maximum accumulation of plutonium in the aqueous phase in the nominal regime amounts to 190 mg/liter (a factor of 6); an increase in the re-extraction section does not change the accumulation; for $N_e = 8$ we find that $X^{max}_{Pu} = 325$ mg/liter (a factor of 11).

The accumulation of plutonium in this process is much less than in the displacement re-extraction process; the highest accumulation value obtained for calculations of separation re-extraction is 80 times the original plutonium concentration (30 mg/liter), while in the displacement re-extraction process even in the nominal regime the accumulation is 70 times the initial value [3]. The relatively low internal accumulation of plutonium is an unquestionable advantage of the process.

The values for the accumulation of microquantities of plutonium are obtained more accurately in the calculation of separation re-extraction than in the calculation of displacement re-extraction, when the plutonium, accumulating in the aqueous phase up to tens of grams, becomes a macrocomponent capable of competing with uranium for the extracting agent. Consequently, weak-acid re-extraction can be used for separating uranium and plutonium. The sensitivity of this process to variation of the parameters is less than in the displacement re-extraction process, and the internal accumulation of plutonium, as indicated above, is considerably lower. In order to obtain the specified separation (10 mg of uranium per liter in the plutonium re-extract and 10 μg of plutonium per kg of uranium) in the nominal regime of operation of [4] we require an apparatus with 24 stages.

Thus, weak-acid re-extraction has advantages over displacement re-extraction. However, we also cannot afford to disregard reductive re-extraction; although it involves a loss of reagents, it does require a far smaller number of stages [1], i.e., has an advantage in the apparatus layout.

A properly justified choice of one or another of the separation schemes (or a combination of several elements from different schemes) requires engineering — economic calculations that take account of the properties of the fuel being reprocessed and the possibilities of automatic control.

LITERATURE CITED

1. V. B. Shevchenko et al., Fourth Geneva Conference, Report No. 435 [in Russian] (1971).
2. US Patent No. 3,714,324, January 30, 1973.
3. A. M. Rozen and M. Ya. Zel'venskii, At. Énerg., 41, No. 2, 91 (1976).
4. J. Ortega and A. Rusheed, Anales de Química, 69, No. 1, 117 (1973).

* This regime corresponds to the point of intersection of the characteristics for Y^{ex}_{Pu} and X^{ex}_U, when high separation is achieved.

LIQUID – VAPOR EQUILIBRIUM IN SYSTEMS WITH DILUTE SOLUTIONS OF METAL FLUORIDES IN URANIUM HEXAFLUORIDE

V. N. Prusakov, V. K. Ezhov, and E. A. Efremov

UDC 541.12.035.4

Investigations of the distribution of a substance between the vapor and liquid phases of a solution have shown that at great dilutions the solute obeys Henry's law [1, 2]. However, Devyatyk and Vlasov [3], and Stepanov et al. [4], postulated the existence of a nonequilibrium state of a dilute solution; they proposed methods for calculating the thermodynamic activity coefficients.

We have therefore made an experimental investigation of liquid – vapor equilibrium in systems with dilute solutions of tellurium, molybdenum, and tungsten hexafluorides and of vanadium, antimony, and tantalum pentafluorides in uranium hexafluoride. The results were compared with the theoretical data.

The uranium hexafluoride used in the experiments was purified by fractional distillation. The purity of the end product was monitored by mass-spectrometric analysis. Radioactive fluorides $^{123+125}TeF_6$, $^{99}MoF_6$, $^{124}SbF_5$, $^{185}WF_6$, and $^{182}TaF_5$ were obtained by fluorination of the corresponding very pure metals, preactivated with thermal neutrons. Vanadium pentafluoride, labeled with the radioactive isotope ^{48}V, was obtained by fluorination of vanadium metal, obtained after evaporation of a radioactive nitric acid solution of vanadium followed by roasting and reduction of the precipitate with hydrogen.

Before use the fluoride was freed from hydrogen fluoride by sorption of the latter on sodium fluoride granules at –195°C.

Fragments of the radioactive metal (0.01-0.02 g) were fluorinated directly in the still in a boat (Fig. 1). The entire apparatus was prepassivated with fluorine and thermostated at 75°C. The boat was heated to 400°C. After the weighed portion of the metal was fluorinated, the still was cooled with liquid nitrogen, and the uranium fluoride from the capsule was condensed in it. The initial composition of the mixture was calculated from the change in weight of the metal and the capsule.

The fluoride solution obtained was subjected to differential distillation at a pressure of 1520 ± 10 mm and 74.0 ± 0.4°C. For this purpose the magnetic stirrer of the still was switched on. The solution vapor passed

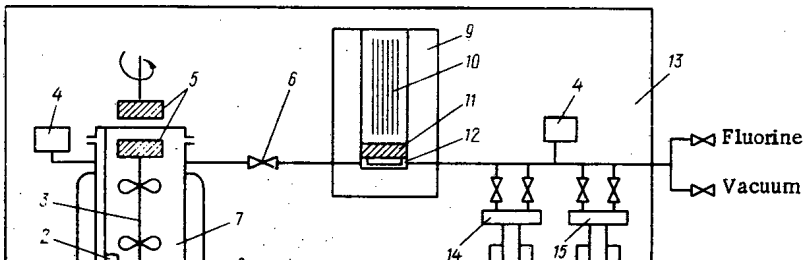

Fig. 1. Schematic diagram of apparatus: 1) jacket; 2) boat; 3) stirrer; 4) manometer; 5) magnet; 6) throttle valve; 7) still; 8) electric furnace; 9) lead housing; 10) FEU-13; 11) crystal; 12) flow cell; 13) airthermostat; 14) capsule; 15) trap.

Translated from Atomnaya Énergiya, Vol. 41, No. 2, pp. 98-101, August, 1976. Original article submitted August 16, 1975.

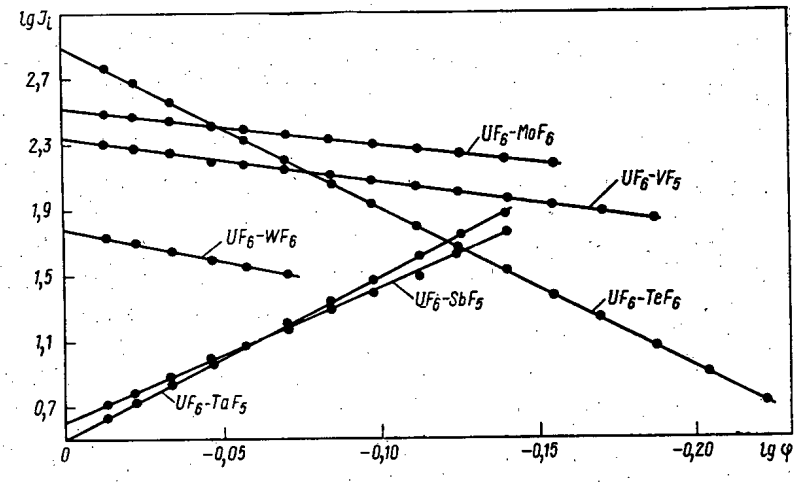

Fig. 2. Logarithmic graph of pulse count rate vs degree of distillation for the systems $UF_6 - MF_6$ and $UF_6 - MF_5$.

through a flow cell and throttle valve to a trap at 5°C. The radioactive vapor was registered by a photoelectric multiplier with continuous recording of the signal on a KSP-4 pen recorder. The solution was thermostated by means of a water thermostat. The precalibrated throttle valve ensured a constant distillation rate at a constant pressure drop.

The maximum degree of compression of the solution in the cell was 30. After distillation the solution was redistilled into the still and the experiment was repeated.

A preliminary investigation was made of the equilibrium conditions for distillation of a solution of TeF_6 in UF_6. This showed that the equilibrium of the process was retained at a stirrer speed of 100-200 rpm and a vapor phase offtake rate of 1-3 g/(cm^2 · min).

The experimental data on distillation of binary solutions were processed by means of the equation

$$\lg I_i = (\alpha - 1) \lg \frac{G_0 - G_i}{G_0} + \lg I_0,$$

where I_0 and I_i are, respectively, the counting rates of pulses from the radioactive label in the vapor being distilled at the beginning of the experiment and during it, G_0 is the initial amount of the solution (in grams), G_i is the amount of distillate obtained (in grams), and α is the separation factor.

The equation is a modification of Rayleigh's integral equation for simple distillation [5] applied to the radiometric method of monitoring the change in the content of a component in vapor being distilled (Fig. 2).

Table 1 lists the values of the separation factors obtained. It also gives the activity coefficients of the solute γ_2, calculated from the equations

$$\alpha = \frac{P_2^0}{P_1^0} \gamma_2 \quad \text{for a highly volatile impurity}$$

and

TABLE 1. Separation Factors of UF_6-Based Binary Systems at 74°C

Dilute solution	Separation factor		Activity coefficient of solute	Investigated concentration range, wt.%
	experimental	ideal		
TeF_6 in UF_6	10,66±0,05	11,73	0,91	$1 \cdot 10^{-2}$—$6 \cdot 10^{-5}$
WF_6 in UF_6	1,39±0,01	2,86	0,49	$2 \cdot 10^{-2}$—$1 \cdot 10^{-2}$
MoF_6 in UF_6	1,22±0,01	1,73	0,70	$1{,}8 \cdot 10^{-1}$—$9 \cdot 10^{-2}$
VF_5 in UF_6	1,28±0,01	1,86	0,69	$7 \cdot 10^{-3}$—$1 \cdot 10^{-3}$
SbF_5 in UF_6	6,53±0,05	26,5	4,06	$1{,}5 \cdot 10^{-2}$—$8 \cdot 10^{-4}$
TaF_5 in UF_6	217±1	661	3,04	$3{,}3 \cdot 10^{-2}$—$9 \cdot 10^{-4}$

TABLE 2. Separation Factors of Metal Fluorides in the Multicomponent System $UF_6 - MoF_6 - SbF_5 - TaF_5$ at 74°C

System	Solute	Separation factor α and α^*	Concentration range investigated, wt.%
$UF_6 - MoF_6$	MoF_6	1,25	10^{-1}—10^{-2}
$UF_6 - SbF_5$	SbF_5	6,40	10^{-2}—10^{-4}
$UF_6 - TaF_5$	TaF_5	215	10^{-2}—10^{-4}

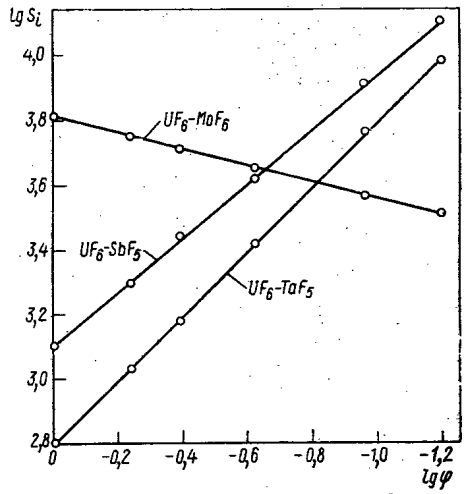

Fig. 3. Logarithmic graph of area under γ spectrum vs degree of distillation.

$$\alpha^* = \frac{P_1^0}{P_2^0}\frac{1}{\gamma_2} \quad \text{for a high-boiling impurity,}$$

where P_1^0 and P_2^0 are, respectively, the saturated vapor pressures of the solvent and solute.

When a multicomponent solution of $MoF_6 - SbF_5 - TaF_5$ in UF_6 was distilled, the signal was sent from the FÉU-13 to a AI-256 pulse-analyzer to register the γ spectra of the vapor being distilled. It is known [6] that in the γ-spectral method of radioisotope analysis the overall pulse count rate through all the analyzer channels from one isotope ΣI_i is proportional to the overall area under all the energy peaks S_i; the experimental data (Fig. 3) were processed by means of the equation

$$\lg S_i = (\alpha - 1)\lg\frac{G_0 - G_i}{G_0} + \lg S_0.$$

Table 2 lists the values of the separation factors obtained.

A linear relation is observed between the logarithm of the counting rate and the logarithm of the degree of distillation (Fig. 2), i.e., the separation factor remains constant at different solution concentrations.

Thus Henry's law holds for these dilute solutions throughout the concentration range investigated.

Using the Hildebrand — van Laar [7], Hildebrand — Scatchard [7], Stepanov — Devyatykh [4], and Vlasov — Devyatykh [3] methods we made a theoretical estimate of the activity coefficients of TeF_6, WF_6, MoF_6, VF_5, SbF_5, and TaF_5 in binary dilute solutions of uranium hexafluoride; the results are given in Table 3. In view of the fact that, unlike the metal hexafluorides, vanadium, antimony, and tantalum pentafluorides may exist in polymerized form [8, 9], their activity coefficients were calculated on the assumption that the degree of association is 1 or 4.

TABLE 3. Activity Coefficients of Fluorides of Certain Metals in Dilute Solutions of Uranium Hexafluoride at 74°C

Solute	Degree of association of solute	Activity coefficient calculated in						Experimental activity coefficient of solute
		[7]	[7]	[4] (cell–solute)	[4] (cell–solvent)	[3] with and without allowance for mutual influence of solvent and solute)		
TeF_6	1	1,408	1,021	1,441	0,979	3,441	0,121	0,91
WF_6	1	1,016	1,013	0,986	0,811	1,337	0,231	0,49
MoF_6	1	1,000	1,015	0,986	0,910	1,448	0,105	0,70
VF_5	1	1,821	7,193	1,097	0,703	15,13	9367	0,69
	4	1,821	291,70	0,114	0,293	15,13	9367	
SbF_5	1	1,868	4,388	1,514	1,271	11,89	11133	4,06
	4	1,868	9,931	0,046	0,139	11,89	11133	
TaF_5	1	3,976	17,508	3,129	3,516	2195	$4,47 \cdot 10^8$	3,04
	4	3,976	2,517	0,095	0,269	2195	$4,47 \cdot 10^8$	

TABLE 4. Activity Coefficients of Components of Dilute Solutions at 74°C

Dilute solution	γ_{calc}	$\gamma_{expl.}$	Discrepancy, %
MoF_6 in UF_6	0,740	0,70	5,7
WF_6 in UF_6	0,494	0,49	0,8
VF_5 in UF_6	0,757	0,69	8,8
SbF_5 in UF_6	5,740	4,06	41,4
TaF_5 in UF_6	3,120	3,04	2,6

From Table 3 it follows that it is only in the case of a solution of vanadium pentafluoride in uranium hexafluoride that the experimental activity coefficient [4] is close to its theoretical value (degree of association 1).

In the other cases the theoretical activity coefficients do not coincide with the experimental values. Note that the behavior of dilute solutions of metal pentafluorides in uranium hexafluoride is best represented by assuming that they exist as monomeric molecules. Dissociation of the compounds at high dilution is not unexpected, but further experimental data are required to confirm that in dilute solutions the predominant form of existence of metal pentafluoride molecules is the monomer.

A dilute solution of antimony pentafluoride in uranium hexafluoride is best described (as in the case of medium concentrations) by the Hildebrand—Scatchard [10] theory of regular solutions.

The coincidence of the experimental separation factors of binary dilute systems UF_6-MoF_6, UF_6-SbF_5, and UF_6-TaF_5 with their values in the multicomponent system $UF_6-MoF_6-SbF_5-TaF_5$ is apparently due to the absence of a mutual influence of the impurity molecules of different species (cf. Tables 1 and 2). It is known that compounds are not formed in binary systems of metal fluorides [10, 12-14].

The experimental data on liquid—vapor equilibrium in systems with binary mixtures of the hexafluorides of uranium, tungsten [12], and molybdenum [14] and pentafluorides of vanadium [15], tantalum [10], and antimony [10] for the region of medium concentrations were approximated in the form of a polynomial of degree n

$$\lg \gamma_i = a_0 + a_1 x + a_2 x^2 + \ldots + a_n x^n,$$

where x is the concentration of the solute in mole fractions.

The use of this equation to determine the activity coefficients of the components of dilute solutions from the data for medium concentrations enabled us to obtain the activity coefficients of the solute (Table 4).

For the systems UF_6-WF_6, UF_6-MoF_6, UF_6-UF_5, and UF_6-TaF_5 the theoretical activity coefficient of the solute is close to the experimental value.

LITERATURE CITED

1. Ya. D. Zel'venskii et al., Teor. Osnovy Khim. Tekh., 1, No. 2, 229 (1967).
2. Ya. D. Zel'venskii, A. A. Efremov, and V. A. Shalygin, Izotopy v SSSR, No. 5, 25 (1966).
3. G. G. Devyatykh and S. M. Vlasov, Zh. Fiz. Khim., 39, 1171 (1965).
4. V. M. Stepanov et al., Zh. Fiz. Khim., 44, 445 (1970).
5. Ya. D. Zel'venskii, J. Feitek, and V. A. Shalygin, Zh. Fiz. Khim., 35, 2602 (1961).
6. V. O. Vyazemskii et al., The Scintillation Method in Radiometry [in Russian], Gosatomizdat, Moscow (1961), p. 299.
7. E. A. Moelwyn-Hughes, Physical Chemistry, Pergamon, Elmsford (1969).
8. C. Hoffman et al., J. Phys. Chem., 62, 364 (1958).
9. E. Lesley, J. Beattle, and P. Jones, J. Chem. Soc., No. 2, 210 (1972).
10. V. K. Ezhov, Zh. Neorgan. Khim., 17, No. 7, 2043 (1972).
11. V. B. Kagan, Azeotropy and Extractive Rectification [in Russian], Goskhimizdat, Leningrad (1961).
12. V. N. Prusakov and V. K. Ezhov, At. Énerg., 25, No. 1, 64 (1968).
13. V. N. Prusakov and V. K. Ezhov, At. Énerg., 28, No. 6, 496 (1970).
14. V. N. Prusakov et al., in: Proc. Symp. SEA (Soviet Economic Aid) "Investigations in the field of irradiated fuel processing," Karlovy Vary, Feb. 26-March 2, 1968 [in Russian], p. 331.
15. R. Shrewsbarry and B. Musulin, Science, 145, 1452 (1964).

DISTRIBUTION OF THE LOSSES DURING THE ACCUMULATION OF ISOTOPES OF THE TRANSURANIUM ELEMENTS

Yu. P. Kormushkin, A. V. Klinov, and Yu. G. Toporov

UDC 621.039.8.002:621.039.554

The authors of [1] investigated for the first time the selection of the costwise optimal accumulation conditions of isotopes of transuranium elements used in radioisotope power generation. We derived in our work an analytic expression for the cost of the unit mass of an isotope to be accumulated; we assumed that the cost of a single absorbed neutron is constant in the simplest accumulation chain with a single end-product.

The simultaneous formation of several products is characteristic of the general isotope-accumulation process. Nevertheless, the selection of economically advantageous accumulation conditions requires knowledge of the production cost of each isotope to be accumulated.

In the reactor irradiation stage, one must consider two loss components whose combination, referred to a single nucleus of the new isotope produced, decides the cost of the isotope. The first component is related to the cost of the raw material consumed and, more specifically, results from the nuclei of the forerunner nuclide which are lost in the accumulation process. The second component results from the losses during the irradiation, i.e., from the production of excess neutrons in the reactor, whose absorption by the forerunner nuclei leads to the formation of the subsequent isotope in the accumulation chain.

In a specialized isotope-producing reactor, the latter component depends upon the total reactor losses. In a multipurpose reactor, the component depends upon the fraction of general reactor losses in a program for isotope accumulation. The determination of this fraction is an independent problem; methods for solving this problem can be found in [2, 3]. When this fraction is known and the losses for winning the initial material are known, the proposed method allows the calculation of the cost of a nucleus of each isotope of any accumulation chain in the stage of the reactor irradiation.

It is generally accepted that the accumulation of isotopes in an open chain without branching can be described by a system of nonlinear differential equations:

$$\left.\begin{aligned}
\frac{dN_0 t}{dt} &= -[b_0(t)+\lambda_0]\,N_0(t);\\
\frac{dN_1(t)}{dt} &= -[b_1(t)+\lambda_1]\,N_1(t)+a_0(t)\,N_0(t);\\
\frac{dN_i(t)}{dt} &= -[b_i(t)+\lambda_i]\,N_i(t)\\
&\quad +a_{i-1}(t)\,N_{i-1}(t),
\end{aligned}\right\} \tag{1}$$

where $N_i(t)$ denotes the number of nuclei of the i-th isotope of the accumulation chain at the time t; $b_i(t)+\lambda_i$ denotes the rate at which nuclei of the i-th isotope disappear via all possible channels; $a_i(t)$ denotes the rate at which the (i + 1)-th isotope is formed; and λ_i denotes the decay constant of the i-th isotope. We have

$$b_i(t)=\int_0^\infty \sigma_a^i(E)\,\Phi(E,\,t)\,dE;$$

$$a_i(t)=\int_0^\infty \sigma_\gamma^i(E)\,\Phi(E,\,t)\,dE,$$

provided that the nuclei of the (i + 1)-th isotope are formed by the capture of neutrons by the forerunner nuclei; $a_i=\lambda_i$, provided that the nuclei of the (i + 1)-th isotope are formed in the decay of forerunner nuclei; $\sigma_a^i(E)$

Translated from Atomnaya Énergiya, Vol. 41, No. 2, pp. 102-104, August, 1976. Original article submitted June 17, 1975; revision submitted December 18, 1975.

denotes the cross section of the absorption of neutrons with the energy E by nuclei of the i-th isotope; and $\sigma_\gamma^i(E)$ denotes the cross section of the radiative capture of neutrons with the energy E by nuclei of the i-th isotope. The condition $N_i(t)|_{t=0} = N_i(0)$ holds.

The equations of system (1) are the equations of the balance and relate the rate of change in the number of nuclei of each isotope of the chain to both the rate at which the nuclei are formed from the preceding isotopes and the rate at which these nuclei disappear over all possible channels.

In analogy to the equations of system (1) one can state differential equations which describe the redistribution of the losses among the isotopes of the accumulation chain during the irradiation process. The approach to the description of the process establishes a relation between the redistribution of the losses and the redistribution of the isotope nuclei and reflects the physics of the phenomenon, because in the case of neutron capture, both a transfer of the losses associated with the cost of the forerunner nucleus and an increase in the cost of the nuclei owing to irradiation losses occur in addition to the transition of the nucleus of one isotope of the chain into a nucleus of the next isotope. In this case the integration of the system of differential equations describing the balance of the losses and the integration of system (1) allow the calculation of the cost of the isotope nuclei of the chain and make it possible to bring into account the physical and thermal characteristics of the irradiating apparatus, the charge of the initial material, etc.

The system of differential equations of the balance of losses, which corresponds to the equation system (1), can be written in the following form*:

$$\left.\begin{aligned}
&\frac{du_0(t)}{dt} = -[b_0(t)+\lambda_0]\,u_0(t);\\
&\frac{du_1(t)}{dt} = -[b_1(t)+\lambda_1]\,u_1(t)\\
&+[b_0(t)+\lambda_0]\,u_0(t)+b_0(t)\,N_0(t)\,v(t);\\
&\frac{du_i(t)}{dt} = -[b_i(t)+\lambda_i]\,u_i(t)+\\
&+[b_{i-1}(t)+\lambda_{i-1}]\,u_{i-1}(t)\\
&+b_{i-1}(t)\,N_{i-1}(t)\,v(t),
\end{aligned}\right\} \qquad (2)$$

where $u_i(t)|_{t-0} = u_i(0)$. In addition to the previously introduced notation, the following notation is used: $u_i(t)$ denotes the total cost of all nuclei of the i-th isotope; $u_i(t) = C_i(t)N_i(t)$ (where $C_i(t)$ denotes the cost of a nucleus of the i-th isotope at the time t).

$$v(t) = \frac{C_{\text{irr}}(t)}{\sum_{i=0}^{n} b_i(t)\,N_i(t)}, \qquad (3)$$

where $C_{irr}(t)$ denotes the target irradiation losses per unit time; and n denotes the number of isotopes of the accumulation chain.

Since the quantity $\sum_{i=0}^{n} b_i(t)N_i(t)$ represents the total number of neutrons absorbed per unit time by the nuclei of the isotopes of the accumulation chain, the function v(t) is equal to the cost of an absorbed neutron at the time t. Furthermore, obviously $\sum_{i=0}^{n} u_i(0)$ denotes the losses incurred in acquiring the initial material.†

In analogy to the equations of system (1), the left side of the i-th equation of system (2) indicates the rate at which the cost of all nuclei of the i-th isotope changes. One can in this way easily determine the meaning of each term of the right sides of equation system (2). The first term of the right side of the i-th equation represents the rate at which the total cost resulting from the disappearance of the nuclei of the i-th isotope decreases. The second term denotes the rate at which the cost is increased by the forerunner nuclei. The rate of nuclei formation in equation system (1) is characterized either by the decay rate of the forerunner nuclei when radioactive decay is the isotope-producing process, or by the rate of neutron capture by the forerunner in the case of radiative capture. In differential-equation system (2), the rate at which the cost increases is characterized (in contrast to the rate at which nuclei arrive) by the rate at which the nuclei of the forerunner

*Naturally, in each real case the form of equation system (1) and of the corresponding system of the balance of the losses depends upon the form of the accumulation chain.

†Usually the material purchased is a mixture of isotopes. In this case one must know the "history" of winning the initial material for obtaining the initial conditions of equation system (2), i.e., for separating the losses incurred in the acquisition of the initial isotopes.

disappear via all possible channels, because the total cost of all expended forerunner nuclei must be ascribed to the nuclei which are formed of each isotope of the chain; one must include the cost of the fission nuclei and the nuclei which decayed outside the chain under consideration.

The third term on the right sides of equation system (2) has no analog in equation system (1) and denotes the rate at which the cost increases owing to irradiation losses. Thus, when the isotope nuclei are formed by the decay of a forerunner, this term of the equation must disappear, because in this case losses related to the absorption of neutrons do not arise. When the isotope nuclei are formed by radiative capture of neutrons by the forerunner, this term of the equation is the product of the rate at which neutrons are absorbed by the forerunner nuclei times the cost of a single absorbed neutron.

We can conclude from Eq. (3) that the neutrons absorbed by fission fragments in the materials of the building and the leakage neutrons are assumed to be neutrons lost for the accumulation process; the cost of these neutrons is distributed among the isotopes of the chain in proportion to the absorption rates (equation system (2)). Thus, the lower the ratio of the number of neutrons absorbed by the isotopes of the chain to the total number of neutrons, the higher the cost of the resulting nuclei. The missing third term in the first equation of system (2) corresponds to the assumption that the cost of the nuclei of the first initial isotope in the open chain is independent of the time of irradiation.

Obviously, at any time the total cost of all accumulated nuclei (including the cost of the nuclei converted after the last isotope of the chain under consideration) must be equal to the sum of the losses incurred in the acquisition of the initial material and the losses incurred in target irradiation. Let us show that the system of differential equations (2) satisfies this condition. To do this, we switch from system (2) to the following system of integral equations:

$$\left.\begin{aligned}
u_0(t) &= -\int_0^t [b_0(t')+\lambda_0]\,u_0(t')\,dt' + u_0^0;\\
u_1(t) &= -\int_0^t [b_1(t')+\lambda_1]\,u_1(t')\,dt'\\
&\quad +\int_0^t [b_0(t')+\lambda_0]\,u_0(t')\,dt'\\
&\quad +\int_0^t b_0(t')\,N_0(t')\,v(t')\,dt' + u_1^0;\\
u_i(t) &= -\int_0^t [b_i(t')+\lambda_i]\,u_i(t')\,dt'\\
&\quad +\int_0^t [b_{i-1}(t')+\lambda_{i-1}]\,u_{i-1}(t')\,dt'\\
&\quad +\int_0^t b_{i-1}(t')\,N_{i-1}(t')\,v(t')\,dt' + u_i^0.
\end{aligned}\right\} \qquad (4)$$

We obtain the formula

$$\sum_{i=0}^{n} u_i(t) + \int_0^t [b_n(t')+\lambda_n]\,u_n(t')\,dt' = \sum_{i=0}^{n} u_i^0 + \int_0^t C_{\text{irr}}(t')\,dt', \qquad (5)$$

by summation over the equations of system (4), where $\sum_{i=0}^{n} u_i(t)$ denotes the total cost of the nuclei of all isotopes in the accumulation chain under consideration; $\int_0^t [b_n(t') + \lambda_n] u_n(t')dt'$ denotes the total cost of the nuclei converted after the last isotope in the chain under consideration; $\sum_{i=0}^{n} u_i^0$ denotes the losses incurred in the acquisition of the initial isotopes; and $\int_0^t C_{irr}(t')\,dt'$ denotes the losses incurred in the target irradiation.

Equation (5) indicates that system (2) satisfies the above condition. The number of nonvanishing terms in the expression $\sum_{i=0}^{n} u_i^0$ is equal to the number of the initial isotopes.

Thus, the method which we developed for calculating the distribution of the losses in the accumulation of isotopes of the transuranium elements makes it possible to calculate the cost of the nuclei of each isotope of any accumulation chain in dependence on the irradiation time; the method makes it possible to take into consideration the influence of the characteristics of both the irradiating apparatus and the target, i.e., it is possible to calculate a quantity which can be the criterion for the economic optimization of those characteristics.

LITERATURE CITED

1. V. P. Terent'ev et al., At. Énerg., 29, No. 4, 260 (1970).
2. V. A. Tsykanov, At. Énerg., 31, No. 1, 15 (1971).
3. V. I. Zelenov, S. G. Karpechko, and A. D. Nikiforov, At. Énerg., 39, No. 1, 9 (1975).

SLOWING DOWN OF PARTICLES IN HIGHLY ANISOTROPIC SCATTERING. STATISTICAL FLUCTUATIONS OF ENERGY LOSSES IN COLLISIONS

Yu. A. Medvedev and E. V. Metelkin

UDC 539.124.17

The theory of the steady-state slowing down of particles in matter is of considerable interest and has a wide range of applications. Information on the spatial and energy spectra of particles is needed to solve a number of problems of reactor physics, shielding physics, nuclear physics, etc. [1-4].

Since an exact solution of the steady-state integrodifferential Boltzmann equation describing the slowing-down process presents formidable mathematical difficulties, a number of approximate methods have been developed which enable the particle spectra to be calculated with sufficient accuracy [1-4]. In most of these methods the distribution function is expanded in a series of spherical harmonics as functions of the direction of the velocity of the particles. This procedure decreases the number of independent variables but increases the number of equations to be solved.

A relatively simple solution was obtained for the elastic slowing down of neutrons for spherically symmetric scattering in the center of mass system. In this case it is sufficient to retain only the first two terms in the expansion of the distribution function in spherical harmonics for neutrons slowing down at "intermediate" distances. This leads to the well-known P_1- or "diffusion" approximation.

As noted in [1] the assumption of spherical symmetry of the angular distribution of elastically scattered neutrons ceases to be valid for energies > 100 keV. At such energies the angular distribution of neutrons is peaked in the forward direction even in the center of mass system [1, 5].

For highly anisotropic scattering a fairly large number of terms must be retained in the expansion of the distribution function in spherical harmonics (see [6] for more details) and a computational technique must be used to obtain the final result.

This difficulty can be circumvented by assuming that in highly anisotropic scattering a particle loses a certain fraction of its energy in each interaction without changing its direction. The first equation describing such a process was derived and solved by Landau [7] in determining the fluctuations of ionization losses of charged particles in thin layers of material when the change in direction of a particle in slowing down can be neglected. The fluctuations (or energy spectrum of the particles) in layers of material whose thickness is comparable with the total ionization range were investigated in [8] using the equation derived in [7]. If a charged particle experiences a negligible change in direction in penetrating a certain layer of material (highly anisotropic scattering) the distribution function obtained in [8] will describe the energy spectrum of the particles (or the fluctuations of ionization losses) at a given distance from the source. Otherwise the result in [8] describes

Translated from Atomnaya Énergiya, Vol. 41, No. 2, pp. 105-110, August, 1976. Original article submitted November 10, 1975; revision submitted March 15, 1976.

the change in the energy spectrum along the actual path of the particle, which is appreciably different from rectilinear because of multiple scattering. The latter result is of interest in determining the energy and mass of particles from the nature of their tracks in photoemulsions, or in the measurement of filters which absorb particles, since it follows from the condition that the particle spectrum at a given distance has a finite width that particles of the same energy can traverse various paths in coming to rest.

The solution obtained in [8] for thin absorbers is rigorous for layers of material of such a thickness that the average energy lost by charged particles in penetrating them is small in comparison with the energy itself. The results of [8] taking account of the change in energy of the particles in slowing down were obtained from qualitative arguments and are not completely rigorous as will be shown later.

In the present paper we calculate analytically the steady-state spatial and energy spectra of particles slowing down in matter when the energy loss per collision is a small fraction of the energy itself. The results can be used to investigate the propagation of gamma rays, neutrons, and charged particles in matter. For highly anisotropic scattering these results describe the particle spectrum at a distance from the source, or after the particles have penetrated a thickness of material, which is small enough so that the direction of a particle has not changed much. Otherwise the results obtained describe the energy spectrum of particles along the actual path, or the energy fluctuations along the trajectory.

The following fact should be noted. For energies high enough so that the effect of anisotropy in the elastic scattering of neutrons cannot be neglected, inelastic scattering processes in which there is an appreciable change in the initial energy can affect the slowing down of neutrons. Therefore the results obtained can be used for neutrons in the energy range $[E^+, E^+ - E_1]$ (here E^+ is the source energy and E_1 is the energy of the first excited state of the moderator nuclei) where the neutron slowing down occurs only as a result of elastic scattering processes, and the effect of inelastic scattering can be taken into account by the method described in [9]. For the same reason these results can be applied for soft gamma rays with energies $E \ll m_e c^2$, where m_e is the mass of an electron and c is the speed of light [2]. Charged particles, particularly heavy particles, lose only a small fraction of their energy in inelastic collisions [3, 4].

The steady-state slowing down in matter of particles from a plane monodirectional monoenergetic source is described by the Boltzmann equation [1]:

$$\mu \frac{\partial \Phi(E; r; \mu)}{\partial r} + (\Sigma_s + \Sigma_a)\Phi(E; r; \mu) = \int_0^\infty dE' \int_{-1}^{1} d\mu' \Sigma_s(E' \to E; \mu' \to \mu) \times \Phi(E'; r; \mu') + \delta(\mu - 1)\delta(r)\delta(E - E^+), \tag{1}$$

where r is the coordinate of a point in space measured along the normal to the source plane, μ is the cosine of the angle between the direction of motion of the particle and the normal to the source plane, $\Phi(E, r, \mu)$ is the neutron flux per unit ranges of E, r, and μ; $\Sigma_S(E' \to E, \mu' \to \mu)$ is the probability per unit path that a particle with energy E' moving in the direction μ' is scattered in the direction μ in an element $d\mu$ and acquires an energy E in the range dE; Σ_S is the total scattering cross section and Σ_a is the total absorption cross section.

We seek the solution of Eq. (1) in the form

$$\Phi(r, E, \mu) = \delta(\mu - 1)\Phi(r, E). \tag{2}$$

Substituting (2) into (1) and integrating over $d\mu$ from -1 to $+1$ we obtain

$$\frac{\partial \Phi(E, r)}{\partial r} + (\Sigma_s + \Sigma_a)\Phi(r, E) = \int_0^\infty dE' \Sigma_s(E') \times P(E' \to E)\Phi(r, E') + \delta(r)\delta(E^+ - E), \tag{3}$$

where

$$P(E' \to E) = \Sigma_s(E' \to E)/\Sigma_s(E');$$

$$\Sigma_s(E' \to E) = \int_{-1}^{1} d\mu \Sigma_s(E' \to E; \mu' \to \mu).$$

If we understand by r the path traversed by the particle, Eq. (3), which agrees with the equation derived in [7], describes the slowing down of particles along the actual path r. For highly anisotropic scattering its solution gives the distribution function at short distances from the source (cf. [2]).

If in Eq. (3) we replace Σ_s by $\nu = v\Sigma_s$, Σ_a by $\gamma = v\Sigma_a$, and r by t, it agrees exactly with the equation describing the slowing down of particles in an infinite medium for a pulsed monoenergetic source uniformly distributed in space, and can be solved by the method developed in [10] for functions ν, γ, and $P(E' \to E)$ of arbitrary form. The result obtained in [10] is valid for $\Delta(E) \ll E$ and $\Sigma_a \ll \Sigma_s$ ($\Delta(E)$ is the average energy lost by a particle in a collision).

If $\Sigma_a \ll \Sigma_s$, absorption, which determines the decrease in the total number of particles, has little effect on the character of the energy spectrum (see [10] with respect to the ratio Σ_a/Σ_s). Therefore from now on we assume that $\Sigma_a \ll \Sigma_s$ and neglect the effect of absorption on the shape of the neutron energy-spectrum. This effect is taken into account directly in using results (22) and (43) of [10]. From results obtained earlier [10] it follows that for $\Sigma_a = \text{const}$ absorption does not affect the shape of the energy spectrum. This conclusion is rather obvious since in this case absorption is eliminated from Eq. (3) by the substitution $\Phi(E; r) = \Phi'(E; r)\exp(-r\Sigma_a)$.

Using the results from [10] and making appropriate changes (cf. above) the solution of (3) can be written in the form

$$\Phi(r; E) = \frac{\varepsilon_m(r)}{E^2}\sqrt{\frac{K(r)}{2\pi}}\exp\left\{-I(r) - \frac{K(r)}{2}\left(\frac{\varepsilon_m(r)}{E} - 1\right)^2\right\}, \tag{4}$$

where ε_m is given by

$$I(r) = \int_{\varepsilon_m}^{E^+} \frac{dE}{\Delta}\frac{\Sigma_a}{\Sigma_s}; \tag{5}$$

$$r = \int_{\varepsilon_m}^{E^+} dE/\Delta\Sigma_s; \tag{6}$$

$$K(r) = \left[\frac{\varepsilon_m}{\Delta(\varepsilon_m)\Sigma_s(\varepsilon_m)}\right]^2 \int_{\varepsilon_m}^{E^+} \frac{dE}{\Delta\Sigma_s^2}\left(1 + \frac{b^2}{\Delta^2}\right)\Bigg\}^{-1}; \tag{7}$$

$$\Delta(E') = \int_0^\infty (E' - E)\,P(E' \to E)\,dE;$$

$$b^2(E') = \int_0^\infty [E' - \Delta(E') - E]^2\,P(E' \to E)\,dE. \tag{8}$$

It follows from (4) that for slowing down along a trajectory the particles are grouped in energy close to a certain average value $\varepsilon_m(r)$ characteristic for each point of the trajectory. This method of focusing can be understood from the following considerations. The rate of displacement of particles down the energy scale as they move along a trajectory ($-d\varepsilon_m/dr = \Delta\Sigma_s$) depends on their energy. Therefore if the quantity $\Delta\Sigma_s$ decreases with decreasing energy, particles whose energy at a given point of the trajectory is smaller (larger) than the average are slowed down less (more) effectively in further motion along the trajectory and fall into the region of average energy. These notions are in a certain sense analogous to concepts of the energy focusing of neutrons from a pulsed monoenergetic source uniformly distributed in space as they slow down in an infinite medium as described in detail in [11].

It follows from the results of [10] that if

$$\Sigma_s = \Sigma_s^{(0)}E^q; \quad \Delta = \Delta^{(0)}E^{(n)};$$
$$\Sigma_s^{(0)} = \text{const}; \ \Delta^{(0)} = \text{const}, \tag{9}$$

the energy focusing of particles will occur for

$$n + q \geqslant 1; \quad n \geqslant 1 \ (\text{for } n = 1, q \neq 0). \tag{10}$$

Mathematically this means that under conditions (9) and (10) the function K(r), which decreases with distance, cannot take on values smaller than $\sim E/\Delta(E) \gg 1$. Otherwise the width of the distribution function could increase without bound.

Let us investigate the nature of the change of the energy spectrum of neutrons as they move along a trajectory. It is known [1] that for elastic scattering of neutrons

$$P(E' \to E) = \frac{1}{\beta E'} \varphi\left[1 - \frac{2}{\beta}\left(1 - \frac{E}{E'}\right)\right] \times \theta(E' - E)\,\theta[E - (1-\beta)E'], \tag{11}$$

where $\varphi(\mu) = 1 + \sum_l (\sigma_l/\sigma_0)\, P_l(\mu)$ is a function characterizing the angular distribution of elastically scattered neutrons in the center of mass system, $\theta(z)$ is a unitary function, $\beta = 4M/(M+1)^2$, and M is the mass number of the moderator nuclei.

Substituting (11) into (8) we obtain

$$\Delta(E) = \frac{1}{2}\beta E\left[1 - \frac{\sigma_1}{3\sigma_0}\right]; \quad b^2(E) = \frac{\beta^2 E^2}{12}\left[1 + \frac{2\sigma_2}{5\sigma_0} - \frac{1}{3}\left(\frac{\sigma_1}{\sigma_0}\right)^2\right]. \tag{12}$$

Since

$$\overline{\mu(E)} = \frac{1}{2}\int_{-1}^{1} d\mu\mu\varphi(\mu) = \frac{\sigma_1}{3\sigma_0}; \quad \overline{\mu^2(E)} = \frac{1}{2}\int_{-1}^{1} d\mu\mu^2\varphi(\mu) = \frac{1}{3} + \frac{2\sigma_2}{15\sigma_0} \tag{13}$$

(where $\bar{\mu}$ is the average value of the cosine of the scattering angle and $\overline{\mu^2}$ is the mean square value), the results (12) can be rewritten in a more physically descriptive form:

$$\Delta E = \frac{1}{2}\beta E\,[1 - \overline{\mu(E)}]; \quad b^2(E) = \frac{\beta^2 E^2}{4}\,[\overline{\mu^2(E)} - \overline{\mu(E)}^2]. \tag{14}$$

It follows from (14) that $b^2(E) \geq 0$ and $\Delta(E) \geq 0$. For $\mu = 1, \Delta(E) = b^2(E) = 0$.

Let us investigate the nature of the neutron spectrum under the conditions

$$\overline{\mu(E)} = \text{const}; \quad \overline{\mu^2(E)} = \text{const}; \quad \Sigma_s = \Sigma_s^{(0)} E^q, \tag{15}$$

which make for easy calculations in (5) and (7) and at the same time are sufficiently general.

Using (5), (7), (14), and (15) we obtain:

for $q = 0$

$$\varepsilon_m(r) = E^+ \exp\left\{-\frac{1}{2}\beta(1-\bar{\mu})\, r\Sigma_s\right\}; \tag{16}$$

$$K(r) = \frac{4}{\beta^2(1-\bar{\mu})^2\delta}\,\frac{1}{r\Sigma_s}; \tag{17}$$

for $q \neq 0$

$$r = \frac{2}{q\beta(1-\bar{\mu})\Sigma_s^0}\left[\frac{1}{\varepsilon_m^q} - \frac{1}{(E^+)^q}\right]; \tag{18}$$

$$K(r) = \frac{4q}{\beta(1-\bar{\mu})\delta}\left[1 - \left(\frac{\varepsilon_m}{E^+}\right)^{2q}\right]^{-1}, \tag{19}$$

where $\delta = 1 + (\overline{\mu^2} - \bar{\mu}^2)/(1-\bar{\mu}^2)^2$.

These results show that for a constant elastic scattering cross section ($q = 0$) the average energy around which the neutrons are grouped in their motion along a trajectory depends on the source energy and decreases exponentially with distance (16). In this case the width of the energy spectrum increases monotonically [$K \approx 1/r$, cf. [17]]. Since our results are valid for $K(r) \gg 1$ [10], Eqs. (16) and (17) can be used at distances

$$r \ll \frac{4}{\beta^2(1-\bar{\mu})^2\delta}\,\frac{1}{\Sigma_s}, \tag{20}$$

which for heavy moderators ($\beta \ll 1$) and highly anisotropic scattering ($1 - \bar{\mu} \ll 1$) are appreciably larger than the neutron mean free path $l_s = 1/\Sigma_s$.

When the elastic scattering cross section increases with energy ($q > 0$), the average neutron energy decreases monotonically with distance [$\varepsilon_m \sim (1/r)$, cf. (18)]. The width of the energy spectrum in this case increases monotonically, approaching the constant value $K_0 = 4q/\beta(1-\bar{\mu})\delta \approx E/\Delta(E) \gg 1$ (19). For $(\varepsilon_m/E^+)^q \ll 1$ the nature of the neutron energy spectrum is independent of the source energy and is determined by the properties of the moderating medium.

If the elastic scattering cross section decreases with increasing energy ($q < 0$) the neutrons in slowing down along the trajectory will accumulate at a distance $r = -2/[q\beta(1-\bar{\mu})\Sigma_s(E^+)]$ (18). In this case the width of the energy spectrum will increase monotonically (19). It follows from the requirement $K(r) \gg 1$ that the results (18) and (19) for $q<0$ are valid at distances where

$$\left(\frac{\varepsilon_m}{E^+}\right)^{-q} \gg \sqrt{\frac{\beta\delta(1-\bar{\mu})}{-4q}} = \sqrt{\frac{\delta}{-2q}\frac{\Delta(E)}{E}} \ll 1. \tag{20a}$$

Now let us investigate the nature of the change of the gamma spectrum along a trajectory. We assume that the change is due mainly to Compton scattering, which is the case over a wide range of gamma energies [2]. Using the differential Compton scattering cross section from [2] it is easy to find from Eqs. (8) in terms of the variables $\alpha = E/m_e c^2$ used in gamma spectroscopy

$$\Sigma_s \approx \rho_{el}\sigma_T[1-2\alpha]; \quad \Delta(\alpha) \approx \alpha^2\left[1-\frac{11}{5}\alpha\right];$$
$$b^2(\alpha) \approx 0.4\alpha^4[1-4\alpha], \tag{21}$$

where ρ_{el} is the electron density, $\sigma_T = 8\pi r_e^2/3$ is the Thomson cross section, and $r_e = e^2/m_e c^2$ is the classical radius of the electron.

Substituting (21) into (5) and (7) we obtain

$$r = \left[1 - \frac{\alpha_m}{\alpha^+} + 4.2\alpha_m \ln\frac{\alpha^+}{\alpha_m}\right] \Big/ (\alpha_m \rho_{el}\sigma_T); \tag{22}$$

$$K(r) = [1-4.2\alpha_m]^{-2} \Big/ \left\{1.4\alpha_m\left[1-\frac{\alpha_m}{\alpha^+} + 6\frac{11}{35}\alpha_m \ln\frac{\alpha^+}{\alpha_m}\right]\right\}. \tag{23}$$

It follows from these results that the gamma energy decreases along a trajectory inversely proportional to the distance (for $\alpha_m \ll \alpha^+$ cf. (22)). The width of the energy spectrum decreases since $K(r) \sim 1/\alpha_m \sim r$ (23). For $\alpha_m \ll \alpha^+$ the average gamma energy and the dispersion of the distribution function obviously do not depend on the source energy but are completely determined by the length of the path traversed (cf. (22) and (23)).

With a decrease in gamma energy the photoelectric absorption in matter becomes important. This can affect the numerical values of $K(r)$ and $\alpha_m(r)$, which is easy to take into account by using the results in [10]. It should also be noted that for $\alpha \ll 1$ the gamma scattering is isotropic and the results obtained describe essentially the evolution of the energy spectrum along the actual path.

We turn now to the penetration of charged particles through matter. In order to compare our results with those of other authors we change to the characteristics used to describe the penetration of charged particles through matter. Let $k_{st} = -dE/dx$ be the energy lost by a particle per unit path length as a result of collisions. It is defined in the following way [3, 5]:

$$k_{st}(E) = \int_0^{E_m} E'\Sigma_s(E; E')\,dE', \tag{24}$$

where $\Sigma_s(E; E')dE'$ is the probability that in a unit path length a particle with kinetic energy E will lose energy E' in the range dE' as a result of collisions; E_m is the maximum energy transfer.

By making these changes of variables it is easy to show that (cf. [8])

$$k_{st}(E) = \Delta(E)\,\Sigma_s(E). \tag{25}$$

Similarly the quantity defined as (cf. Eq. (10.4) of [3])

$$\rho^2 = \int_0^{E_m} (E')^2\,\Sigma_s(E; E')\,dE', \tag{26}$$

is expressed in terms of a combination of quantities (8)

$$\rho^2 = \Sigma_s(E)[b^2(E) + \Delta^2(E)]. \tag{27}$$

Using the newly introduced characteristics, neglecting absorption, and taking account of the fact that $K \gg 1$ we can write Eq. (4) in the form

$$\Phi(r, E)\,dE = \frac{dE}{\sqrt{2\pi\Omega^2(r)}} \exp\left\{-\frac{[\varepsilon_m(r)-E]^2}{2\Omega^2(r)}\right\}, \tag{28}$$

where

$$\Omega(r) = \frac{\varepsilon_m^2(r)}{K(r)} = k_{cr}^2(\varepsilon_m)\int_{\varepsilon_m}^{E^+}\frac{dE\rho^2(E)}{k_{st}^3(E)}, \tag{29}$$

and $\varepsilon_m(r)$ is determined from

$$r = \int_{\varepsilon_m}^{E^+}\frac{dE}{k_{st}(E)}. \tag{30}$$

We assume as in [8] that the particles penetrate a thin enough layer of material so that the average change in energy is small in comparison with the energy itself. In this case assuming that $\rho^2(E)$ and $k_{st}(E)$ are constants we obtain

$$\Omega^2(r) = r\rho^2; \quad \varepsilon_m(r) = E^+ - rk_{st}. \tag{31}$$

Substituting (31) into (28) gives a result which agrees with [3, 8].

The change in energy of particles during slowing down was taken into account qualitatively in [8]. To do this it was proposed to replace the multiplication by r on the right-hand side of the first of Eqs. (31) by integration over dr and then to transform this integral into an integral over energy by using (30). Thus the result obtained in [8] agrees in form with (28) where $\Omega(r)$ has the following form:

$$\Omega_0(r) = \int_{\varepsilon_m}^{E^+}\frac{dE\rho^2(E)}{k_{st}(E)}. \tag{32}$$

We illustrate the difference between (32) and (29) by considering the propagation of nonrelativistic fast heavy charged particles in matter. In this case [3, 4]

$$\rho^2(E) = 4Cm_e^2c^4z^2 = \text{const}; \tag{33}$$

$$k_{st}(E) = \frac{2Cm_emc^4z^2}{E}\ln\left[\frac{4E}{I}\frac{m_e}{m}\right], \tag{34}$$

where m and ze are the mass and charge of the moving particle, and $C = \pi\rho_{el}r_e^2$. The final result can be obtained in a simple and descriptive form.

By substituting (33) and (34) into Eq. (32) of [8] it follows that

$$\Omega_0^2 = r\rho^2, \tag{35}$$

where r is the path length traversed by a particle.

Substituting (33) and (34) into (29) and (30) and treating the logarithm as a slowly varying function we obtain

$$\varepsilon_m(r) = E^+\sqrt{1-\frac{r}{R}}; \tag{36}$$

$$\Omega^2(r) = \frac{m_e}{2m}\frac{(E^+)^2}{\ln\left[\frac{4E^+}{I}\frac{m_e}{m}\right]}\frac{[1-(1-r/R)^2]}{[1-r/R]}, \tag{37}$$

where $R = E^+/2k_{st}(E^+)$.

It is obvious that R is only of the same order of magnitude as the total range of a charged particle in matter since it has already been noted that Eq. (34) is valid only in the high-energy region (for energies > 1.5 MeV for protons and > 5 MeV for alpha particles [3]). For fast particles this agreement may be close (when E^+ is large).

Using (35) and (37) we obtain

$$\frac{\Omega_0^2(r)}{\Omega^2(r)} = \frac{2x(1-x)}{[1-(1-x)^2]} \quad \left(x = \frac{r}{R}\right). \tag{38}$$

It follows from (38) that our results agree with those of [8] for thin layers of material, i.e., for small x, since as $x \to 0$

$$\frac{\Omega_0^2(r)}{\Omega^2(r)} \approx \left(1-\frac{x}{2}\right). \tag{39}$$

Equation (35) was well confirmed experimentally [12]. It should be noted that in this case samples of rather thin foils ($x \ll 1$) were used. For a foil thickness even of the order 0.2 R we find from (39) that the difference betwee (35) and (37) is 10%, which is within the limits of experimental error. The difference between (35) and (37) begins to be important for penetration through sufficiently thick layers of material ($x = 0.5$, $\Omega_0^2/\Omega^2 = 0.67$).

It follows from (38) that in the penetration of sufficiently thick layers of material the width of the energy spectrum of the particles must increase more rapidly than predicted by the results in [8], approaching infinity as $r \to R$. However our results are valid so long as the width of the energy spectrum is small, i.e., for $K \gg 1$, and also as long as Eq. (34) is valid. Using (29), (36), and (37) we obtain

$$K(r) = 2\frac{m}{m_e}\ln\left[\frac{4E^+}{I}\frac{m_e}{m}\right]\frac{(1-r/R)^2}{\left[1-\left(1-\frac{r}{R}\right)^2\right]}. \tag{40}$$

In this case we find from the condition $K \gg 1$ that our results are valid at distances

$$\frac{R-r}{R} \gg \sqrt{\frac{m_e}{2m}\frac{1}{\ln\left[\frac{4E^+}{I}\frac{m_e}{m}\right]}} \ll 1, \tag{41}$$

i.e., along most of the path traversed by a particle before coming to rest if Eq. (34) holds. This shows that energy fluctuations are negligible along most of the path.

LITERATURE CITED

1. A. Weinberg and E. Wigner, The Physical Theory of Neutron Chain Reactors, Univ. Chicago (1958).
2. O. I. Leipunskii, B. V. Novozhilov, and V. N. Sakharov, Propagation of Gamma Rays in Matter [in Russian], Fizmatgiz, Moscow (1960).
3. B. Rossi, High Energy Particles, Prentice-Hall, New York (1952).
4. S. V. Starodubtsev and A. M. Romanov, Penetration of Charged Particles Through Matter [in Russian], Akad. Nauk UzbekSSR, Tashkent (1962).
5. M. N. Nikolaev and N. O. Bazazyants, Anisotropy of Elastic Scattering of Neutrons [in Russian], Atomizdat, Moscow (1972).
6. E. Oblow, K. Kin, and H. Goldstein, Nucl. Sci. and Engng., 54, 72 (1974).
7. L. D. Landau, On the Ionization Loss of Fast Particles. Collected Works, Vol. 1 [in Russian] Nauka, Moscow (1969), p. 482.
8. I. Ya. Pomeranchuk, Zh. Éksperim. Teor. Fiz., 18, No. 8, 759 (1948).
9. Yu. A. Medvedev, E. V. Metelkin, and G. Ya. Trukhanov, At. Énerg., 36, 277 (1974).
10. Yu. A. Medvedev et al., At. Énerg., 38, 156 (1975).
11. M. V. Kazarnovskii, Trudy FIAN, 11, 176 (1959).
12. C. Madsen and P. Venkateswarlu, Phys. Rev., 74, 1782 (1948).

TOTAL BACKSCATTERING COEFFICIENTS FOR OBLIQUELY INCIDENT 15-25-MeV ELECTRONS

V. V. Gordeev, V. P. Kovalev, and V. I. Isaev

UDC 539.171.2

Total coefficients, angular distributions, and other characteristics of backscattered electrons are needed for shielding calculations, the shaping of radiation fields, etc.

It is rather difficult to describe differential and total characteristics theoretically. Satisfactory results have been obtained under a number of restrictions [1, 2]. At the same time total election backscattering coefficents have been measured in only a few cases [3, 4].

Total backscattering coefficients for 4.7-14-MeV electrons incident obliquely on aluminum and lead targets of semiinfinite thickness were measured in [3]. Similar measurements for aluminum, iron, copper, and lead using 12.8-25-MeV electrons were reported in [4]. We have performed relative measurements of total electron backscattering coefficients as a function of target thickness and the angle of incidence of the electron beam for aluminum, copper, and lead targets.

The measurements were performed at the LUÉ-25 electron linear accelerator [5]. A beam of electrons 1 cm in diameter from the accelerator was incident on a target in air at a distance of 7 cm from the exit window of the accelerator. The targets were 10 cm in diameter and varied in thickness from 0.81 to 10.5 g/cm^2. In order to record the electrons which penetrated a target of thickness less than the electron range in the target material a copper hemispherical shell 2 cm thick and 10 cm in outside diameter was connected to the target. The hemisphere was placed so that the electrons which penetrated the target were incident nearly normally on the hemisphere, since the total electron backscattering coefficient is minimum for normal incidence. The target and hemisphere were rotated by remote control. The charge deposited on the target and hemisphere was collected on a 100-mF energy-storage capacitor whose potential was measured by an electrometer amplifier. The discharge time of the whole circuit was approximately three orders of magnitude longer than the irradiation time. The charge incident on the target was monitored by a secondary emission detector. Following [4] we can write

$$\frac{1-\eta(\theta, x)}{1-\eta_0(x)}=\frac{q_t(\theta, x)+q_s(\theta, x)}{q_{t0}(x)+q_{s,0}(x)}, \quad (1)$$

where $\eta(\theta, x)$ is the backscattering coefficient for electrons incident on the target surface, θ is the angle between the normal to the target and the direction of the incident beam, x is the target thickness, $q(\theta, x)$ is the

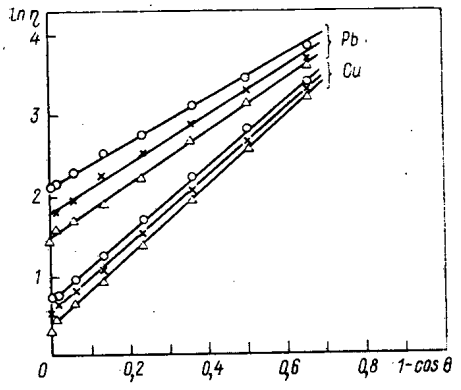

Fig. 1. Total electron backscattering coefficients for copper and lead targets at ○) 15, ×) 20, and Δ) 25 MeV.

Translated from Atomnaya Énergiya, Vol. 41, No. 2, pp. 110-112, August, 1976. Original article submitted August 6, 1975.

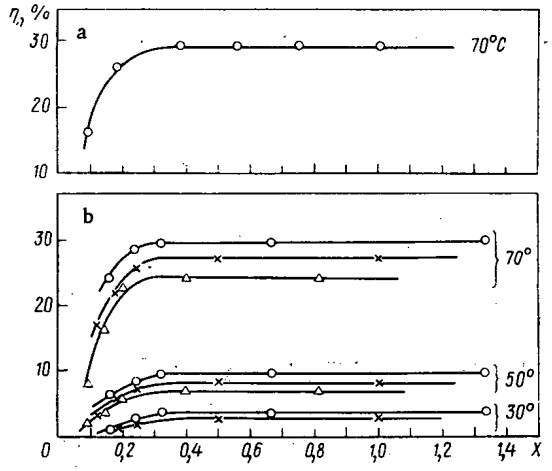

Fig. 2

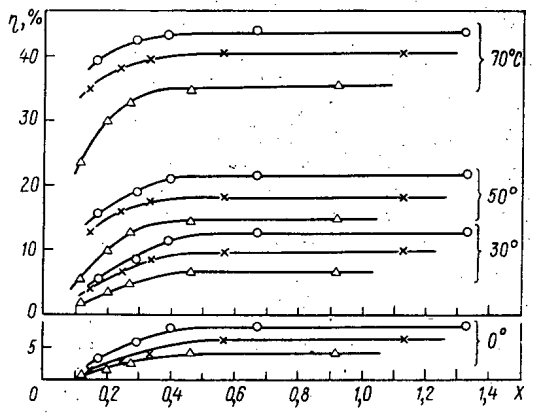

Fig. 3

Fig. 2. Dependence of electron backscattering coefficients on target thickness and the angle of incidence for a) aluminum and b) copper at ○) 15, ×) 20, and △) 25 MeV.

Fig. 3. Dependence of total electron backscattering coefficients on target thickness and the angle of incidence for lead at ○) 15, ×) 20, and △) 25 MeV.

charge deposited on the target and hemisphere, $q_s(\theta, x)$ is the charge of secondary electrons, $\eta_0(x)$, $q_{t0}(x)$, and $q_{s0}(x)$ are, respectively, the backscattering coefficient, the charge taken from the target and hemisphere, and the charge of secondary electrons for normal incidence of the electron beam on the target. The values of $q_t(\theta, x)$ and $q_{t0}(x)$ were obtained during the course of the experiment, and the values of $\eta_0(\infty)$ were taken from [6, 7]. Following [8] the values of $q_s(\theta, x)$ were calculated from the expression

$$q_s(\theta, x) = q_{s0}(x)\,\delta_0[1+\beta\eta(\theta, x)], \tag{2}$$

where δ_0 is the secondary emission coefficient for the incident beam, and β is the efficiency of scattered electrons in forming secondary electrons. For the range of electron energies investigated $\beta = 1$. The values of δ_0 given in [6] are 2.1, 2.8, and 4% for aluminum, copper, and lead, respectively. δ_0 varies slowly with energy and was assumed constant in the calculations.

Using Eqs. (1) and (2) it is easy to obtain the relation

$$\eta(\theta, x) = \frac{1-\delta_0}{1+\delta_0}\left[1 - \frac{q_t(\theta, x)}{q_{t0}(x)}\right] + \eta_0(x)\frac{q_t(\theta, x)}{q_{t0}(x)}. \tag{3}$$

The results were processed in the following way. Using Eq. (3) the value of $\eta_0(x)$ was calculated as a function of the target thickness for normal incidence of the electron beam. Then $\eta(\theta, x)$ was calculated by using these values.

Figure 1 shows the measured values of the total electron backscattering coefficients for various angles of incidence of the electron beam on targets of semi-infinite thickness.

The experimental data are adequately described by the empirical formula

$$\eta(\theta, \infty) = \exp[a + b(1-\cos\theta)], \tag{4}$$

where a and b are coefficients depending on energy and the target material. For lead $a = 3 - 0.06\,E$, $b = 2 + 0.05\,E$; for copper $a = 1.15 - 0.03\,E$, $b = 3.8 + 0.02\,E$ (here E is the electron energy in MeV). For aluminum a and b are equal to 0.35 and 4.71 respectively at E = 15 MeV. The values of $\eta(\theta, \infty)$ in Eq. (4) are given in percent.

Figures 2 and 3 show the measured values of the total electron backscattering coefficients as functions of the target thickness for various angles of incidence of the initial beam. The values of $\eta(\theta, x)$ increase with increasing target thickness and reach a maximum for a thickness approximately equal to $x = \cos\theta/(1+\cos\theta)$, where x is in units of the extrapolated electron range in the target material. This is true for the whole energy range studied. The error of the relative measurements is determined mainly by the error of the electrometer

amplifier, and is ±10% for the ratio $q_t(\theta, x)/q_{t0}(x)$. The maximum error of the measurements in [7] is no more than ±12.5%. Because of its small absolute value the error in the determination of δ_0 does not appreciably affect the error in the measured value of $\eta(\theta, x)$.

LITERATURE CITED

1. R. Dashen, Phys. Rev., 134A, A1025 (1964).
2. N. P. Kalashnikov and V. A. Mashinin, in: Proc. Second All-Union Symp. on the Interaction of Atomic Particles with a Solid [in Russian] (1972), p. 362.
3. S. Okabe, T. Tabata, and R. Ito, Ann. Rep. Rad. Center Osaka Pref., 4, 50 (1963).
4. V. P. Kovalev et al., At. Énerg., 32, 342 (1972).
5. V. I. Ermakov et al., At. Énerg., 29, 206 (1970).
6. T. Tabata, Phys. Rev., 162, 336 (1967).
7. D. Harder and L. Metger, Z. Naturforsch., 23a, 1675 (1968).
8. L. N. Dobretsov and T. L. Matskevich, Zh. Tekh. Fiz., 27, 734 (1957).

50-MeV ELECTRON SYNCHROTRON WITH CYCLOTRON PREACCELERATION

S. P. Velikanov, V. I. Kvochka
V. S. Panasyuk, V. V. Sanochkin,
Ya. M. Spektor, B. M. Stepanov,
Yu. M. Tereshkin, and V. B. Khromchenko

UDC 621.3.038.61

The operating principles and design of pulsed accelerators with an extremely strong magnetic field have been described [1]; in [2], there is a model of an electron cyclic accelerator with a pulsed magnetic field with which experiments were performed on the acceleration of electrons to 2 MeV in the field of an H_{111} standing wave. Elements of the theory of cyclic acceleration of particles in a cylindrical cavity containing an H_{111} wave have been presented [3]. One of the characteristics of the acceleration principle is the preacceleration of particles to relativistic energy along a spiralling orbit by the electric field of a standing wave at a fixed frequency. Further acceleration is carried out in the field of this same wave and also in a rotational electric field to maximum energy along an orbit of constant radius.

This paper discusses a cyclic electron accelerator constructed for use as a source of synchrotron radiation in the vacuum ultraviolet region and also discusses the results of preliminary experiments intended to check the theory given in [3]. The operating principles of the accelerator have been described [1-3].

Accelerator Design

The main design feature of the accelerator is that the electromagnet for the guide magnetic field is at the same time an accelerating uhf resonant cavity and a vacuum chamber [1-3]. Because of this, the frequency of the uhf oscillator is selected on the basis of minimal energy capacity in the excitation system for the electromagnet. Optimization of the normal mode of the resonant cavity with respect to this parameter leads to an oscillator frequency value $\omega_0 \leq 1.8 \cdot 10^{10}$ sec^{-1}, which corresponds to a relativistic orbit radius $r_r = 1.6$ cm. It is necessary to accelerate electrons to an energy $\varepsilon = 50$ MeV in order to obtain particle radiation in the required wavelength region ($\lambda_s \leq 600$ Å).

The following basic units in the design of the accelerator can be identified: electromagnet, resonant cavity, acceleration chamber, excitation system for the electromagnet, oscillator for the accelerating field, and particle injector.

Translated from Atomnaya Énergiya, Vol. 41, No. 2, pp. 113-117, August, 1976. Original article submitted July 14, 1975.

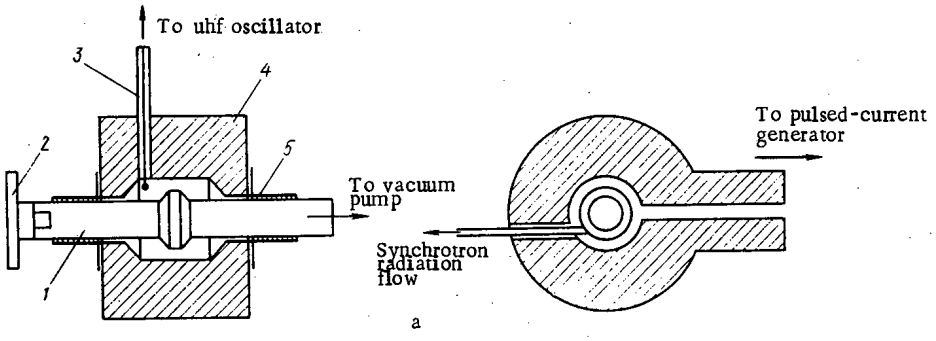

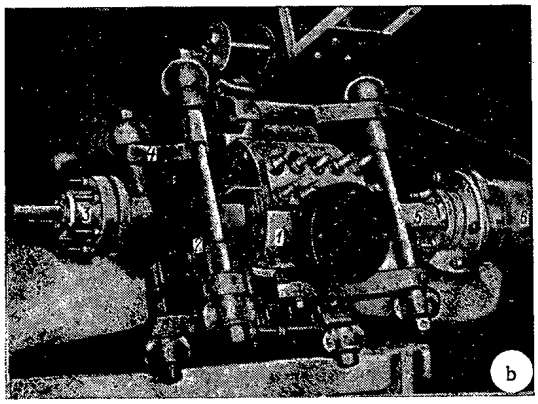

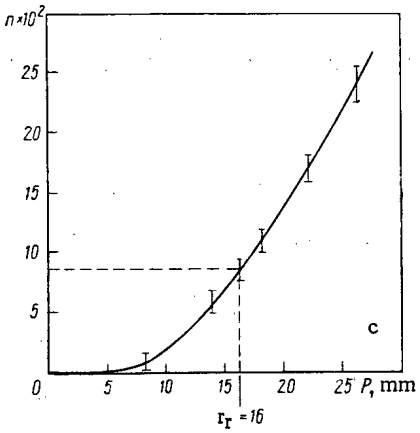

Fig. 1. a) Diagram of electromagnet with acceleration chamber: 1) acceleration chamber; 2) injector; 3) unit for excitation of resonant cavity; 4) electromagnet; 5) guard cylinders. b) External view of electromagnet assembled with acceleration chamber: 1) electromagnet; 2) guard cylinders; 3) injector; 4) tightening clamps; 5) acceleration chamber; 6) vacuum channel. c) Dependence of magnetic field decay index in median plane of electromagnet on distance from the axis.

Electromagnet, Resonant Cavity, and Acceleration Chamber. To obtain the specified accelerator parameters, it is necessary to excite a guiding magnetic field with an induction $B \approx 10$ T on the orbit. This explains the choice of an iron-free design for the electromagnet. The electromagnet (Fig. 1a, b) is a massive single-turn loop, the internal surface of which must create the required falloff of the magnetic field and act as a cavity resonator with a normal frequency equal to the frequency of the accelerating field. Figure 1c shows the dependence of the decay index on distance from the electromagnet axis in the median plane. The shape of the internal profile of the electromagnet is selected so that the decay index at the relativistic orbit is sufficiently removed from the condition for parametric resonance. As shown by calculations, resonance coupling and nonlinear resonances represent no hazard for the accelerated electrons.

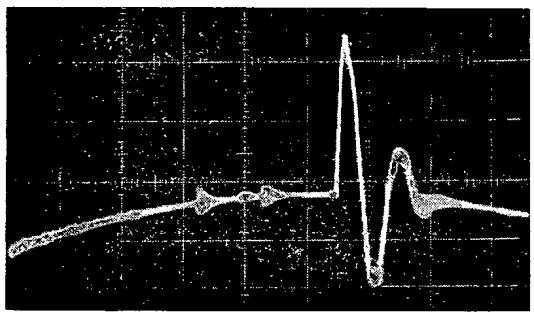

Fig. 2. Current trace for excitation system for magnetic field.

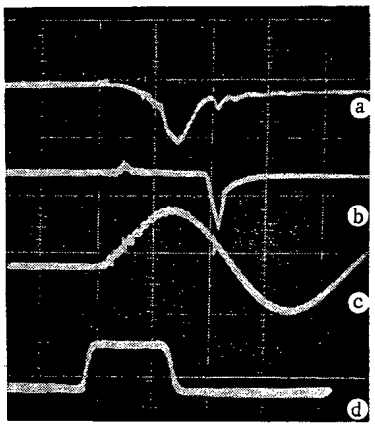

Fig. 3

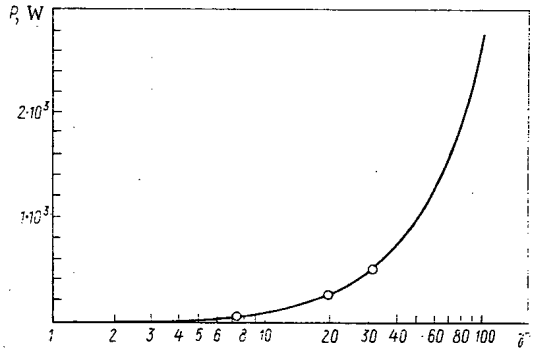

Fig. 4

Fig. 3. Oscilloscope traces of basic processes in the accelerator: a) light, b) γ-ray, c) magnetic field, and d) accelerating-field pulses.

Fig. 4. Dependence of minimum uhf-oscillator power on accelerator energy: O) experiment.

The magnetic fields near the ends of the electromagnet reach 30 T. Therefore measures must be taken to insure mechanical stability of the system. In our case, where the actual length of the current pulse ($\tau \leq 10^{-5}$ sec) is small in comparison with the period of the natural oscillations of the system, mechanical stability is provided by the choice of a sufficiently thick wall for the copper loop and by tightening of the loop with clamps at the point of current feed.

The resonance properties of the resonant cavity (frequency and Q) are mainly determined by the shape and size of the internal surface of the loop and by the degree of screening of the cavity. The dimensions of the internal cavity were selected so that the resonance frequency corresponded to the optimal oscillator frequency $f \approx 3000$ MHz. Reduction in the diameter of the opening of the loop near its ends (see Fig. 1a) makes it possible to obtain not only the required configuration of the magnetic field in the electromagnet but also considerable screening of the internal cavity with respect to high frequencies. To increase the screening of the resonant cavity at the ends of the loop, guard cylinders transparent to the guide magnetic field are installed at the ends of the loop. This makes it possible to obtain a resonant cavity with $Q \approx 10^3$.

An acceleration chamber can be either the internal cavity of an electromagnet in which the required vaccum is produced or a glass vacuum envelope installed in an electromagnet that is not vacuum-tight. As shown by experiment, the use of the internal cavity of the electromagnet as a vacuum chamber limits the maximum energy of the accelerator to $\varepsilon = 15$ MeV because of breakdown of the vacuum gap at the point where the electromagnet is connected to the excitation system. The cause of the breakdown is plasma from the uhf discharge and from the particle injector. A glass vacuum chamber (see Fig. 1a, b) increases the electrical stability of the electromagnet and simplifies its design. It should be noted that the plasma from the uhf discharge within the vacuum chamber screens the quasistatic electric field of the electromagnet, which has a perturbing effect on the accelerated electron bunch, and also removes from the walls of the acceleration chamber the charge of accelerated particles striking them.

For an acceleration cycle about $2.5 \cdot 10^{-6}$ sec long, the electron range does not exceed 1000 m, which offers an opportunity to decrease the demands on the vacuum system of the accelerator. Calculations using the technique in [4] show that the relative particle losses through scattering by residual gas are no more than 1% for a vacuum of $\sim 10^{-4}$ mm Hg and an initial electron energy of 5 eV. A vacuum of 10^{-4}-10^{-5} mm Hg is maintained in the acceleration chamber.

Excitation System for Electromagnet. If one assumes a sinusoidal variation of the magnetic field (using the first quarter-cycle for acceleration) [3], the system for excitation of the guiding magnetic field then degenerates into the simplest pulsed current generator (PCG) in which the current in the load is produced by discharge of a condenser bank into an inductive load (electromagnet). The energy stored in the condensers of the PCG must exceed the energy in the magnetic field of the electromagnet; in addition, one should strive to reduce the parasitic inductance of the PCG, including the inductance of condensers, spark gaps, and leads,

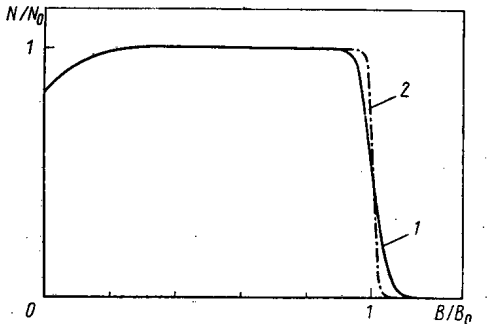

Fig. 5

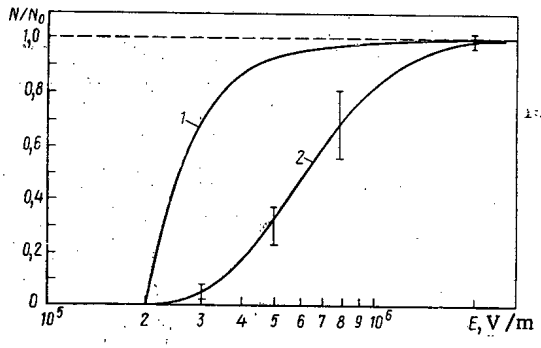

Fig. 6

Fig. 5. Dependence of accelerator intensity on level of initial magnetic field for 1) P = 10 kW and 2) 2.5 kW.

Fig. 6. Dependence of accelerator intensity on intensity of accelerating field.

in comparison with the inductance of the electromagnet. In our case, the PCG is a bank of 24 low-inductance, high-voltage IK-50-3 condensers which are switched into the total load by three low-inductance, vacuum spark gaps. The parasitic inductance of the PCG is 10^{-8} H; the inductance of the electromagnetic is $2 \cdot 10^{-8}$ H. The total energy capacity of the bank is 90 kJ; the maximum current in the electromagnet is 2.5 MA; the frequency of the natural oscillations of the LC circuit is 10^5 Hz.

The excitation system also includes a preliminary field bank (PFB) which produces a field of low amplitude (~0.1 T) in the electromagnet but one of sufficient duration to produce the required condition of cyclotron resonance at the center of the acceleration chamber. The bank consists of four IMU-5-140 condensers which are connected to the electromagnet by a vacuum spark gap through a Bitter solenoid with an inductance $L_c = 2 \cdot 10^{-6}$ H. The maximum current of the bank is $4 \cdot 10^4$ A; the frequency of the circuit is $5 \cdot 10^3$ Hz.

An oscilloscope trace of the magnetic field of the electromagnet at small values of the main magnetic field (for convenience of illustration) is shown in Fig. 2.

The repetition rate of current pulses in the electromagnet, and consequently of cycles of acceleration, is determined by the time for restoration of the electrical stability of the vacuum spark gaps and by the charging rate of the PCG device. The time between two successive firings of the spark gaps is ~5 min.

Oscillator for Accelerating Field. An acceleration mode with the initial rate of rise of the magnetic field different from zero is possible with sufficiently high intensity of the accelerating field, as has been shown [3]. Using the parameters for the excitation system for the magnetic field, and setting $\omega_0 = 1.8 \cdot 10^{10}$ sec^{-1} and ε = 50 MeV, we obtain a minimum intensity of the accelerating field $E = 5 \cdot 10^5$ V/m, which corresponds to an accelerating-field oscillator power $P = 2.7 \cdot 10^3$ W when the accelerating resonant cavity has a $Q \approx 600$. Such oscillator power corresponds to zero intensity of the accelerator. The working power of the oscillator should be selected so that the intensity of the accelerating field is greater than the intensity of the space-charge field of a bunch. A magnetron is used in the accelerator which has a power of 200 kW in a pulse of $2.5 \cdot 10^{-6}$ sec; this permits acceleration of up to 10^{11} particles [5].

Electron Injector. According to the operating principles of the accelerator, the source of particles should be located at the center of the acceleration chamber. There are several methods for realizing such an injector; it is most convenient to use as a source of electrons an erosion plasma which is injected along the magnetic lines of force into the central region of the acceleration chamber by means of a coaxial plasma accelerator (Marshall gun) [16]. The density of the plasma injected by the gun into the center of the acceleration chamber is ~10^{11} cm^{-3}. The diameter of the plasma beam at the center of the accelerator is no more than 10 mm (for an axial field with an induction of 0.1 T). The axial velocity of the plasma is no more than $5 \cdot 10^6$ cm/sec which is acceptable for the capture of electrons into the acceleration mode. Reproducibility of plasma flux parameters is not worse than 20%.

EXPERIMENTAL RESULTS

Particle acceleration can occur only with a rate of rise of the magnetic field in the electromagnet that is not too high and with a fixed intensity of the accelerating field in the resonant cavity [3]. The relation

determining the maximum permissible rate of rise of the magnetic field as the initial time through the intensity of the accelerating hf field was found by detection with a scintillation counter of the γ-ray pulses produced by the accelerated particles during their deceleration in a target (Fig. 3). This dependence is shown in Fig. 4 after conversion to the coordinates "oscillator power — accelerator energy" with allowance for the parameters of the device. The curve in Fig. 4 makes it possible to determine the minimum uhf oscillater power required for acceleration to an energy $\varepsilon = \gamma m_0 c^2$ for constant length of acceleration cycle and sinusoidal rise in the magnetic field. Good agreement is observed between theory and experiment.

The dependence of accelerator intensity (in relative units) on the level of the initial magnetic field set by the PFB (see Fig. 2) is shown in Fig. 5. Here the accelerator intensity is assumed proportional to the bremsstrahlung intensity. A certain increase in intensity with increase in B_i at small values of B_i is explained by an improvement in the operating mode of the injector. The steepness of the drop in the curve at $B_i = B_0$ depends on the amplitude of the accelerating electric field. The width of the region of the drop increases as the amplitude increases, which indicates an increase in the area bounded by the phase-stability curve. This result is in accord with theory [3].

The energy spread of the accelerated electrons also depends on the intensity of the accelerating field. Writing the equation for the separatrix in the coordinates $u = p - p_c$, φ, where p_c is the momentum of the equilibrium particle and φ is the particle phase with respect to the wave of the accelerating field [3], we obtain at the time of completion of acceleration $(\partial B/\partial t|_{T/4} = 0)$ with $p_c \gg m_0 c$,

$$eE(\sin\varphi - 1) = -\frac{\omega_0}{p_c} u^2. \tag{1}$$

Then it is easy to determine the maximum energy spread of the accelerated particles:

$$\frac{\Delta\varepsilon}{\varepsilon} = \sqrt{\frac{2eE}{m_0 c \gamma \omega_0}}. \tag{2}$$

The relative amplitude of radial phase oscillations $\Delta r/r$ is also determined by Eq. (2). Substituting $E = 2 \cdot 10^6$ W/m and $\gamma = 30$ in it, we obtain $\Delta r/r_c \approx 0.07$ or the diameter of the electron bunch $d = 2\Delta r \approx 2$ mm. The diameter of the electron bunch is determined experimentally from the width of the γ pulse emitted when the beam of accelerated electrons impinges on a target with allowance for the variation of the magnetic field in the system. The resultant value of the diameter ($d \approx 2.5$ mm) is in agreement with the theoretically determined value. Visual observations and photography of the synchrotron radiation from an accelerated electron bunch confirm this value.

As is well known, synchrotron radiation from electrons accelerated to relativistic energies is a source of information about accelerator intensity. Keeping in mind the features of the injector used in this accelerator and taking into account the results of [3], we obtain the expression

$$N = N_0 \left\{ \frac{1}{2} + \frac{1}{\pi} \arcsin\left[1 - 2\left(\frac{\dot{B}_p}{\dot{B}_{p\,max}} \right)^3 \right] \right\}, \tag{3}$$

for accelerator intensity, where $N_0 = n_0 V$ (V is the volume of the region in which particle capture into the acceleration mode occurs; n_0 is the density of the plasma electrons from the source at the center of the acceleration chamber).

The resultant dependence is shown in Fig. 6 (curve 1) in the coordinates $(N/N_0, E)$. Also shown is an experimental curve obtained by measurement of the intensity of synchrotron radiation from electrons accelerated to 20 MeV and normalized at the maximum intensity (curve 2). The discrepancy between experimental and theoretical relations can be explained by the influence of space charge at the time of electron bunch formation [5].

The absolute value of the numbers of accelerated particles can be found by comparing the intensity of a narrow spectral range of synchrotron radiation with the radiation from a lamp calibrated against an absolute black body in the same spectral range. The intensity of synchrotron radiation is converted into accelerator intensity by means of the formulas given in [7]. Measurements showed that the intensity of the accelerator was better than $5 \cdot 10^8$ particles per pulse for an amplitude of the high-frequency field $E = 2 \cdot 10^6$ V/m.

In conclusion, the authors are grateful to A. A. Sokolov for valuable advice furnished during the period of accelerator startup and testing and to the staff of the Department of High-Voltage Engineering at the Leningrad Polytechnic Institute for help in the development of the PCG.

LITERATURE CITED

1. V. S. Panasyuk, A. A. Sokolov, and B. M. Stepanov, At. Énerg., 33, No. 5, 907 (1972).
2. A. V. Gryzlov et al., in: Proc. II All-Union Conference on Charged-Particle Accelerators [in Russian], Vol. 1, Nauka, Moscow (1972), p. 170.
3. A. V. Gryzlov et al., Zh. Tekh. Fiz., 42, No. 1, 13 (1972).
4. A. G. Vlasov, Izv. VUZ, Ser. Fiz., No. 1, 20 (1961).
5. M. Yu. Novikov, Yu. M. Tereshkin, and V. B. Khromchenko, At. Énerg., 41, No. 2, 125 (1976).
6. P. N. Dashuk et al., Technology of High Pulsed Currents and Magnetic Fields [in Russian], Atomizdat, Moscow (1970).
7. Synchrotron Radiation in Solid-State Studies [in Russian], A. A. Sokolov (editor), Mir, Moscow (1970).

PROSPECTS FOR THE USE OF NUCLEAR-PHYSICS ANALYTIC METHODS IN BIOLOGY AS ILLUSTRATED BY THE WILT PROBLEM

V. Ya. Vyropaev, I. F. Kharisov, O. D. Maslov, E. L. Zhuravleva, and L. P. Kul'kina

UDC 543.53:633.51

The investigation of the role of microelements in various biological processes is undoubtedly not only of purely scientific interest but also of great national economic significance.

It is well known that such elements (macroelements) as C, H, O, N, S, P, K, Na, and Ca form vitally necessary components of parts of plant cells and the microelements Cu, Fe, Co, Mn, Zn, Mo, Se, Sb, I, and tens of others play an important role in the biological processes occurring in living things.

According to Vinogradov [1, 2], one can assume the presence of all chemical elements in living matter, and it is natural to expect that they perform a definite biological task. However, the question of exactly what biological task is performed by a given microelement has not been resolved thus far [3]. Obviously, one of the reasons is the absence of reliable analytical methods which would make it possible to perform analysis over the entire spectrum of elements on the test samples of small mass (0.1-0.01 g) that are typical of biology [4].

Biological objects (plants or living organisms) have a remarkable property from the viewpoint of activation analysis — their matrix is described by the mean conventional "formula of life" $H_{2960}O_{1480}C_{1480}P_{18}N_{16}S$, i.e., those elements which yield short-lived radioisotopes under neutron activation. This circumstance makes it possible to perform neutron activation analysis of a series of elements with high instrumental sensitivity and places the method of neutron activation in prime position for the analysis of biological objects for elemental composition from the viewpoint of discovering the biological task of microelements. The combination of neutron activation analysis with such nuclear-physics methods as autoradiography, tracer atoms, etc., is even now proving to be of significant help to the biological sciences in the solution of scientific and practical problems.

In this regard, we discuss a very important specific example — the problem of cotton-plant wilt. Wilt is a fungous disease which leads to withering and death of the cotton plant. The disease is a typical one for many agricultural crops. At the present time, the causes of this phenomenon have not been completely explained, but there are two basic hypotheses: Withering of the cotton plant occurs because of failure in feeding through the action of the parasite fungus resulting in blockage of transport vessels in the plant; withering and death of the plant occur through the action of toxins developed by the parasite fungus which enter the organs of the plant.

Translated from Atomnaya Énergiya, Vol. 41, No. 2, pp. 118-122, August, 1976. Original article submitted October 18, 1974.

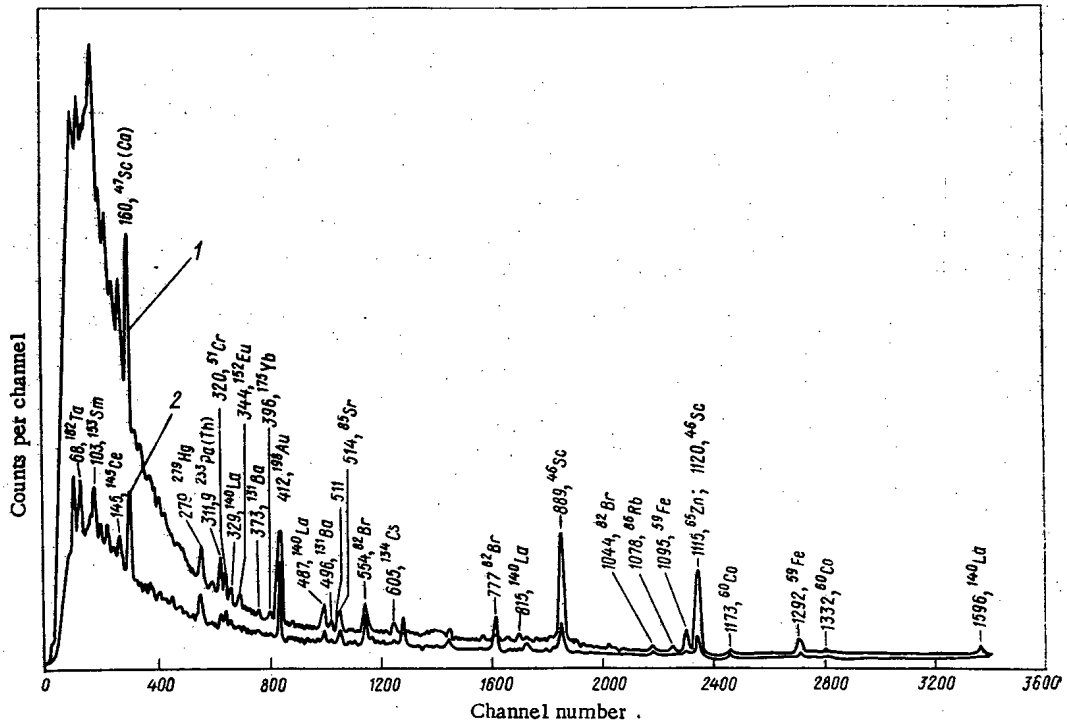

Fig. 1. Gamma spectra from samples of cotton-plant roots: 1) diseased, 2) healthy.

Wilt causes tremendous economic loss and hinders further increase in cotton productivity. The disease is so widespread that it reduces the cotton harvest significantly. Losses because of wilt amount to 10-30% and more in all the cotton-growing areas of the world.

At the present time, no one disputes the fact that it is possible the infection of the cotton plant by wilt is connected in some degree with definite anomalies in the content of certain microelements in soil and plants which affect both the wilt-resistance of cotton plants and the vital activity of the parasite fungus [5-7].

Because of this, healthy and wilt-infected cotton plants were examined for the content of various microelements by means of neutron activation. The main purpose of these studies was to determine the quantitative content of microelements in various plant organs and to attempt to establish on the basis of the experimental data some regularity in the behavior of the relative content of these elements.

Cotton-plant samples were selected from plants of a single crop cultivated under identical soil conditions and were prepared from five to 10 plants, i.e., they were averaged for a given field. The selected samples were separated into parts for irradiation: roots, stems, leaves, bolls, and fibers.

Since neutron activation analysis makes it possible to perform studies of microelement content with a sensitivity as high as 10^{-9} g/g, it is necessary to maintain particular sterility in the preparation of samples for irradiation. In addition, one ought not subject the samples to any physical or chemical effects since it has been established that up to 75% of certain elements is lost in thermal and chemical incineration [8].

The samples were prepared in the following manner: The cotton-plant samples, after being thoroughly cleansed of dust, were dried in a drying cabinet without ashing at a gradual rise in temperature from 50 to 120°C over a period of 10-15 h. The air-dried samples were ground into a powder in an agate mortar. Samples in the form of pellets 20 mm in diameter, 2-4 mm thick, and weighing ~1000 mg were prepared from this powder by compression at pressures up to 250 atm. Such samples proved to be very convenient and practical to work with. They were compact, had sufficiently high mechanical strength, small volume, high density and mass (which is very important in the preparation of samples from plants and other biological objects), and also fixed sized and shape. In addition, accuracy of calibration is considerably increased for them, and an optimal geometry for spectral measurement is easily selected.

The samples were packaged (each pellet separately) in polyethylene and placed in a stack along with standards in a special container of pure aluminum. The irradiation was carried out with a thermal neutron fluence of 10^{16} n/cm^2 ($f = 2.3 \cdot 10^{12}$ n/cm^2-sec, $\tau_{irr} = 70$ min). The neutron fluence was determined from the induced activity of standards with known activation cross sections.

TABLE 1. Microelement Content in Healthy (H) and Wilt-Infected (W) Parts of Plants, %

Element	Root			Stem			Leaf			Ball			Fiber		
	H	W	W/H	H	W	W/H	H	W	W/H	H	W	W/H	H	W	W/H
Na	0,1	0,12	1,2	0,03	0,011	0,37	0,049	0,055	1,1	0,019	0,022	1,16	$3\cdot10^{-3}$	$8\cdot10^{-3}$	2,7
K	0,6	1,18	1,9	1,65	2,32	1,4	4,1	2,1	0,5	4,46	6,0	1,35	0,6	0,97	1,6
Ca	1,2	2,	1,5	3,7	1,76	0,5	1,5	1,43	0,96	3,5	3,0	0,85	0,6	0,5	0,86
Sc	$7,4\cdot10^{-6}$	$2,1\cdot10^{-5}$	2,8	$6,4\cdot10^{-6}$	$8,4\cdot10^{-5}$	1,32	$2,5\cdot10^{-5}$	$4,2\cdot10^{-5}$	1,7	$1,5\cdot10^{-5}$	$3,7\cdot10^{-5}$	2,5	$2,4\cdot10^{-6}$	$3,1\cdot10^{-6}$	1,3
Cr	$1,5\cdot10^{-4}$	$1,5\cdot10^{-4}$	1,0	$3,2\cdot10^{-3}$	$3,8\cdot10^{-3}$	1,2	0,004	0,007	1,7	—	$<0,001$	—	—	$<0,001$	—
Fe	0,015	0,04	2,6	0,004	0,008	2,0	0,082	0,12	1,5	0,036	0,078	2,0	0,024	0,024	1,0
Co	$2\cdot10^{-5}$	$5,1\cdot10^{-5}$	2,0	$1\cdot10^{-4}$	$8\cdot10^{-5}$	0,8	$7,3\cdot10^{-5}$	$8,8\cdot10^{-5}$	1,2	—	$<10^{-5}$	—	$4,8\cdot10^{-5}$	$3,1\cdot10^{-5}$	0,6
Cu	$7\cdot10^{-5}$	$9\cdot10^{-5}$	1,3	$7,8\cdot10^{-4}$	$8,1\cdot10^{-4}$	1,05	$2,9\cdot10^{-4}$	$1,8\cdot10^{-4}$	0,6	$1,1\cdot10^{-3}$	10^{-4}	0,9	$3,8\cdot10^{-4}$	$4,2\cdot10^{-4}$	1,1
Zn	$4,2\cdot10^{-4}$	$5\cdot10^{-3}$	13	$8\cdot10^{-3}$	$1,3\cdot10^{-2}$	1,6	$7\cdot10^{-3}$	$3\cdot10^{-2}$	4,3	$7\cdot10^{-4}$	$2,2\cdot10^{-3}$	3,0	$3\cdot10^{-3}$	$4,0\cdot10^{-3}$	1,4
Ga	$3,2\cdot10^{-5}$	$2,4\cdot10^{-5}$	0,75	$1,2\cdot10^{-3}$	$1\cdot10^{-3}$	0,83	$1,3\cdot10^{-3}$	$9,0\cdot10^{-4}$	0,7	$6,7\cdot10^{-3}$	$4,2\cdot10^{-3}$	0,6	$4,5\cdot10^{-4}$	$7\cdot10^{-5}$	0,16
Br	$4,4\cdot10^{-3}$	$2,2\cdot10^{-3}$	0,5	$8,5\cdot10^{-4}$	$5,8\cdot10^{-4}$	0,7	$4,2\cdot10^{-3}$	$3,2\cdot10^{-3}$	0,7	$2,5\cdot10^{-3}$	$1,6\cdot10^{-3}$	0,6	$6\cdot10^{-5}$	$4,6\cdot10^{-4}$	7,5
Sr	$5,1\cdot10^{-3}$	$5,5\cdot10^{-3}$	1,1	$2,4\cdot10^{-2}$	$2,2\cdot10^{-2}$	0,9	$3,7\cdot10^{-2}$	$2,6\cdot10^{-2}$	0,7	—	$<0,01$	—	$1,2\cdot10^{-2}$	$1,3\cdot10^{-2}$	1,1
Mo	—	$<0,000\,01$	—	$4,8\cdot10^{-4}$	$4\cdot10^{-4}$	0,8	$1,6\cdot10^{-4}$	$8\cdot10^{-5}$	0,5	—	$<1\cdot10^{-5}$	—	—	$<1\cdot10^{-5}$	—
Ba	$3,6\cdot10^{-3}$	$4\cdot10^{-5}$	1,1	—	$<0,001$	—	$6,1\cdot10^{-3}$	$7,9\cdot10^{-3}$	1,3	—	$<0,0001$	—	—	$<0,001$	—
La	$2\cdot10^{-5}$	$7\cdot10^{-6}$	3,4	—	$<0,00001$	—	$5,8\cdot10^{-5}$	$11\cdot10^{-5}$	1,8	$2,9\cdot10^{-5}$	$3\cdot10^{-5}$	1,0	—	$<0,00001$	—
Th	$7,0\cdot10^{-6}$	$1,8\cdot10^{-5}$	2,6	$0,5\cdot10^{-6}$	$1\cdot10^{-6}$	2,0	$2,7\cdot10^{-6}$	$7,8\cdot10^{-6}$	2,9	—	$<0,000001$	—	—	$<0,000001$	—
Au	$2,4\cdot10^{-6}$	$2,7\cdot10^{-4}$	1,1	$4,8\cdot10^{-7}$	$11\cdot10^{-7}$	2,4	$4,1\cdot10^{-6}$	$2,7\cdot10^{-6}$	0,7	$0,9\cdot10^{-6}$	$2\cdot10^{-6}$	2,3	$7,4\cdot10^{-7}$	$5,2\cdot10^{-7}$	0,7
Cs	$2,5\cdot10^{-6}$	$1\cdot10^{-6}$	4,0	—	—	—	—	—	—	—	—	—	—	—	—
	$0,9\cdot10^{-5}$	$1,1\cdot10^{-5}$	1,2	—	—	—	—	—	—	—	—	—	—	—	—
	$4,5\cdot10^{-9}$	$1,6\cdot10^{-4}$	3,6	—	—	—	—	—	—	—	—	—	—	—	—
	$3\cdot10^{-6}$	$8,4\cdot10^{-6}$	2,8	—	—	—	—	—	—	—	—	—	—	—	—
	$1,4\cdot10^{-6}$	$2,9\cdot10^{-6}$	1,4	—	—	—	—	—	—	—	—	—	—	—	—
	$2,2\cdot10^{-6}$	$5,3\cdot10^{-6}$	2,4	—	—	—	—	—	—	—	—	—	—	—	—
	$7,8\cdot10^{-5}$	$7,8\cdot10^{-5}$	1,0	—	—	—	—	—	—	—	—	—	—	—	—
	$0,9\cdot10^{-4}$	$2,8\cdot10^{-4}$	3,1	—	—	—	—	—	—	—	—	—	—	—	—

Declassified and Approved For Release 2013/09/23 : CIA-RDP10-02196R000700080002-8

TABLE 2. Relative Content of Microelements in Various Parts of the Cotton Plant, g/g

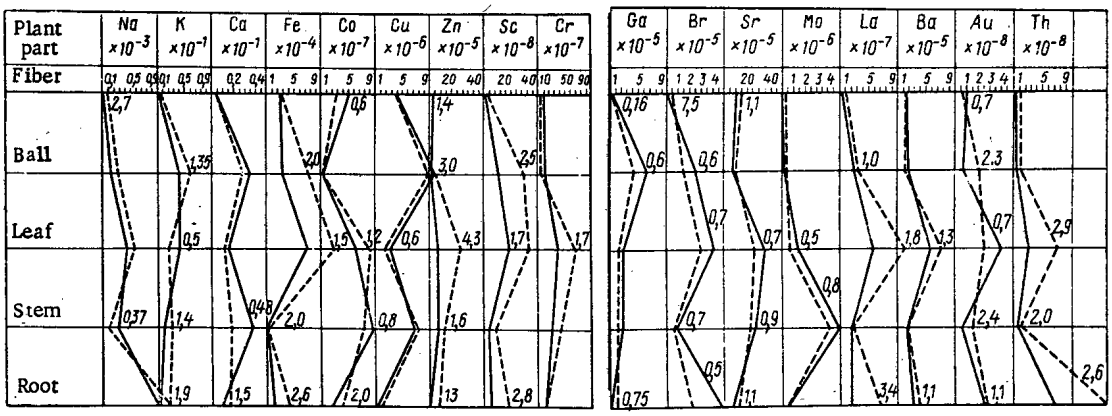

Note. Healty (—) and wilt-infected (-----) plants.

In this cycle of experiments, analysis was made of the content of long-lived radioactive isotopes. Because of this, the samples were "cooled" for two days in order to allow decay of the short-lived radioisotopes, which give rise to considerable interference in the determination of other elements because of high activity. A detector with a volume of 40 cm^3 having a resolution of 3 keV for the ^{137}Cs photopeak (E_γ = 661.65 keV) was used. Spectra were analyzed on a Minsk-32 computer (determination of areas under the peaks including subtraction of background and corrections for detector efficiency, holding time, and counting time for each isotope analyzed as a function of decay constant, etc.) [9].

Each sample was counted twice — two and four days after irradiation. In this situation, the counting time increased from 20 min to several hours. Such a counting procedure resulted from an attempt to obtain information about the comparatively short-lived isotopes and to reduce the Compton background from them in the development of the long-lived isotopes.

Isotopes contained in the test samples were identified from known γ-transition energies and half-lives for radioactive isotopes [10]. A quantitative determination of the content of elements was made by an absolute method from the known thermal neutron fluence and the handbook on nuclear-physics constants [11]. Spectra from samples of diseased and healthy roots of cotton plants are shown in Fig. 1 for τ_{irr} = 4 days and τ_{cool} = 10 h.

The final results of the analysis are shown in Table 1. As is clear from Table 1, the activation method makes it possible to perform multielement high-sensitivity analysis of cotton plants and to reveal the differences in elemental content in parts of diseased and healthy plants. Up to 25 elements were determined simultaneously with sensitivities to 10^{-7}-10^{-8} g/g. (This is not a limit, as is clear from the spectra of these samples.)

As already noted, the quantitative determination of elemental content was made by an absolute method. It is obvious that the calculated results contain an error in this case since the handbook nuclear-physics constants are not always exact. Nevertheless, the error of the resultant data is no more than 20% when one considers the fact that the energy spectrum of the neutrons with which the samples were irradiated was extremely pure in thermal neutrons (cadmium ratio greater than 100).

The errors of the ratios W/H given in Table 1 are minimal since these are ratios of the net areas of photopeaks produced under completely identical conditions (irradiation, cooling, and counting times, normalization with respect to mass, identical spectrometer, etc.).

Special conclusions drawn from the results of our studies are the task of the biologists, but it is impossible not to point out the significant difference in the content of most of the elements in the parts of healthy and wilt-infected plants. While it is known what biological task is performed by such elements as Na, K, Ca, Fe, and Cu, the identified elements Sc, Cr, Co, Zn, Ga, Br, Mo, Au, Cs, Sb, Rb, Th, and rare-earths show that the difference in their content is evidence of their biological role in the life of the cotton plant and in the activity of the parasite fungus.

Table 2 gives data for the relative content of 17 elements (ratio of the isotopic content in parts of wilt-infected and healthy cotton plants) in the parts of a cotton plant. Analyzing the resultant data, one can say that the relative concentrations of such elements as K (except for leaves), Sc, Cr, Fe, Zn, Ba, La, and Th are considerably higher in all parts of a cotton plant infected by wilt, and the relative concentrations of Ga, Br (except for fiber), and Mo are considerably lower. The relative content of Na, Ca, Co, Cu, Sr, and Au varies

over broad limits, for example, from ~0.3 to ~3.0 for Na. A higher concentration of Cs, Sb, Ce, Sm, Eu, Yb, and Rb is observed in the roots of wilt-infected cotton plats as compared to healthy plants. Such a variation in microelement concentration is obviously the cause or the result of infection of the cotton plant by wilt.

Solution of the wilt problem requires the organization of systematic analysis over a number of years in order to reveal the specific role of the elements and to establish a definite regularity in their content and behavior. The problem can undoubtedly be solved through collaboration of specialists at centers for activation analysis and scientists studying this problem.

In conclusion, the authors express their gratitude to G. N. Flerov for supporting this work and for continuing interest, and to A. A. Kist and Z. É. Bekker for valuable discussions of the results.

LITERATURE CITED

1. A. P. Vinogradov, Uspekh. Khim., 1, 13 (1944).
2. A. P. Vinogradov, Geochemistry of Rare and Distributed Elements in Soils [in Russian], Izd. Akad. Nauk SSSR, Moscow (1957).
3. A. A. Kist, Biological Role of Chemical Elements and the Periodic Law [in Russian], Fan, Tashkent (1973).
4. I. I. Orestova, Cand. Dissertation, Uglubek, Inst. Yad. Fiz., Akad. Nauk Uzbek SSR (1970).
5. R. Rustamov et al., At. Énerg., 33, No. 6, 975 (1972).
6. R. Rustamov et al., At. Énerg., 34, No. 6, 476 (1973).
7. R. Rustamov, Author's Abstract of Candidate's Dissertation, Uglubek, Inst. Yad. Fiz., Akad. Nauk Uzbek SSR (1974).
8. Ya. S. Abdullaev, Author's Abstract of Candidate's Dissertation, Uglubek, Inst. Yad. Fiz., Akad. Nauk Uzbek SSR (1973).
9. V. B. Zlokazov and L. P. Kul'kina, JINR Preprint 10-8162, Dubna (1974).
10. I. Pagden, G. Pearson, and J. Bewers, J. Rad. Chem., 9, 101 (1971).
11. C. Lederer, J. Hollander, and I. Perlman, Tables of Isotopes, J. Wiley and Sons, New York (1968).

PROBLEM OF THE INTENSITY OF AN ELECTRON SYNCHROTRON WITH CYCLOTRON PREACCELERATION

M. Yu. Novikov, Yu. M. Tereshkin, and V. B. Khromchenko

UDC 621.384.634:621.384.683

The paper is devoted to a theoretical estimate of the intensity of the electron synchrotron with cyclotron preacceleration, described in [1]. With this method of injection, the limiting intensity of the electron beam is determined mainly by the effect of Coulomb forces at the instant of electron capture in the acceleration cycle. Synchrotron oscillations are considered, taking account of the azimuthal component of the electric field of the beam space-charge, and the limiting intensity is found from the conditions which correspond to collapse of stability of these oscillations. The general procedure for the calculations is taken from [2, 3] and differs only in that the radius of curvature of the beam considered (~1.6 cm) is comparable with its dimensions. As the main purpose of the paper consists in finding the lower estimate for the limiting intensity, the screening effect of the walls on the beam is not taken into account and, moreover, only the azimuthally homogeneous charge distribution is considered [2, 3]. The beam is assumed to be infinitely long in the axial direction. Figure 1 shows the dependence of the intensity on the amplitude of the uhf field for the case when the guiding magnetic field increases according to the resonance law found in [4]. Figure 2 shows the dependence of the intensity on the delay time $\tau = [(2\ddot{B}/B)|_{t=0}]^{1/2}$, depending on the parasitic reactivity in the GIT circuit. It can be seen that a reduction of the delay above a certain characteristic value leads to a sharp fall in intensity of the beam. The curves obtained are found to be in qualitative agreement with the experimental curves [1].

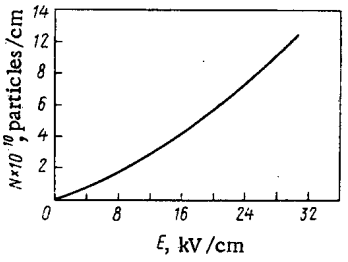

Fig. 1

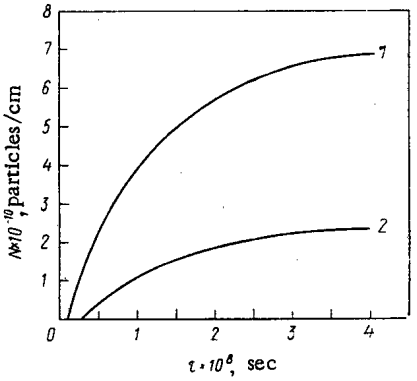

Fig. 2

Fig. 1. Dependence of limiting beam intensity on the amplitude of the field.

Fig. 2. Dependence of limiting beam intensity on the delay time 1) E = 25 and 2) 12.5 kV/cm.

LITERATURE CITED

1. S. P. Velikanov et al., At. Énerg., Vol. 41, No. 2, 113 (1976).
2. A. N. Lebedev, Author's Abstract of Candidate's Dissertation, Fiz. Inst. Akademii Nauk SSSR, Moscow (1968).
3. Yu. A. Khlestkov and Yu. M. Tereshkin, Zh. Tekh. Fiz., 41, 339 (1971).
4. A. V. Gryzlov et al, Zh. Tekh. Fiz., 42, 13 (1972).

Translated from Atomnaya Énergiya, Vol. 41, No. 2, pp. 125-131, August, 1976. Original article submitted July 24, 1975.

EFFECT OF HARD ORE-ENCLOSING ROCK ON THE EFFICIENCY OF UNDERGROUND LEACHING

I. K. Lutsenko, A. A. Burykin, and V. K. Bubnov

UDC 669.823

In this project, a group of experiments is carried out to determine the effect of the granulometric composition of ore-enclosing rock, crushed by an explosion, on the uranium extracted from it, by studying the dynamics of motion of solutions of sulfuric acid into the interior of ore fragments, the kinetics of the leaching process, and the completeness of uranium extraction. Widely abundant ore-enclosing rocks were used in the experiment (Table 1) containing almost identical uranium minerals — pitchblende and sooty uraninite, forming veins and impregnations.

It is determined that the rate of movement of a solution of acid in the ore fragments is not constant and decreases with penetration into the fragment. The maximum rate is observed at a depth of 10 mm.

The process of capillary leaching of uranium with solutions of sulfuric acid from different rocks proceeds with unequal kinetics, as a result of which the uranium extraction varies from 20 to 98%. The rocks can be arranged in the following series, according to the intensity and completeness of uranium extraction: felsite-porphyry, granite, argillite, trachydacite, and basalt.

TABLE 1. Characteristics of Rock and Dynamics of Motion of Solutions of H_2SO_4 inside Ore Fragments

Ore-enclosing rock	Porosity		Solution movement rate, mm/h, to depths 10; 20;30;40;60, and 100 mm resp.
	total	effective	
Felsite-porphyry	1,5	1,1	0,16; 0,1; 0,08; 0,06; 0,005
Granite	2,4	0,89	0,1; 0,09; 0,03; 0,01; 0,003
Basalt	1,3	0,61	0,01; 0,008; 0,002; 0,001; 0,0003
Trachydacite	2,54	0,57	0,3; 0,01; 0,008; 0,003; 0,001; 0,0005
Argillite	1,1	0,72	0,1; 0,05; 0,008; 0,003; 0,001; 0,0005

Table 2 shows the granulometric composition of the ore fragments, which must be achieved during crushing of the various rocks by an explosion, to prepare them for the process of sulfuric acid leaching, with the aim of extracting uranium in quantities of 77-93.5%.

TABLE 2. Results of Uranium Leaching from Rock

Ore-enclosing rock	Granulometric composition of batch		Uranium content, %	Duration of leaching, days		Extracted uranium in solution, %
	size, mm	yield of grades, %		active time	total time	
Felsite-porphyry	—200+100	9,9				
	—100+50	21,8	0,215	102	150	93,5
	—50+25	24,2				
	—25+0	44,1				
Granite	—200+100	13,0				
	—100+50	22,0	0,055	83	120	91,0
	—50+25	28,0				
	—25+0	37,0				
Argillite	—200+100	10,0				
	—100+50	15,8	0,079	84	180	84,0
	—50+25	22,0				
	—25+0	52,2				
Trachydacite	—200+100	5,0				
	—100+50	9,0	0,050	160	280	77,5
	—50+20	30,0				
	—25+0	56,0				

Original article submitted May 21, 1975.

INTERPRETATION OF AUTOIONIC IMAGES OF THE DISLOCATION STRUCTURE OF URANIUM BY MEANS OF A COMPUTER

A. L. Suvorov and T. L. Razinkova

UDC 535.82:546.791

In order to interpret autoionic images of samples of α-uranium containing dislocations, a simulation program has been developed and carried out for the matching contrast of images by means of a computer. The program takes into account the anisotropy of the elastic properties of the material; the calculation of the atomic shifts in the dislocation field is carried out in accordance with [1]. The basis of the simulation is the method of thin shells [2]. The local brightness of the images of different atoms is taken into account by the method proposed previously in [3].

The calculations were carried out for two possible uranium orientations: [010] and [001]. The radius of the cusp of the sample was equal to ~110 Å and the thickness of the surface layer mapped was 0.4 Å. Certain parameters of the atom environment were calculated in passing: the maximum number of neighbors of the i-th order, translation vectors to the corresponding neighboring atoms, and the distance to these atoms.

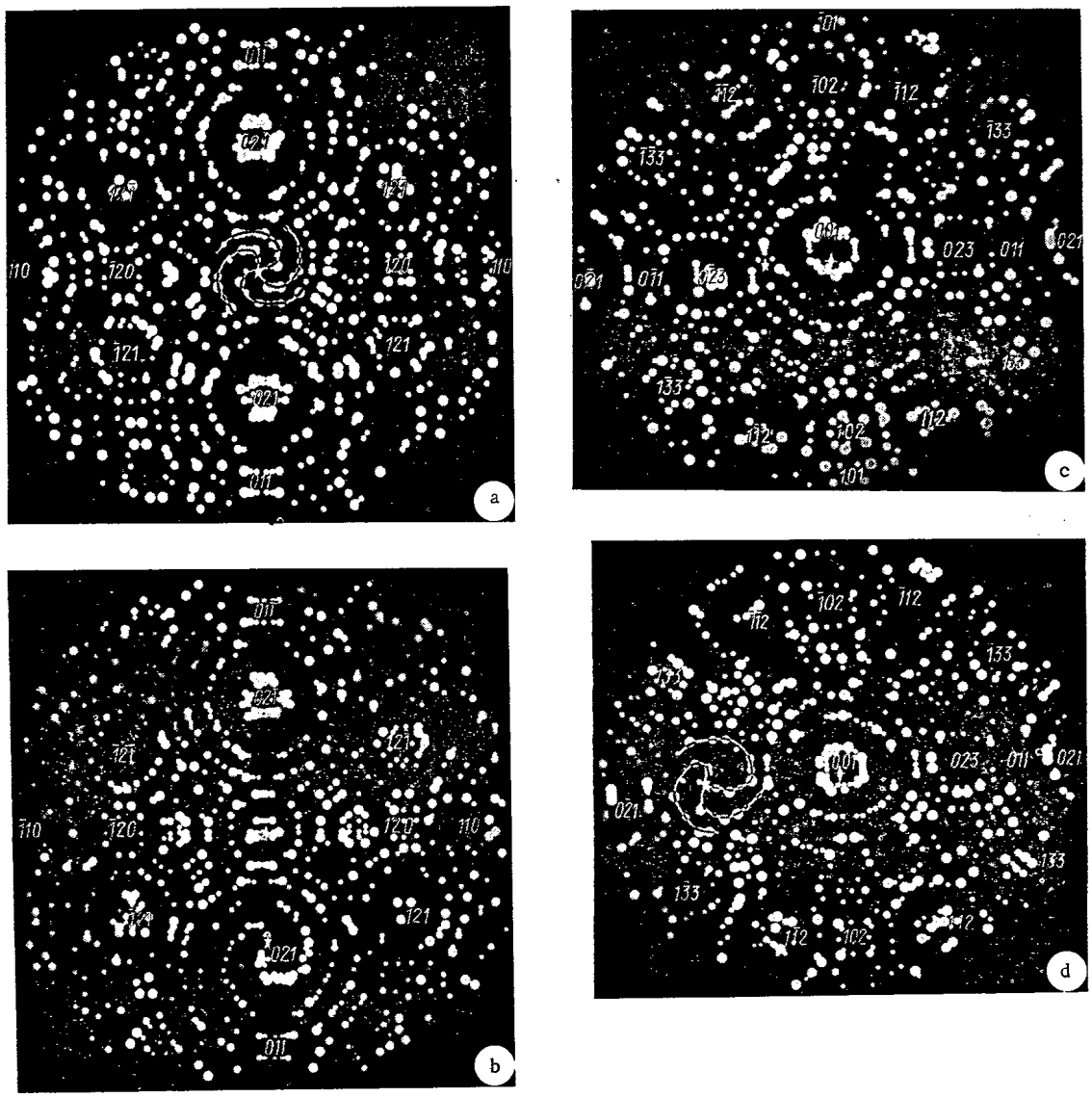

Fig. 1. Models of autoionic images of uranium samples, calculated by computer, oriented along a, b) [010] and c, d) [001]. The point of emergence of the line of dislocation ($b = b_0$ [010] for a and b; $b = c_0$ [001] for c and d) at the surface of the sample is marked by a star.

Examples of the calculated models are shown in Fig. 1. The models correspond to autoionic images of a sample containing a spiral dislocation $\mathbf{b}=b_0[010]$; the orientation is [010]. For model *a*, the line of dislocation emerges at the center of the (010) pole, converting the mapped edge of the crystallographic planes to a four-turn spiral (n=4). For model b, the line of dislocation is shifted parallel to [010] along [001] by 10 c_0 [exit at pole (021)]; the spiral has two turns, n=2. Models c and d are calculated for samples oriented along [001], containing a dislocation $\mathbf{b}=c_0[001]$. The line of dislocation is shifted parallel to [001] along [010] by $5b_0$ in (c) and $10b_0$ (d). The interpretation of the models is not single-valued: n=1 or 2 (c) and $n \approx 3$ (d).

The analysis carried out in this paper of the many models permits a conclusion to be drawn about the nonvalidity of application to uranium of the $(\mathbf{g} \cdot \mathbf{b})$ criterion [4]. Therefore, machine simulation of autoionic images of the dislocation structure of uranium represents a unique method for their interpretation.

LITERATURE CITED

1. M. Yoo and B. Loh, J. Appl. Phys., 43, 1373 (1972).
2. A. Moore, Phys. Chem. Solids, 23, 907 (1962).
3. T. L. Razinkova and A. L. Suvorov, Preprint No. 48, Inst. Teor. i Éksperim. Fiz., Moscow (1974).
4. S. Ranganathan, J. Appl. Phys., 37, 4346 (1966).

Original article submitted August 14, 1975.

DETERMINATION OF THE DEGREE OF SENSITIVITY OF MASS-SPECTROMETERS TO MICROIMPURITIES

M. L. Aleksandrov, N. A. Konovalova and N. S. Pliss

UDC 53.089.52:621.384.8

If a sample being investigated by means of a mass spectrometer contains, in addition to the substance of certain mass M, also a substance of mass $M_1 = M + \Delta M$, $|\Delta M| \leq 1$ to 2, the amount of which in the sample is very small in comparison with M, then we call M_1 a microimpurity to M. The mass M_1 is assumed to lie in the region of mass-scanning in which is extended the so-called "tail" of the peak of the mass M, and therefore reliable and accurate qualities of the detection and estimation of the parameters of the mass-M_1 signal must be determined by the intensity and instability of both the noise signal of the "tail" at this mass, and by the effective signal of the microimpurity at the output of the sensing system (multiplier — amplifier).

In this paper, an algorithm of detection is proposed, based on the theory of statistical solutions and making it possible to introduce an objective measure of the sensitivity of a mass spectrometer to microimpurities. The proposed algorithm takes into account nonlinearity of the multiplier — amplifier system.

The statistical formulation of the problem of detection reduces to verification of the statistical hypothesis concerning the equivalence of the mean values of two sets $H_0: EY = EX$ with a one-sided alternative $H_1: EY > EX$, where the set X defines the measurements outside of the mass peak M_1 and Y defines the measurements at the peak, i.e., H_0 is the confirmation of the absence of an impurity and H_1 is the confirmation of the presence of an impurity.

As the statistical criterion in the paper, the well-known Student criterion t is assumed, with a correction to the number of degrees of freedom in view of the uncertainty of the dispersions [1, 2]. The quantity t is calculated by measurements at the mass peak M_1 and outside of it, and its value is compared with the threshold value t_α, determined by the Student distribution with the corresponding number of degrees of freedom, so that $P(t > t_\alpha) = \alpha$, if H_0 is correct. If it is shown that $t > t_\alpha$, then the solution is applied in favor of H_1. In this case, for every chosen value of α (usually $\alpha \approx 0.01$–0.05), the power of the criterion can be calculated, i.e., the value of $1 - \beta = P(t > t_\alpha)$ with the accuracy of M_1. It is clear that α is the probability of a false detection, and $1 - \beta$ is the probability of a true detection. We call the pair $(\alpha, 1 - \beta)$ the reliability of detection.

Suppose that at the input of the sensing system of the mass spectrometer there is applied a mixture of a useful signal and noise. They can be assumed to be Poisson ion currents with intensities of λ_s and λ_n, respectively. It is clear that the measured output data depend both on λ_s and λ_n and on the characteristics of the sensing system. The paper investigates the dependence of the reliability of detection on λ_s and λ_n and the

characteristics of the system. If λ_p is the intensity of the main peak (mass M), then the ratio λ_s/λ_p, detected with a specified reliability (α, $1-\beta$) can be assumed for the objective microimpurity sensitivity of the instrument.

Examples are given of the calculation of the detection reliability for certain ratios of λ_s/λ_n and for certain characteristics of the sensing system (different electron – electron emission coefficient). Moreover, the construction of a confidence interval is given in the paper, for the intensity of microimpurity signal and for values of the upper and lower levels ($P_1 = 0.95$; $P_2 = 1 - P_1 = 0.05$) of its explicit form.

LITERATURE CITED

1. B. Welch, Biometrika, 29, 350 (1938).
2. B. Welch, Biometrika, 34, 28 (1947).
3. M. L. Aleksandrov, L. N. Gall, and N. S. Pliss, Zh. Teor. Fiz., 44, No. 6, 1302 (1947).
4. J. Neyman and B. Tokarska, J. Amer. Stat. Assoc., 31, 318 (1936).
5. T. E. Harris, Theory of Branching Processes, Vol. 19, Springer-Verlag, New York (1963).

Original article submitted October 6, 1975.

γ FIELD INITIATED BY A MONODIRECTIONAL NEUTRON SOURCE IN AIR

A. V. Zhemerev, Yu. A. Medvedev, and B. M. Stepanov

UDC 539.124.17

We investigate analytically the γ field generated in air as the result of the capture by nitrogen nuclei of neutrons (in the general case from a pulsed source) with energies ≤ 0.45 MeV. The source of unscattered neutrons is assumed monodirectional and the scattered neutrons are treated in the age approximation. Assuming isotropic elastic scattering of neutrons after the first collision the following expression can be derived for the source of capture γ radiation $Q(r, \xi, t)$:

$$Q(r, \xi, t) = q(r, t)\,\Phi(\alpha, \beta\xi). \tag{1}$$

Here $q(r, t)$ is a function describing the capture γ radiation from an isotropic neutron source [1], r is the polar radius, ξ is the cosine of the polar angle, $\alpha = \sqrt{\tau}/\lambda$, $\beta = r/2\sqrt{\tau}$, $\tau(t)$ is the age of a neutron undergoing moderation and depends on the time, and λ is the range of a neutron at the source energy.

Equation (1) is written in spherical coordinates with the origin at the neutron source and the z axis along the direction of emission of the neutrons. $\Phi(\alpha, \beta\xi)$ describes the anisotropy of the source of capture gamma radiation

$$\Phi(\alpha, \beta\xi) = \sqrt{\pi}\,\alpha \exp\{(\alpha - \beta\xi)^2\}\,[1 - erf(\alpha - \beta\xi)],$$

where $erf(x)$ is the error function. The anisotropy decreases as α increases as a result of the spreading out of the neutrons over a larger volume. The anisotropy increases as $\beta\xi$ increases because of the increasing role of neutrons experiencing their first collision close to the point of observation.

Equation (1) was used to investigate the intensity of the γ radiation initiated by a monodirectional neutron source in air.

It was shown that the anisotropy of the intensity of the γ radiation is more pronounced than the anisotropy of the source of capture γ radiation $\Phi(\alpha, \beta\xi)$ and decreases with increasing distance. This results from the fact that the range of capture γ rays is longer than λ and $\sqrt{\tau}$.

LITERATURE CITED

1. A. V. Zhemerev et al., At. Énerg., 38, 174 (1975).

BASIC LAWS FOR THE FORMATION OF TISSUE DOSES FROM COLLIMATED BEAMS OF MONOENERGETIC NEUTRONS

V. N. Ivanov

UDC 577.3:539.12.04+539.125.52

The distribution of the neutron tissue dose produced by collimated beams is a little-studied area of radiation tissue dosimetry [1]. Tissue doses of neutrons with energies from 100 eV to 1 MeV were calculated in [2] for beams with radii from 0.5 to 6.5 cm.

The present article studies the laws for the formation of the neutron tissue dose and its components using the data from [2]. The recoil nuclei dose buildup factors in the cross section of the beam and the relative neutron depth tissue doses and their components were analyzed for neutron beams of various diameters. These values were compared with similar data for the broad-beam neutron irradiation of the human body.

Figure 1 shows the variation of the recoil-nuclei dose with the beam diameter. It is clear from the figure that the buildup factor varies most rapidly for beams with radii < 3 cm. For larger radii the curves approach a rather gently sloping plateau, more rapidly the lower the neutron energy. As the neutron energy increases, the slope of the plateau increases and its length decreases. For example, for 1000 keV neutrons the plateau region at a depth of 9 cm begins for radii of more than 4 cm where the buildup factor changes from 3.8 to 4.8, i.e., by 26%. Naturally it is higher for broader beams and low-energy neutrons.

Figure 1 shows broad-beam buildup factors corresponding to an infinite beam radius. A comparison of these data with the buildup factors for finite-radius beams shows that the scattering of neutron energy beyond the limits of finite beams increases with increasing depth.

The scattering of energy beyond the beam limits for the dose components arising from the capture of thermal neutrons in nitrogen and hydrogen is appreciably larger than for recoil nuclei. For beams from 2.5 to 6.5 cm in radius at tissue depths < 15 cm the proton dose from the $^{14}N(n, p)^{14}C$ reaction in the cross section of the beam is ~10-75% of this dose for broad beams. The gamma dose from the $^{1}H(n, \gamma)^{2}H$ reaction in the cross section of the beams does not exceed 40% of the broad beam dose.

The recoil-nuclei dose remains constant over the cross section of the beams independently of their size. The dose from the capture of thermal neutrons at the edges of beams with radii > 2.5 cm is 10-20% smaller than the average dose in the cross section of the beams. Immediately beyond the beam limits the recoil-nuclei

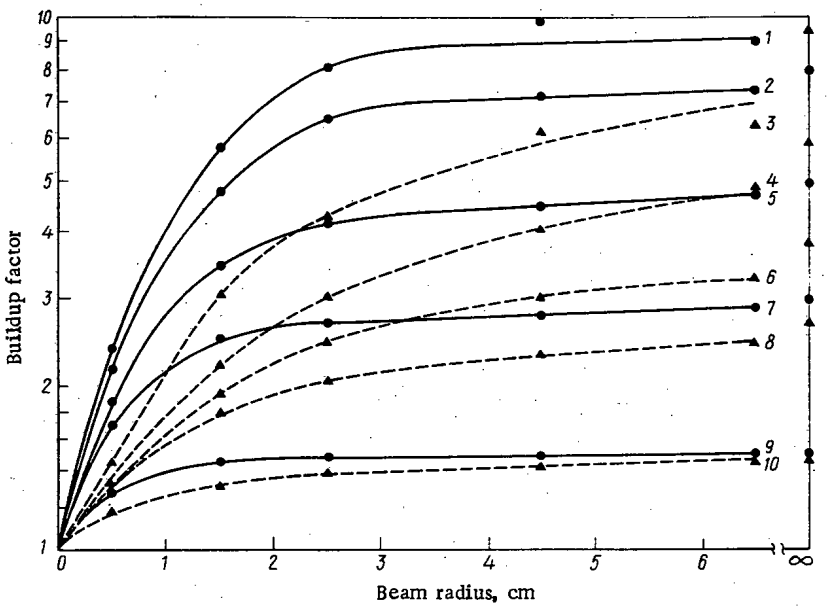

Fig. 1. Recoil proton dose buildup factor as a function of beam radius for various tissue depths along the beam axis, cm. 1) z = 4.5, 2) 3.5, 3) 1.5, 4) 2.5, 5) 9.0, 6) 4.5, 7) 1.5, 8) 2.5; 9, 10) 0.5; ——, — — — —) initial neutron energy 0.1 and 1000 keV, respectively.

dose decreases by a factor of 10-50 at the tissue surface and by 3-10 at a depth of 6-8 cm, depending on the neutron energy and the beam diameter. The dose from the products of the (n, p) reaction in nitrogen and (n, γ) in hydrogen varies almost exponentially with the distance from the beam axis.

The article also discusses the laws for the formation of the integral absorbed dose.

LITERATURE CITED

1. V. G. Zolotukhin et al., Neutron Tissue Doses in the Human Body [in Russian], Atomizdat, Moscow (1972).
2. V. N. Ivanov et al., At. Énerg., 39, No. 5, 360 (1975).

Original article submitted November 5, 1975.

TOTAL CROSS SECTION FOR THE INTERACTION OF COLD NEUTRONS WITH WATER

S. B. Stepanov and V. E. Zhitarev

UDC 539.171.02.162.2

Using a longwave crystal spectrometer we have measured the total cross sections for the interaction of cold neutrons with light water in the liquid and gaseous states at several temperatures by the transmission method. The measurements were performed [1] with liquid water for neutron wavelengths $\lambda = 15$-19 Å and with water vapor in the $\lambda = 8$-19 Å range. The total cross sections obtained are shown in Tables 1 and 2.

For the range of wavelengths investigated there were no appreciable deviations from a linear dependence of the cross section σ_s on λ. The temperature dependence of the scattering cross sections and the slopes $\Delta\sigma_s/\Delta\lambda$ for the liquid are related to the temperature changes of the structure and the dynamics of water, in particular to the change of the concentration of free molecules. The cross sections obtained for vapor are 5-10% larger than those calculated from the Krieger — Nelkin model, while the slopes agree with the calculated values to within ~4%.

TABLE 1. Total Interaction Cross Section for Liquid Water, b

T, °K	λ, Å				
	15	16	17	18	19
294	302±8	308±10	321±7	331±11	342±8
353	379±8	404±8	423±8	442±10	455±15
403	461±12	477±11	509±9	534±9	558±10
453	524±16	539±14	582±15	614±18	649±25
488	590±18	629±22	653±22	697±24	715±18
523	686±27	693±16	733±35	767±18	823±31

* $1\,b = 10^{-28}\ m^2$.

TABLE 2. Total Interaction Cross Sections for Water Vapor

T, °K	λ, Å											
	8	9	10	11	12	13	14	15	16	17	18	19
403							530±30	568±29	583±26	633±30	686±21	696±18
423	335±31	379±20	405±21	415±19	479±21	506±19	556±13	584±16	627±17	649±16	682±14	751±19
453	323±19	389±19	428±19	457±18	501±17	524±23	580±12	624±16	645±12	704±11	748±11	767±14
473	353±13	382±14	435±24	480±18	522±20	553±21	595±16	637±16	674±14	713±14	751±13	780±34
513	361±15	412±15	433±13	495±13	536±14	580±7	613±6	660±10	691±8	731±12	751±9	807±9
553	376±21	408±12	451±23	484±14	540±14	587±14	612±10	670±13	691±15	738±12	790±16	832±16

LITERATURE CITED

1. S. B. Stepanov et al., At. Énerg., 37, No. 4, 351 (1974).

Original article submitted November 12, 1975.

EFFECT OF THE COMPOSITION OF FRIABLE ORE-BEARING ROCKS ON THE EFFECTIVENESS OF THE PROCESS OF UNDERGROUND LEACHING

A. A. Burykin, I. K. Lutsenko,
B. V. Vorob'ev,* and S. I. Korotkov

UDC 669.823

The intensity of the process of underground leaching and the completeness of the extraction of uranium from a nonuniform ore-bearing stratum is determined by the rate and degree of extraction of uranium from the individual layers of rock which have different lithological composition. In the present communication we give the results of experiments on the extraction of uranium from samples of a productive horizon composed of continental gray sands, argillaceous sands, silts, and clays, with some fragments of carbonified flora (Table 1).

The tests were carried out in cylindrical Plexiglas tubes 0.25 m long and 9 cm^2 in cross-sectional area, The ore was charged into the tubes when the model was in a vertical position, a little at a time, with gradual wetting of the investigated material from below with water. When the tests were carried out, the model was subjected to a constant pressure gradient equal to unity (J = 1). In the tests involving the extraction of uranium from coals, fragments of carbonified wood measuring 6×3×3 cm were placed in sterile quartz sand. The rate of filtration of the solution through the sand—coal system was maintained at 0.18 m/day.

* Deceased.

TABLE 1. Characteristics of Ore Samples

Samp No.	Rock	0.01-mm fraction, %	Filtration coef. K, m/day	U in sample, %
1	Medium-grained slightly clayey sands	5,8	0,16	0,049
2	The same	6,4	0,14	0,080
3	Uneven-grained clayey sands	25,9	0,01	0,075
4	The same	22,6	0,01	0,048
5	Medium-grained and large-grained sands	3,0	1,0	0,022
6	The same	3,1	1,2	0,029
7	Medium-grained sands with organic remnants*	5,5	0,3	0,019
8,9	Carbonified wood remnants	—	20†	2,10; 1,20

*C_{org} = 1.5%.
†With respect to the surrounding sands.

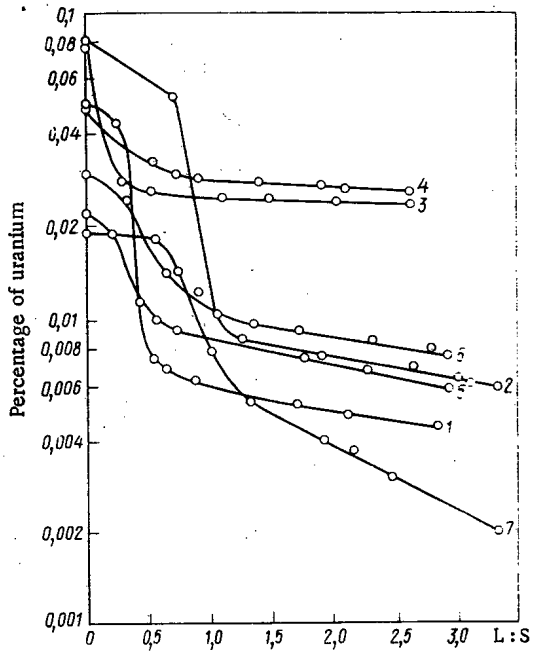

Fig. 1. Variation of uranium content of samples during the leaching process (the numbers next to the curves correspond to the numbers of the samples in Tables 1 and 2).

Translated from Atomnaya Énergiya, Vol. 41, No. 2, pp. 132-133, August, 1976. Original article submitted May 21, 1975; revision submitted February 16, 1976.

TABLE 2. Extraction of Concentration of Uranium in Product Solutions

Sample No.	U in sample, %	First stage				Second stage								U in sample after test, %
		L:S = 0,5		L:S = 1,0		L:S = 1,5		L:S = 2,0		L:S = 2,5		L:S = 3,0		
		C	E	C	E	C	E	C	E	C	E	C	E	
6	0,029	0,26	45	0,1	63	0,03	68	0,01	71	0,01	74	0,01	76	0,007
5	0,022	0,23	55	0,02	60	0,02	65	0,013	68	0,013	71	0,013	72	0,006
1	0,049	0,65	65	0,22	88	0,01	89	0,01	90	0,01	91	—	—	0,004
2	0,080	0,40	25	0,9	87	0,03	89	0,16	90	0,016	91	0,015	92	0,006
3	0,075	0,99	66	0,03	67	0,015	68	0,013	69	—	—	—	—	0,024
4	0,048	0,30	32	0,096	43	0,01	44	0,01	45	0,01	46	—	—	0,026
7	0,019	0,016	4	0,167	48	0,1	76	0,013	79	0,017	84	0,02	90	0,002

Notes. C = concentration, g/liter; E = extraction, %.

The leaching reagent used was a 30 g/liter solution of sulfuric acid. The tests ended with a uranium concentration of 1-3 g/liter in the production solutions. The results of the experiments on the extraction of uranium from ores, as a function of the yield of the production solutions, are shown in Table 2 and Fig. 1, from which it can be seen that two stages can be distinguished in the uranium-leaching process from the standpoint of intensity of extraction.

In the first stage ($L:S \leq 1$) the uranium enters intensively into solution, with the intensity determined by the direct interaction of the filtering solvent with the surface of the ore particles. The process takes place predominantly with convective diffusion [1, 2].

From clayey sands with a pelite fraction of 22-26% the extraction of uranium in this stage amounts to 43-67% (see Fig. 1, curves 3 and 4), with a residual content of 0.028-0.025% in the sample. The extraction of uranium from samples with a pelite-fraction content of 3-6.4% (see Fig. 1, curves 1, 2, 5, and 6) is 60-88% in the first stage, with a residual uranium content of 0.06-0.012% in the sample.

In the second stage the uranium goes into solution extensively because molecular diffusion predominates. In this stage the increment in the extraction of uranium from clayey sands (samples 3 and 4) is no more than 1% per unit of L:S, and the value for sands with a low pelite-fraction content (samples 1, 2, 5, and 6) is 1.6% (see Table 2). The extraction for L:S = 2.5-3.0 amounts to 72-92% for ores of this lithological type.

For the leaching of uranium from samples with a high organic-remnant content ($C_{org} = 1.5\%$) we observe a more complete extraction of the uranium into the solution. For L:S = 1 the extraction of uranium is 48% when it is present in an amount of 0.167 g/liter in the solution (see Table 2). When the L:S ratio is further increased to 3, we can increase the uranium-extraction level to 90%, with a residual content of 0.002% in the sample (see Fig. 1, curve 5).

The extraction of uranium from carbonified wood remnants with an initial content of 2.1% and 1.2% amounted to 94-95% over a 32-day period, with a residual content of 0.078-0.111% in the coals. The maximum, average, and minimum uranium content values in the production solution at the end of the test were 0.5, 0.04, and 0.01 g/liter, respectively.

Thus, the intensity and completeness of extraction of uranium from a multilayer ore-bearing stratum with nonuniform water-bearing properties depends on the coefficients of filtration of the lithological types of the ore-bearing rocks. The higher the coefficient of filtration, the more intensive will be the leaching of the uranium. Nonuniformity in the lithological composition of the ore-bearing rocks must result in uneven extraction of the uranium from the ore-bearing horizon.

The process of leaching of uranium from ores is divided into two stages according to the intensity of extraction. The first stage is characterized by intensive leaching, during which 63-88% of the total uranium content of the ore is extracted under experimental conditions, while in the second stage the extraction intensity is low.

LITERATURE CITED

1. V. G. Bakhurov, S. G. Vecherkin, and I. K. Lutsenko, Underground Leaching of Uranium Ores [in Russian], Atomizdat, Moscow (1968).
2. I. K. Lutsenko, V. G. Bakhurov, and R. S. Meshcherskaya, At. Énerg., 27, No. 6, 500 (1969).

DETERMINATION OF SPECIFIC ENERGY LOSSES BY CHARGED PARTICLES IN MATTER

G. N. Potetyunko

UDC 539.12.04

One of the methods for determing specific energy losses by charged particles in matter is based on measurement of the reduction in the energy of a beam of particles passing through a layer of test material; one transmits a beam of charged particles through a layer of absorber of thickness d and measures the energy of the beam ahead of the absorber (E_1) and beyond it (E_2). One takes the ratio

$$\Delta E/\Delta x=(E_1-E_2)/d \tag{1}$$

as the value of dE/dx at an energy E given by

$$E=(E_1+E_2)/2. \tag{2}$$

It is assumed that the method described gives a value of dE/dx which differs little from the true value for sufficiently thin absorbers.

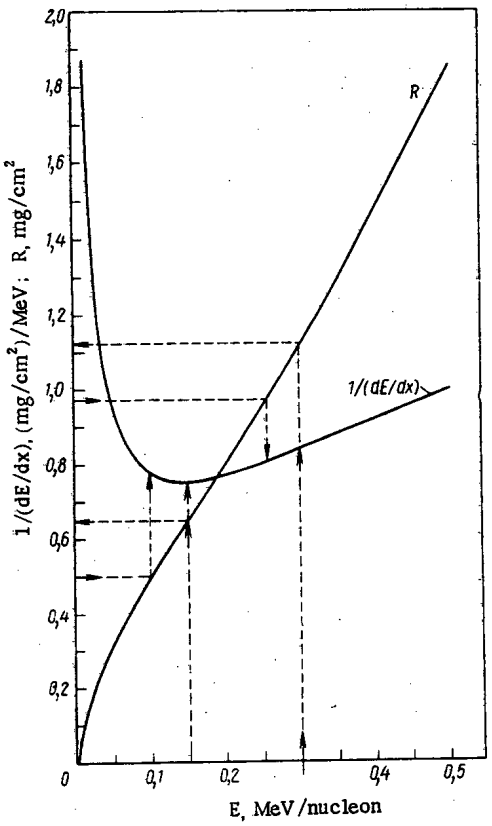

Fig. 1. Range R(E) and quantity 1/(dE/dx) for the case of ^{4}He-ion transmission through aluminum (see tables in [1]).

Translated from Atomnaya Énergiya, Vol. 41, No. 2, pp. 134-135, August, 1976. Original article submitted October 23, 1975; revision submitted February 23, 1976.

In the present paper, an attempt is made at rigorous justification of this method for the determination of dE/dx, and the factors influencing its error are investigated. In addition, another method for the analysis of experimental data obtained in the type of experiment described is proposed which is of a more universal nature.

We have

$$R(E)=\int_0^E \frac{dE}{dE/dx}. \tag{3}$$

Here, R(E) is the range of the particles in matter.

We assume that in some interval $[E_1, E_2]$ the function dE/dx is closely approximated by the following expressions:

$$\frac{dE}{dx}=\frac{1}{a_1+2a_2E} \tag{4}$$

or

$$\frac{1}{dE/dx}=R'_E(E)=a_1+2a_2E. \tag{5}$$

We then have from Eqs. (5) and (3)

$$R(E)=a_0+a_1E+a_2E^2. \tag{6}$$

From Eq. (6) we obtain

$$R(E_1)-R(E_2)=a_1(E_1-E_2)+a_2(E_1^2-E_2^2). \tag{7}$$

The difference $R(E_1) - R(E_2)$ is the thickness d of the absorber, and we finally have in place of Eq. (7)

$$\frac{\Delta E}{d}=\frac{1}{a_1+a_2(E_1+E_2)}, \tag{8}$$

where $\Delta E = E_1 - E_2$.

The right side of Eq. (8) completely matches the right side of Eq. (4) if in the latter we take into account the condition (2), and the left side of Eq. (8) matches the right side of Eq. (1).

Thus it is shown that if in the interval $[E_1, E_2]$ the range of a particle is exactly described by Eq. (6), then Eq. (1) under the condition (2) gives a completely accurate value of dE/dx regardless of the thickness of the absorber.

We estimate the effect of an error in the approximation (6) on the error in the determination of dE/dx. We assume that

$$R(E)=a_0+a_1E+a_2E^2+\Delta(E), \tag{9}$$

where $\Delta(E)$ is the error of the approximation. We assume that $\Delta(E)$ and its derivative Δ'_E are sufficiently small quantities. We then have

$$\frac{dE}{dx}-\frac{\Delta E}{d}\approx\frac{-\Delta'_E\left(\frac{E_1+E_2}{2}\right)+\frac{\Delta(E_1)-\Delta(E_2)}{\Delta E}}{[a_1+a_2(E_1+E_2)]^2}. \tag{10}$$

Equation (10) makes it clear that the error of this method for the determination of dE/dx is determined by the errors $\Delta(E)$ and Δ'_E and the quantity ΔE. It is typical that, as is learned, this method gives sufficiently reliable results only in the case where within the interval $[E_1, E_2]$ there is sufficiently accurate simultaneous approximation of two quantities — the range and its derivative:

$$\begin{aligned} R(E)&=a_0+a_1E+a_2E^2;\\ R'_E(E)&=\frac{1}{dE/dx}=a_1+2a_2E. \end{aligned} \tag{11}$$

We now investigate how the error of the method varies with change in ΔE. We assume

$$\Delta(E)\approx a_3E^3. \tag{12}$$

We then obtain in place of Eq. (10)

$$\frac{dE/dx-\Delta E/d}{(dE/dx)_{\exp}} \approx \frac{a_3}{4}\Delta E^2\left(\frac{dE}{dx}\right)_{\exp}, \tag{13}$$

where $(dE/dx)_{exp}$ is the experimental value of dE/dx found by the method described. Consideration of higher powers in Eq. (12) for $\Delta(E)$ does not change the nature of the dependence of the error of the method on ΔE.

For a visual evaluation of the validity of approximation (11) in the interval $[E_1, E_2]$ for various absorber thicknesses and incident particle energies, it is very convenient to use a diagram in which two curves are plotted $-R(E)$ and $1/(dE/dx)$ (see Fig. 1). We assume that the thickness of the aluminum foil is 150 $\mu g/cm^2$. From Fig. 1, it is clear that for ^{4}He-ion energies of 0.30 or 0.15 MeV/nucleon we arrive respectively at the linear or curvilinear portions of the $1/(dE/dx)$ curve, i.e., the approximation (11) either holds or does not hold.

Thus this method for the determination of dE/dx gives sufficiently reliable results only at energies which are sufficiently removed from the region of the maximum in the dE/dx curve. In order to obtain such results by the method described for energies in the region of the maximum in the dE/dx curve, or ahead of it, it is necessary to prepare very thin films of test material (~20-30 $\mu g/cm^2$), which is complicated and leads to additional uncontrollable errors because of possible nonuniformity in thickness. Nevertheless, the experimental scheme for the determination of dE/dx can be maintained as before in this energy region also if one uses another method for analyzing the experimental data. We briefly describe this method.

We assume that in the interval $[E_{min}, E_{max}]$ the range is approximated by a polynomial of n-th degree with respect to energy,

$$R(E)=a_0+a_1E+a_2E^2+\ldots+a_nE^n. \tag{14}$$

Then

$$\frac{dE}{dx}=\frac{1}{R'_E(E)}=\frac{1}{\sum\limits_{k=1}^{n} ka_kE^{k-1}} \tag{15}$$

and

$$d/\Delta E=y=a_1F_1+a_2F_2+\ldots+a_nF_n. \tag{16}$$

Here,

$$\left.\begin{aligned} &F_1=1;\ F_2=E_1+E_2;\\ &F_3=E_1^2+E_1E_2+E_2^2;\\ &F_n=E_1^{n-1}+E_1^{n-2}E_2+\ldots+E_1E_2^{n-2}+E_2^{n-1}. \end{aligned}\right\} \tag{17}$$

The general scheme of the proposed method is as follows. We assume there is a set of experimental results

$$d_i,\ E_{1ij},\ E_{2ij}. \tag{18}$$

Using them, we construct a table of the quantities appearing in Eq. (16):

$$F_{2p},\ F_{3p},\ \ldots,\ F_{np},\ y_p;\quad p=1,\ 2,\ \ldots,\ N, \tag{19}$$

following which we determine the parameters a_k, k = 1, 2, ..., n, by the method of least squares. Knowing these parameters, we calculate the difference $R-a_0$ and dE/dx from Eqs. (14) and (15). To determine the parameter a_0, it is necessary to know the range at any value of the energy in the interval $[E_{min}, E_{max}]$.

The basic feature of this method for the analysis of experimental data is that its use is not associated with any limitations on absorber thickness; only one limitation is important here — the particles must pass through the absorber. This circumstance makes it possible to improve the experimental scheme. Using a sufficiently thick absorber, we measure the energy E_{2ij}; we simultaneously record the backscatter spectrum and reconstruct dE/dx from it [2]. Thus dE/dx can be determined by two completely independent methods from the results of a single experiment.

In conclusion, the author takes great pleasure in thanking É. T. Shipatov for valuable discussions of the problems touched on in this paper.

LITERATURE CITED

1. L. Northcliffe and R. Schilling, Nucl. Data, A7, 233 (1970).
2. E. Sirotinin et al., Rad. Eff., 15, 149 (1972).

USE OF "BEAM UNFOLDING" FOR CALCULATION OF β-FLUX ABSORPTION IN THE SEGMENT MODEL

V. A. Kuz'minykh and S. A. Vorob'ev

UDC 539.121.7

This paper discusses the use of the segment method in the solution of the problem of β-particle interaction with nonflat absorbers. In the segment method, the function of the particle differential flux I(T, x, u) is represented in the form of an expansion in Fourier series and Legendre polynomials. The transition from the j-th segment of particle trajectory to the (j+1)-th segment is performed through the recurrence relations for the coefficients of the expansion. Entrance into the computing cycle at j = 0 is accomplished by assignment of the coefficients in the expansion of the source function $I_0(T, x, u)$ [1, 2].

$$I_{lk}=\frac{2\pi}{L}\int_{-L/2}^{L/2} dx \exp\left(-i\frac{2\pi}{L}kx\right)\int du I_0(T, x, u)P_l(u), \tag{1}$$

where L is the period of the expansion in Fourier series; $U=\cos\theta$; θ is the angle between the direction of particle motion and the OX axis.

If the variables are separated in the source function in order to bring out the angular dependence in explicit form, we have

$$I_0(T, x, u)=N(T)f(x)\varphi(u), \tag{2}$$

where N, f, and φ are functions describing the energy spectrum, spatial distribution, and angular distribution of source particles, respectively.

For a monoenergetic particle beam, one can write

$$I_0(x, u)=\delta(x-x_0)\varphi(u), \tag{3}$$

where x_0 is the coordinate of the front face of the absorber.

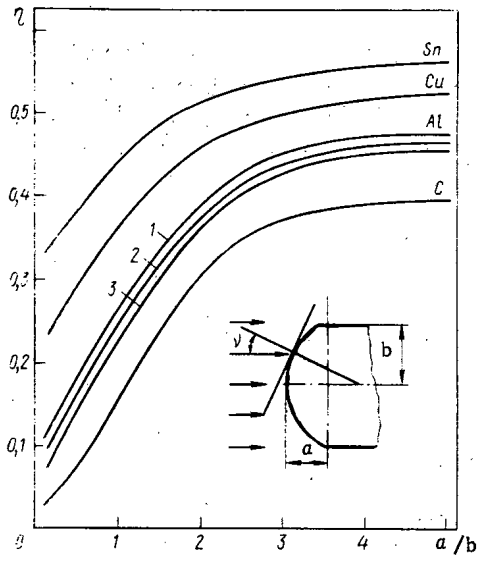

Fig. 1. Dependence of the backscattering coefficient of 0.5-MeV positrons for C, Cu, and Sn on the ratio a/b of the semiaxes of the ellipsoid; 1, 2, 3) respectively 0.2-, 0.5-, and 1-MeV positrons on aluminum.

Translated from Atomnaya Énergiya, Vol. 41, No. 2, pp. 136-137, August, 1976. Original article submitted November 6, 1975.

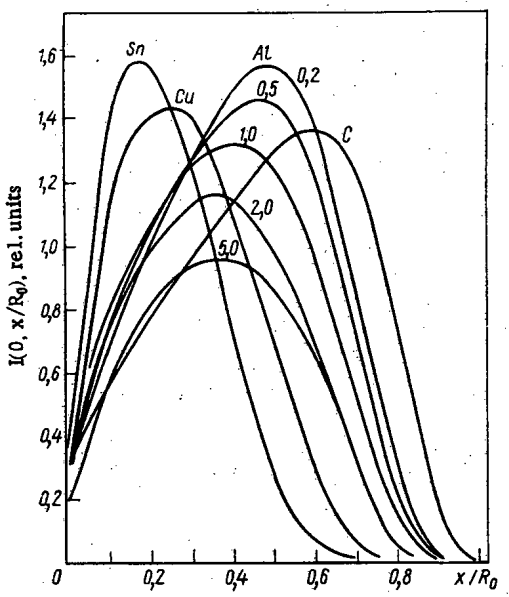

Fig. 2

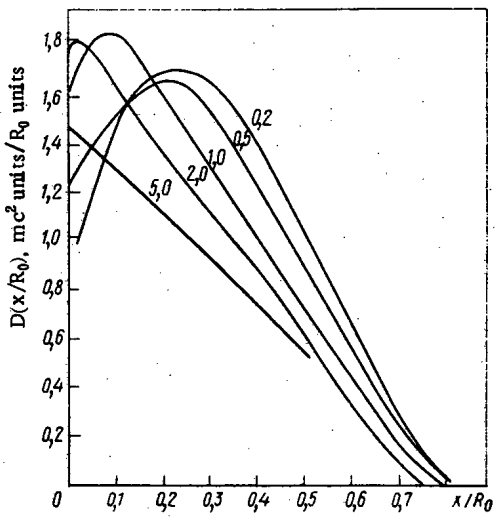

Fig. 3

Fig. 2. Distribution of annihilation centers with depth for C, Cu, and Sn absorbers, an initial positron energy of 0.5 MeV, and $a/b = 1$; numbers above the curves for aluminum denote the value of a/b.

Fig. 3. Distribution of absorbed energy over depth for an aluminum absorber and 0.5-MeV positrons; numbers denote the value of a/b.

In writing down the source functions (2) and (3), the interaction of some arbitrary particle flux I_0^1 with a nonflat absorber can be represented as the interaction of a particle flux I_0 with a flat absorber. For this purpose, the original distribution of particles in the beam should be "unfolded" into a distribution over angle with respect to the normal to the absorber surface. The problem is solved by the general scheme of the segment method [2] using the resultant angular distribution $\varphi(u)$. The described operation of "beam unfolding" makes it possible to obtain from the segment method integral characteristics at the absorber surface for particle interaction with matter and provides an opportunity to calculate problems involving different geometries by means of a single program.

Here we solve the problem for a parallel uniform beam of particles (beam radius r_0) incident on an absorber with a front face that has the shape of an ellipsoid of rotation. The geometry of the calculation is shown in Fig. 1. The operation of "beam unfolding" consists of the transition from the radial beam density $\varphi_1(y) = y/\pi r_0^2$ to the probability density $\varphi(u)$ for the impact of particles on the surface of the absorber at an angle θ with respect to the normal.

The desired angular distribution has the form

$$\varphi(u) = y(u)\frac{dy}{du} = \frac{a^2 u}{\pi r_0^2 [1 - u^2(1 - a^2/b^2)]^2} \tag{4}$$

and the cosine of the maximum angle of particle incidence on the surface is

$$u_{max} = \{(b^2 - r_0^2)/[b^2 - r_0^2(1 - a^2/b^2)]\}^{1/2}. \tag{5}$$

If the ratio of the semiaxes of the ellipse $a/b \to 0$, the angular distribution approaches the distribution corresponding to normal incidence of particles on the absorber, $\varphi(u) \to \delta(u - 1)$.

Input data obtained from Eqs. (1), (3), and (4) for $u_{max} = 0$ were used in a program for calculation of the characteristics of positron transport through matter in which fluctuations of energy loss and positron annihilation in flight were included. The results obtained describe the interaction of an "unfolded beam" of particles with a flat absorber and of a uniform beam with a solid of rotation, the size of which is considerably greater than the particle range R_0 in the given material. In the present case, $b > R_0$.

Figure 1 shows the dependence of the total backscattering coefficient for 0.5-MeV positrons on the ratio a/b of the semiaxes of the ellipsoid of rotation. The magnitude of the total backscattering coefficient depends

strongly on the angle of particle incidence for a flat absorber [3]. For an ellipsoidal absorber, this dependence is manifested in integral form. For slight curvature of the sample surface, $(a/b) < 2$, the backscattering coefficient increases rapidly as a/b increases with the dependence $\eta(a/b)$ being stronger for light materials than for heavy materials. When the curves are extrapolated to $a/b = 0$, the values $\eta(0)$ agree with the previously calculated backscattering coefficients for normal incidence of particles on a flat absorber [4]. Significant changes in the relationship $\eta(a/b)$ do not occur when there is a change of incident-particle energy to 1 MeV.

The distribution with absorber depth of annihilation centers and of absorbed energy broadens markedly with increase in a/b and the maxima are shifted toward the face. Furthermore, the maximum depth of particle penetration is unchanged for an aluminum absorber (Figs. 2 and 3). The curves are compressed and shifted toward the face (Fig. 2) when $a/b = 1$ as the atomic number of the absorber material increases because of the increasing importance of the role of elastic scattering. The tail of the distribution curve for absorbed energy becomes linear as a/b increases. This is clearly seen in Fig. 3. The results indicate strong dependence of spatial distributions and backscattering on the form of the initial angular particle distribution $\varphi(u)$. This makes it possible to talk about the applicability of the "beam unfolding" operation for the determination of the form of $\varphi(u)$ for which the absorbed energy, or any characteristic associated with it, is distributed over absorber depth according to a previously assigned law. With linear dependence, one can obtain a uniform value of absorbed dose over thickness by bilateral irradiation of an object.

LITERATURE CITED

1. O. Evdokimov and A. Yalovets, Nucl. Sci. and Engng., 55, 67 (1974).
2. S. A. Vorob'ev and V. A. Kuzminykh, in: Applied Nuclear Spectroscopy [in Russian], V. G. Nedovesov (editor), No. 5, Atomizdat, Moscow (1975), p. 3.
3. S. A. Vorob'ev and V. A. Kuz'minykh, Program and Reports of XXV Conference on Nuclear Spectroscopy and Nuclear Structure [in Russian], Nauka, Moscow (1975), p. 483.
4. Y. Kuzminykh, I. Tsekhanovski, and S. Vorob'ev, Nucl. Instrum. and Methods, 118, 269 (1974).

MEASUREMENT OF SPECTRAL CHARACTERISTICS OF SLOW-NEUTRON FIELDS USING CADMIUM RATIOS OF ACTIVATION DETECTORS

I. A. Yaritsyna, E. P. Kucheryavenko, I. A. Kharitonov, and T. M. Kuteeva

UDC 539.125.516.22.074.85.08

In moderating systems, the energy distribution of the slow-neutron flux density has the form

$$\varphi(E)=\varphi_{th}\frac{E}{(kT_n)^2}\exp(-E/kT_n)+\varphi_{epi}\frac{\Delta(E/kT_n)}{E^{1+\alpha}}, \quad (1)$$

where φ_{th} is the thermal-neutron flux density; $\varphi_{epi}/\varphi_{th}$ is the ratio between the epithermal flux density and the thermal flux density; T_n is the neutron temperature; α is a parameter which takes into account the deviation of the epithermal neutron spectrum from a 1/E spectrum.

The limit function $\Delta(E/kT_n)$ determines the nature of the distribution near the lower energy threshold for epithermal neutrons μkT_n and has no significant effect on the shape of the spectrum.

A method was proposed [1] for the determination of T_n, φ_{th}, and $\varphi_{epi}/\varphi_{th}$ based on the irradiation of a set of three resonance detectors in a test field, for example, ^{197}Au, Cu, and ^{176}Lu. Compiled tables make it possible to determine the spectral characteristics, except for α, from measurements of the saturation activity of the detectors.

In this report, a method is proposed which makes it possible to determine the spectral characteristics including α using only two resonance detectors in all.

The cadmium ratio for a resonance detector of thickness t [2] is given by the expression

$$R_{Cd}(t)=\frac{G_{th}(t)\,g(T_n)+fC(\alpha,\ T_n)\,G_r(t)\,h}{\frac{g(T_n)}{\hat{R}}-fC(\alpha,\ T_n)\,W'-\frac{1}{F_{Cd}}}\times\frac{(\alpha,\ G_r)\frac{I'}{\sigma_0}}{C(\alpha,\ T_n)\,G_r(t)\,h(\alpha,\ G_r)\frac{I'}{\sigma_0}}, \quad (2)$$

where $C(\alpha,\ T_n)$ is a renormalization correction for the epithermal-neutron fraction

$$f=\frac{1}{1+\varphi_{th}\sqrt{\pi\mu/4}\varphi_{epi}};$$

$h(\alpha,\ G_r)$ is a correction of the reduced resonance integral I' when $\alpha \neq 0$; $\hat{R}$ is the cadmium ratio for a thin 1/V detector; $g(T_n)$ is a coefficient which allows for deviation of neutron absorption cross section from 1/V behavior in the range $E < \mu kT_n$; W' is a coefficient which allows for deviation of the cross section from 1/V behavior in the range $\mu kT_n < E < E_{Cd}$; F_{Cd} is a correction for the absorption of epithermal neutrons in the cadmium filter; G_{th} and G_r are the self-shielding factors for thermal and epithermal neutrons.

TABLE 1. Detector Parameters and Cadmium Ratios

Element	Parameter						
	t, mg/cm^2	F_{Cd}	G_{th}	G_r	σ_0, b	I', b	R_{Cd}
^{197}Au	18,6	1,01	0,981	0,53	98,8±0,3	1513±40	6,32±0,03
^{55}Mn	15,0	1,00	0,992	0,92	13,23±0,10	7,8±0,4	47,7±0,4
^{51}V	63,7	1,00	0,985	1.0	4,93±0,06	0,48±0,1	91±2

Translated from Atomnaya Énergiya, Vol. 41, No. 2, pp. 138-140, August, 1976. Original article submitted November 25, 1975.

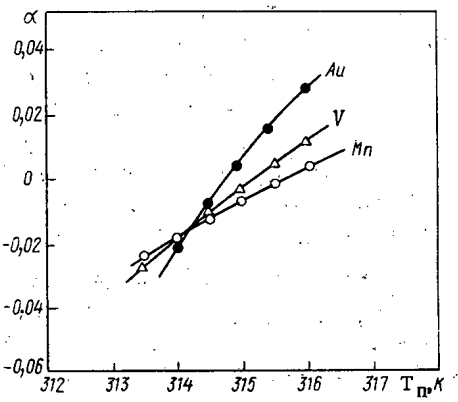

Fig. 1

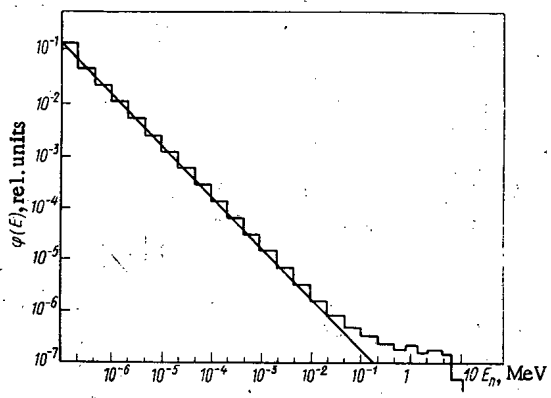

Fig. 2

Fig. 1. Determination of spectral characteristics of a slow-neutron field in a cavity.

Fig. 2. Shape of neutron spectrum in a cavity: ——) 1/E spectrum; histogram gives computed spectrum.

The cadmium ratio for a thin 1/V detector can be expressed after some transformation through the parameter $k(\delta)$ tabulated by Westcott [3] for two values of E_{Cd}:

$$\hat{R}=\frac{0.5+\alpha}{fC(\alpha, T_n)}\left[\frac{4k(\delta)}{\sqrt{\pi}}\right]^{1+2\alpha},$$
$$k(\delta)=\frac{1}{4}\sqrt{\frac{\pi E_{Cd}}{kT_0}}. \qquad (3)$$

The renormalization correction [4] is calculated from the expression

$$C(\alpha, T_n)=(0.5+\alpha)\left(\frac{\mu T_n}{T_0}\right)^{0.5+\alpha}. \qquad (4)$$

According to [5], the coupling equation can be written in the following form:

$$\frac{T_n-T_m}{T_m}=Cf, \qquad (5)$$

where T_m is the moderator temperature and C is a coupling constant.

An analysis of neutron temperatures in various moderators for T_m close to $T_0=293.7$°K showed that $C=3.46\pm0.09$ [6].

After substitution of Eqs. (3)-(5) in Eq. (2), we have

$$R_{Cd}(t)=\frac{G_{th}(t)\frac{3.46g(T_n)T_0}{T_n-T_0}\frac{1}{0.5+\alpha}\left(\frac{\mu T_n}{T_0}\right)^{-0.5-\alpha}+G_r(t)\frac{I'}{\sigma_0}h(\alpha, G_r)}{g(T_n)\frac{1}{0.5+\alpha}\left[\frac{\sqrt{\pi}}{4k(\delta)}\right]^{1+2\alpha}-W'+\frac{1}{F_{Cd}}G_r(t)\frac{I'}{\sigma_0}h(\alpha, G_r)}. \qquad (6)$$

Equation (6) indicates that the cadmium ratio for a resonance detector depends only on T_n and α. By solving a system of equations like Eq. (6) for two resonance detectors, one can determine T_n and α, find f by using Eq. (5), and determine φ_{th} from the saturation activity of one of the resonance detectors by the cadmium-difference method.

Table 1 gives the detector parameters and measured cadmium ratios used for the determination of the spectral characteristics of slow-neutron fields inside a cavity 120 mm in diameter in a polyethylene moderator in the form of a 690-mm cube. The spectra of slow neutrons were obtained by moderation of fast neutrons from six $^{239}Pu(\alpha, n)Be$ sources located symmetrically with respect to the center of the cavity in the moderator at a depth of 33 mm.

The detector parameters σ_0, I' and G_r, F_{Cd} were taken, respectively, from [7, 8].

Values of the characteristics α and T_n were determined by a graphic method from the intersection of the functionals $R_{Cd}(\alpha, T_n)$ in the α–T_n plane (Fig. 1). The average value of the neutron temperature was $T_n = (314 \pm 3)$ °K and $\alpha = -0.015 \pm 0.003$. Analysis of the quantities appearing in Eq. (6) shows that the error in the determination of T_n and α is mainly associated with the group $G_r(t)I'/\sigma_0$, which is determined by the parameters of the detector. To achieve the required accuracy, therefore, one should select detectors for which the resonance parameters and absorption cross sections are well known. The fraction of epithermal neutrons was $f = 0.028 \pm 0.001$ according to Eq. (5). The thermal neutron flux density determined by the cadmium-difference method from the saturation activity of the gold detector was $\varphi_{th} = (5.73 \pm 0.06) \cdot 10^8$ n/m^2-sec.

To obtain an independent estimate of the parameter α, the spectrum of slow neutrons in a cavity in a polyethylene moderator was calculated by the Monte Carlo method. The program BNAB-26 [9] for producing group constants was used in the calculation. The actual source — moderator system was idealized; the fast-neutron sources were represented in the form of a spherical layer with a volume equal to the total volume of all the actual sources and a mean radius of 100 mm; the moderater was represented in the form of a spherical system with the actual volume maintained.

The computed shape of the neutron spectrum in the cavity is shown in Fig. 2 on a logarithmic scale.

To evaluate α, it is necessary to approximate some portion of the spectrum by a straight line. The question of assignment of definite points to the line $y = \alpha \ln E$ can be solved by seeking a line of the indicated form with least variance.

The minimum variance is determined by the error of the calculation performed, which is the result of the uncertainty in the shape of the primary spectrum from the ^{239}Pu(α, n)Be fast-neutron sources, the uncertainty in the values of the microscopic neutron-interaction constants used, and the idealization of the actual source — moderator system.

As shown by analysis, the maximum error is contributed by the uncertainty in the spectrum of the ^{239}Pu (α, n)Be neutron sources. By comparing spectra from ^{239}Pu(α, n)Be sources measured by various methods [5, 10, 11] and representing the entire spectrum in the range 1.0-11.0 MeV in the form of partial amplitudes with an energy width of 1 MeV, one can estimate the mean-square deviation for the partial amplitudes for each of the methods cited. Assuming that the neutrons in the partial amplitudes make an equally probable contribution to the 1/E spectrum in the cavity, which is acceptable in the evaluation of an error, the uncertainty of the source spectrum in the range 1-11.0 MeV makes a contribution $\sigma = \pm 10\%$ to the error of the 1/E spectrum. Fitting the equation of a line with a variance corresponding to $\sigma = 10\%$ showed that the spectrum in the range $1\text{-}5 \cdot 10^3$ eV can be approximated by the line $y = \alpha \ln E$ where $\alpha = -0.015 \pm 0.002$. The calculated and experimental values of the parameter are in satisfactory agreement within the limits of estimated error.

Thus the proposed method has a number of advantages: it makes possible the additional determination of the parameter α; it requires a total of two activation detectors for the determination of all spectral parameters; in the determination of T_n and α, it uses cadmium ratios, for which the measurement technique is simpler than the measurement of detector activities.

The authors are grateful to G. G. Orlov for calculation of the slow-neutron spectrum in the moderator.

LITERATURE CITED

1. R. Nisle, in: Proc. Symp. IAEA on Neutron Dosimetry, Vol. 1, Vienna (1963), p. 111.
2. T. Ryves and E. Paul, J. Nucl. Energy, 22, 759 (1968).
3. C. Westcott et al., in: Proc. II Intern. Conf., Geneva, Vol. 16, (1958), p. 70.
4. T. Ryves, Metrologia, 5, 119 (1969).
5. Neutron Fluence, Neutron Spectra, and Kerma, Rep. ICRU-13, Washington (1969).
6. O. L. Andreev and E. P. Kucheryavenko, Metrologiya, No. 5, 31 (1974).
7. Neutron Cross Sections, Rep. BNL-325, 3rd ed., Vol. 1, USAEC (1973).
8. Proc. Symp. IAEA on Neutron Fluence Measurements, Vienna (1970).
9. L. P. Abagyan et al., Group Constants for Nuclear Reactor Calculations [in Russian], Atomizdat, Moscow (1964).
10. N. D. Tyufyakov et al., At. Énerg., 34, No. 5, 349 (1973).
11. N. D. Tyufyakov and L. A. Trykov, Pribory i Tekh. Éksperim., No. 2, 73 (1973).

INVESTIGATION OF THE REMOVAL OF T AND ^{85}Kr DURING PROCESSING OF IRRADIATED UO_2 IN AN OXYGEN MEDIUM

A. T. Ageenkov and E. M. Valuev

UDC 621.039.713

The development of efficient methods of removal and decontamination of radioactive gaseous fission products of uranium is linked with a study of the removal of T and ^{85}Kr during the processing of irradiated uranium dioxide in an oxygen medium at elevated temperature. This process is considered one of the principal manufacturing operations in the reprocessing of nuclear fuel [1]. The reaction $3UO_2 + O_2 = U_3O_8$ leads to conversion of the dense UO_2 into a finely dispersed powder of U_3O_8 and is accompanied by a change of the cubic crystalline lattice of UO_2 first of all to the face-centered tetragonal lattice of U_3O_7 and then to orthorhombic U_3O_8. The double recrystallization of the fuel considerably increases the mobility of the fission products, including the gaseous products [2]. An increase in the rate of removal of the gaseous fission products promotes crushing of UO_2 during oxidation into uranous—uranic oxide powder with a particle size of up to several microns.

Samples of 3%-enriched UO_2 were investigated in a cladding of zirconium alloy with a diameter of 9.1 mm and length 40 mm; they were opened at the ends. The fuel burnup, calculated by the ^{137}Cs content, amounted to 5600-22,000 MW · day/ton U.

Preliminary experiments on the oxidation of unirradiated samples with the same geometry showed that at a temperature of 400-500°C during the initial time of interaction of oxygen with the oxide fuel, distributed near the open ends of the sample, it takes place quite rapidly. However, the access of oxygen into the reaction zone is hindered in proportion with the consolidation of the U_3O_8 powder formed, and further oxidation of UO_2 almost ceases. In consequence of the high strength and plasticity of the zirconium alloy, rupture of the cladding, as was observed in [3], did not take place. Therefore, the claddings of the samples were subjected to preliminary hydrogenation [4], as a result of which the zirconium alloy completely lost its plasticity and its strength was reduced from 35 to 1-3 kg/mm^2 [5]. During the oxidation processing, the hydrogenated cladding was ruptured by the action of the U_3O_8 pressure, which assisted to completion the reaction $UO_2 \rightarrow U_3O_8$.

A diagram of the experimental facility is shown in Fig. 1. The samples were inserted in the leak-tight ampoule and, with the periodic addition of oxygen, they were maintained for 2 h at a pressure of 300-760 mm

TABLE 1. Conditions and Results of Experiments on the Removal of T and ^{85}Kr from Irradiated UO_2

No. of expt.	Amount of U in sample, g	Conditions of oxygen treat.		Content in original samples, Ci/ton U		Removal of gaseous fission products from UO_2							
						hydrogen treatment				oxygen treatment			
		temperature, °C	holding time, h	T	^{85}Kr	Ci/ton U		% of initial content		Ci/ton U		% of original content after hydrogen treatment	
						T	^{85}Kr	T	^{85}Kr	T	^{85}Kr	T	^{85}Kr
1	8,1	420	2	43±6	1100±300	10,0	11,0	23,3	1,0	14,0	85	42,5	7,7
2	10,2	420	2	170±15	5600±500	31,0	55,0	18,5	1,0	71,4	1250	51,3	25,5
3	7,5	420	4	64±8	2200±500	10,0	11,1	17,2	0,9	28,0	368	53,7	16,7
4	9,5	420	4	110±12	3100±500	25,5	42,0	23,2	1,3	67,4	600	80,2	21,3
5	10,2	520	3	170±15	5600±500	35,0	49,0	20,5	0,9	79,2	1166	58,7	23,8
6	10,0	520	3	170±15	5600±500	25,0	57,0	14,7	1,0	77,0	1130	53,1	23,1
7	12,8	520	3	170±15	5600±500	36,0	52,0	21,2	0,9	75,7	1410	56,5	28,8
8	11,0	620	2	64±8	2200±500	11,0	68,0	17,2	0,8	27,6	403	52,0	18,3
9	11,4	620	2	110±12	3110±500	17,0	114,0	15,4	3,7	54,0	706	58,0	22,8
10	12,3	620	4	43±6	1100±300	8,0	6,0	18,6	0,5	43,7	167	80,0	15,2
11	13,2	620	4	170±15	5600±500	33,0	32,0	19,4	0,6	112,5	1916	82,2	39,1

Translated from Atomnaya Énergiya, Vol. 41, No. 2, pp. 140-142, August, 1976. Original article submitted December 1, 1975.

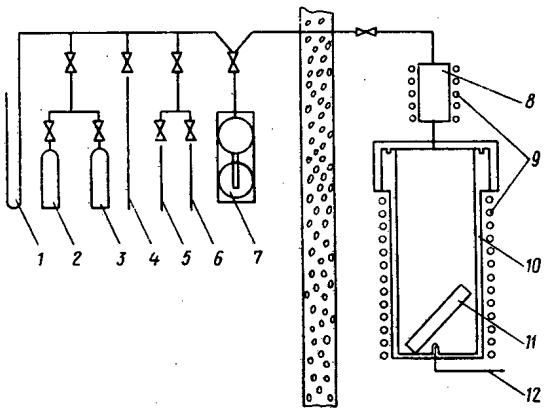

Fig. 1. Diagram of experimental facility: 1) mercury manometer; 2, 3) vessels for collection of gases; 4) vacuum connections; 5) oxygen supply line; 6) hydrogen supply line; 7) mercury compresser; 8) moisture decomposer; 9) heating element; 10) reaction ampoule; 11) sampler; 12) thermocouple.

Hg and a temperature of 650-700°C. At the end of the process the gas phase was pumped out from the reaction ampoule into a calibrated vessel for analysis. Then, at a pressure of 100-200 mm Hg, oxygen was fed into the reaction ampoule and held for a specified time. The gas, after the oxidation treatment, was pumped out into a vessel for analysis through manganese heated to 700°C to decompose moisture. The content of T and ^{85}Kr were determined in the gas by a radiochromatographic method [6]. In order to determine the initial and final content of T and ^{85}Kr in the uranium oxides, the samples were dissolved in HNO_3 with heating and the aqueous and gas phases were analyzed. The total content of T and ^{85}Kr in the samples being investigated were determined as the sum of their quantities in the samples during hydrogenation, oxidation, and dissolution. In addition, the content of T in the zirconium cladding was taken into account [7].

The most important factors which affect the principal parameter (the removal of gaseous fission products from the fuel) are: the degree of burnup of the fuel, and the temperature and time of oxidation treatment. In order to explain the dependence of the removal of T and ^{85}Kr on these factors, it was necessary to produce a mathematical model of this process. For this, a complete 2^3 factor experiment was planned and carried out [8]. The conditions for its accomplishment and the results of the experiments are shown in Table 1. Experiments 1-4 and 8-11 were not duplicated. In order to determine the dispersion of the reproducibility, the experiment was repeated three times at the reference level (columns 5-7).

It can be seen from the results obtained that T and ^{85}Kr are removed from the fuel in the gaseous phase during hydrogen and oxygen treatment. As a result of the hydrogen treatment, ~18.5% T and ~0.9% ^{85}Kr is released. The relatively large release of T in comparison with ^{85}Kr obviously is due to its greater mobility in the fuel, and also the effect of isotopic exchange with the protium present in the gas phase.

The results of the experiments on the oxidation treatment enabled a mathematical model of the process to be compiled in the form of regression equations, which can be used to calculate the amounts of T and ^{85}Kr removed from the fuel. The total removal of T and ^{85}Kr during the hydrogen and oxygen treatment can be calculated by the equations

$$N_T = 69{,}4 + 0{,}58\,(B - 14{,}5) + 9.4\,(\tau - 3) + 0.046\,(T\,^\circ C - 520);$$

$$N_{Kr} = 24.9 + 1.15\,(B - 14{,}5) + 0.03\,(T\,^\circ C - 520) + 2.25\,(\tau - 3),$$

where N_T and N_{Kr} is the total removal of T and ^{85}Kr during hydrogen – oxygen treatment, as % of the initial content; B is the fuel burnup, MW · day/ton U · 10^3; τ is the time of oxidation treatment, h; and T° is the temperature of the oxidation process, °C.

The removal of 7.7 to 39.1% of ^{85}Kr during the oxidation treatment of the fuel does not contradict previously published data. Thus, in the oxidation of UO_2 with air in a boiling layer at 450°C, 27% of ^{85}Kr was removed [9].

The release of T by gas-thermal processing amounted to 90%. The published data on the removal of T during oxidation of irradiated UO_2 are contradictory and are found in wide limits from 8% [10] to 99.9% [11]. The low values for the removal of T, probably were obtained under conditions of incomplete oxidation of UO_2.

The investigations carried out and the equations obtained permit the yield of T and ^{85}Kr to be determined by a numerical method, for fuel with different burnup at the temperature and during the time of treatment

within the limits studied, and also permit one to plan means of ensuring the required degree of removal from fuel of gaseous fission products.

The authors express their thanks to Z. V. Ershov for useful discussions, to A. F. Shvoev, A. A. Buravtsov and V. V. Kravtsev for assistance in carrying out the experiments.

LITERATURE CITED

1. Z. A. Mezhov, Atomnaya Tekhnika za Rubezhom, No. 6, 16 (1972).
2. B. Lastman, Radiation Phenomena in Uranium Dioxide [in Russian], Atomizdat, Moscow, 93 (1964).
3. J. Bodine et al., J. Nucl. Sci. Engng., 19, 1 (1964).
4. A. T. Ageenkov and V. F. Savel'ev, At. Énerg., 32, No. 6, 474 (1972).
5. A. T. Ageenkov et al., Izv. Akad. Nauk SSSR, Metally, No. 4, 160 (1973).
6. P. Van Urk and L. Lindner, Intern. J. of Appl. Rad. and Isotopes, 25, No. 5 (1972).
7. A. T. Ageenkov et al, At. Énerg., 40, No. 7, 23 (1976).
8. F. S. Novik, Mathematical Methods of Planning Experiments in Physical Metallurgy, Section 1 [in Russian], Izd. MISIS, Moscow (1972).
9. A. Chilengkay, Nucl. Appl., 5, 11 (1968).
10. J. Good, Trans. Amer. Nuc. Soc., 15, No. 1, 87 (1972).
11. V. Shraer, in: Proceedings of Symposium of the Council for Mutual Economic Aid, Investigations in the Field of Reprocessing of Irradiated Fuel, Vol. 1 [in Russian], izd. Komissiya po Atomnoi Énergii, Czech. SSR, Prague (1974), p. 84.

PULSED AIR-CORED BETATRON POWERED FROM A MAGNETOCUMULATIVE GENERATOR

A. I. Pavlovskii, G. D. Kuleshov, R. Z. Lyudaev, L. N. Robkin, and A. S. Fedotkin

UDC 621.384.634.3

The power supply for charged-particle accelerators, operating in the single-pulse regime, usually is effected from condensers of inductive storage devices of electrical energy. More frequently, condenser banks are used, whose power capacity often reaches tens and hundreds of kilojoules and have a mass of many tons. These power supply sources can be used mainly under steady-state conditions. At the same time, there are problems which require the use of transportable accelerator facilities. Because of this, a power supply system has been considered for high-powered pulsed air-cored betatrons from magnetocumulative generators (MCG) [1], with a specific power capacity which is greater by a factor of thousands and tens of thousands than condenser storage devices. The generation of powerful electrical pulses in MCG is achieved by the efficient conversion of the chemical energy of explosives into electromagnetic energy by means of the compression of a magnetic field by conductors moving under the action of the explosion.

The relatively high inductivity of the electromagnet winding of air-cored pulsed betatrons of the coil type [2], makes difficult the efficient transfer of energy from the MCG. Therefore, for experiments with MCG, a design of pulsed air-cored betatron was developed with profiled field-shapers of the type shown in [3], which enables its electromagnet to be matched easily with the MCG.

The special feature of the design is the shaping of the betatron field from a randomly pulsed axisymmetrical magnetic field by positioning in it azimuthal-open circuit conducting shells of the required shape [4].

The conducting shells (Fig. 1) ensure the shaping of the betatron field with a stepped configuration:

Translated from Atomnaya Énergiya, Vol. 41, No. 2, pp. 142-144, August, 1976. Original article submitted December 1, 1975.

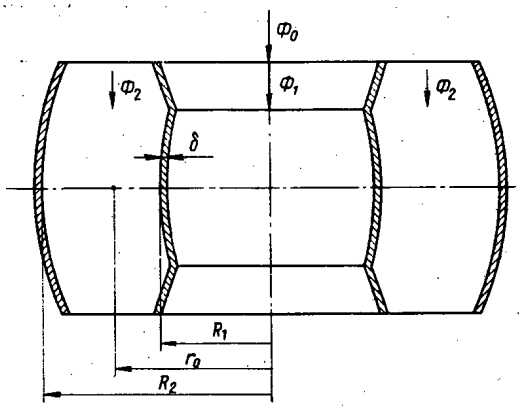

Fig. 1

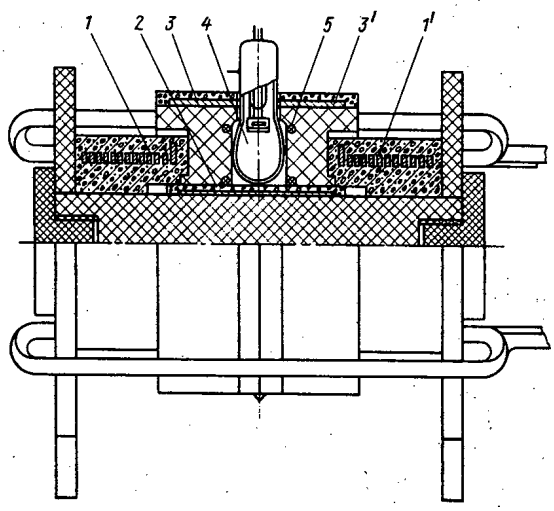

Fig. 2

Fig. 1. Diagram of betatron field shaping with conducting shells.

Fig. 2. Structure of the pulsed air-cored betatron.

$$H(r) = H_1(r) \text{ when } 0 \leqslant r \leqslant R_1 - \delta;$$
$$H(r) = H_0 (r_0/r)^n \text{ when } R_1 \leqslant r \leqslant R_2,$$

where r_0 is the radius of the equilibrium orbit; H_0 is the field in it; $0 < n < 1$ is the field decay index; δ is the thickness of the conducting shells (δ is chosen equal to several thicknesses of the skin layer).

The required ratio between the magnetic field strength (Wider condition) is achieved by separation of the initial current Φ_0 into currents Φ_1 and Φ_2 and their further deformations. The required decay of the field in the region of stability is provided by the curvature of the shells or, in the case of cylindrical shells, by an azimuthal gap on the outside of the shaper, symmetrically relative to the median plane of the betatron.

Figure 2 shows a schematic section of an air-cored inductive accelerator. The initial axisymmetrical magnetic field is created by two triple-loop four-turn coils of the electromagnet 1 and 1', connected in series, with a total inductivity of 3 μH. The coil windings are made of copper with cross section 4 · 10 mm^2 and a pitch of 28 mm. The distance between the coils is 3 mm. The inside diameter of the winding and the height are 160 and 38 mm, respectively.

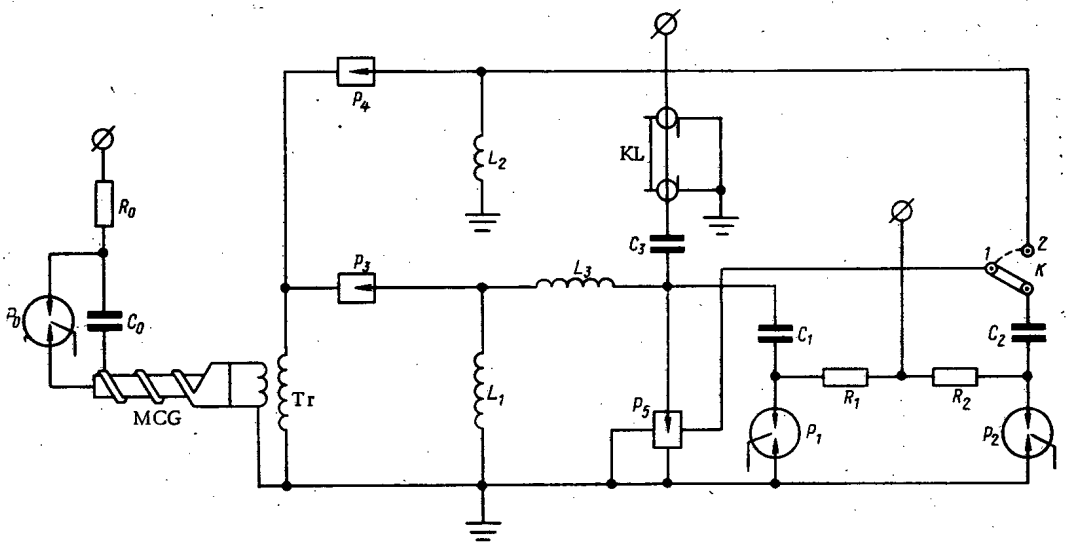

Fig. 3. Electrical circuit diagram of a pulsed air-cored betatron with power supply from a magnetocumulative generator.

The required magnetic field distribution in the working region is created by cylindrical shapers, positioned coaxially with the coils and symmetrically relative to the median plane.

The inside shaper 2, in order to ensure sufficient magnetic resistance of the gap, is made in the form of a wound-on eight-layered cylinder of copper foil with a size of 0.25×2 mm with lavsan insulators between layers (0.05×3 mm). The height of the shaper and its inside diameter are 180 and 92 mm, respectively.

The outer shaper consists of copper cylinders 3 and 3', cut along the generatrix with a gap of 3 mm. The inside diameter of the shaper is 270 mm, the height of the cylinder is 80 mm and the wall thickness is 5 mm. Along the slit of the cylinder are laid six layers of lavsan with with a thickness of 0.05 mm. In order to improve the azimuthal structure of the field, copper screens with a thickness of 0.8 mm, a height of 80 mm, and an azimuthal extent of 90° are installed on the inside wall of the cylinders, symmetrically relative to the slit. Lavsan insulation is also laid between the screens and the cylinder.

The required magnetic field decay in the region of stability is provided by an azimuthal gap with a height of 40 mm between the cylinders of the outer shaper. A sealed-off vacuum chamber 4 is used in the betatron. The injector is a triple-electrode electron beam with a straight-channel tungsten cathode. The target is fastened on the rear side of the anode. The spread of accelerated electrons at the target was achieved by local perturbation of the magnetic field on the orbit created by the sector winding 5.

For mechanical strength of the accelerator, along the outer surface of the electromagnet coils, the inner and outer field-shapers, a binding of glass tape is laid with subsequent impregnation in ÉPK-4 vacuum compound. In order to ensure intercoil insulation and mechanical strength, the coils, before binding, were soaked with an epoxy compound with quartz filler of the type ÉZK-1. The design of the betatron was calculated on a single triggering with the MCG. The duration of the acceleration cycle was $\sim 100\,\mu$sec.

The radius of the equilibrium orbit of the betatron is $r_0 = 7.8$ cm; the energy of the accelerated electrons is $E = 0.1\sqrt{W}$ MeV, where W is the energy in joules transferred to the coils of the electromagnet from the MCG.

In order to ensure the optimum and stable conditions of injection, electron capture in the acceleration cycle, and convenience of preliminary adjustment, a two-stage cycle of operation of the betatron was chosen (Fig. 3).

The initial betatron field is created by the discharge of the condenser bank C_1 through the winding of the electromagnet L_1 and the auxiliary inductance L_3. In this phase of field change, electrons are injected into the chamber and are accelerated up to an energy of 1 MeV. Then the spark-gap P_3 connects the magnetocumulative generator to the betatron and the main acceleration cycle begins. The electron cutoff at the target is effected by switching-in the winding of the coil L_2 through the spark-gap P_4 to the MCG. In the tuning cycle, the switch K is changed over to position 2 and the winding of the coil is energized from the capacitor C_2 at the end of the first phase of the acceleration cycle.

The spark-gaps P_0, P_1 and P_2 are of the trigatron type, P_3 and P_4 are of the explosive type, controlled by explosive delay lines, P_5 has a solid dielectric in the working gap, which disintegrates on discharge of C_2 through the Nichrome wire located inside the dielectric. Startup of the injection unit is effected through the isolation capacitor C_3 and the cable line of the delay KL. Capacitors C_0, C_1 and C_2 were charged from the rectifier through resistors R_0, R_1 and R_2.

As the power supply source for the accelerator electromagnet was used a dual-cascade spiral MCG with a spiral diameter of 160 mm and a length of 1 m, which permitted an energy of up to 3 MJ to be produced in a load, moved to a safe distance (depending on the degree of matching between the load and the MCG), with an initial energy of 1 kJ (power amplification up to $3 \cdot 10^3$, efficiency 10%) [1]. Matching of the load (electromagnet of the accelerator) with the MCG was effected by means of the line transformer Tr. The current in the load circuit was switched in only at the last stage of operation of the MCG, by means of the explosive contractor ("cut-off" low-voltage front of the current pulse). The energy from the MCG was transferred to the accelerator along a cable line with a length of ~10 m.

In the explosive test after capture of the electrons and their preliminary acceleration up to an energy of 1 MeV, an "interception" cycle of the electrons and their further acceleration up to an energy of ~100 MeV was achieved. The maximum current in the windings was $\sim 8 \cdot 10^5$ A. The amplitude of the magnetic field at the equilibrium orbit at the instant of discharge was ~40 kOe. The energy transferred to the load (the betatron electromagnet) from the MCG amounted to ~1MJ.

The injection cycles, acceleration, and discharge of the electron beam at the betatron target were controlled by means of synchrotron and bremsstrahlung radiation sensors.

LITERATURE CITED

1. A. D. Sakharov et al., Dokl. Akad. Nauk SSSR, 165, No. 1, 65 (1965).
2. A. I. Pavlovskii et al., Dokl. Akad., Nauk SSSR, 160, No. 1, 68 (1965).
3. A. I. Pavlovskii et al., Byul. Izobret, No. 34, 185 (1971).
4. L. Ferrari, K. Rogers and A. Jermakian, Rev. Sci. Instrum., 38, No. 12, 1697 (1967).

INCREASE IN BEAM RADIUS AND SIZE OF IMAGE ELLIPSOID BECAUSE OF ERRORS IN A LINEAR PROTON ACCELERATOR

A. D. Vlasov

UDC 621.384.64.01

Random errors in linear proton accelerators lead to an increase in the radius of the accelerated beam. From the work of Smith and Gluckstern [1], this increase was defined as the increase in the transverse oscillations of individual particles where only the first power of the errors were taken into consideration. However, it was discovered in 1972, in computer simulation of the effects of errors, that the growth of beam radius in large accelerators markedly exceeded the values predicted by existing theory [2]. Subsequently, a method was developed for calculation of the radius from the oscillations of individual particles which took into account the second power of the errors and which eliminated the observed discrepancies [3-5].

Another approach to the problem was proposed [2] in which the radius of the beam was defined as the largest of the transverse coordinates x and y of the points of the ellipsoid representing the beam in the four-dimensional phase space xx'yy'. In this case the volume of the ellipsoid was assumed constant and the calculation performed to an accuracy that included the second power of the errors. The effect of separately selected forms of parametric errors — inaccuracies of the field gradient in quadrupole lenses and lens rotation around the longitudinal axis — were calculated analytically on the basis of the ellipsoid approach, first approximately [2] and then more precisely [3, 4]. It was established that the ellipsoid approach was applicable only when particle phase oscillations and time variation of errors were absent or did not have a significant effect.

This paper discusses the increase in beam radius on the basis of the ellipsoid approach for the combined effect of all parametric and coherent errors (transverse displacements and tilts of lenses belong in the latter).

Particle motion in the direction of the x axis in a periodic accelerating and focussing system with errors is described by the equation

$$(d^2x/dz^2)+(\nu_0^2+\Delta\nu_x^2)\,x+\Delta\nu_{xy}^2 y-\nu_q^2(x-x_c)=\Delta_x. \tag{1}$$

The equation for the y axis is similar. These equations give values of x, x', y, and y' only at the boundaries of periods; x_c and y_c are the coordinates of the center of a bunch; ν_0 is the characteristic frequency without consideration of Coulomb repulsion; ν_q^2 is the Coulomb repulsion coefficient; the coefficients $\Delta\nu_x^2$ and $\Delta\nu_{xy}^2$ depend on parametric errors and the term Δ_x on coherent errors. A bunch of accelerated particles can have the shape of a uniformly charged ellipsoid. Setting $x=x_c+x_e$ and $y=y_c+y_e$, i.e., $r=r_c+r_e$, we separate Eq. (1) into two equations:

$$(d^2x_c/dz^2)+(\nu_0^2+\Delta\nu_x^2)\,x_c+\Delta\nu_{xy}^2 y_c=\Delta_x; \tag{2}$$

$$(d^2x_e/dz^2)+(\nu_0^2-\nu_q^2+\Delta\nu_x^2)\,x_e+\Delta\nu_{xy}^2 y_e=0, \tag{3}$$

and do the same for the y axis. This separation is only possible when the coefficients in Eq. (2) which vary with phase oscillations are identical for all particles. This condition is satisfied since it conforms to the general condition for the applicability of the ellipsoidal approach. Thus the initial portion of the problem is separated into two simpler problems previously considered. Equation (3) describes the motion of a particle within the bunch, which is subject only to the effects of parametric errors. For its calculation, we use the

Translated from Atomnaya Énergiya, Vol. 41, No. 2, pp. 144-145, August, 1976. Original article submitted December 9, 1975.

solution $r_e = r_0\theta_{par}$ obtained on the basis of the ellipsoid approach [4]. Equation (2) describes the motion of the center of a bunch, which can be calculated as the motion of an individual particle using [5]. Let the initial amplitude of the oscillations of the center of a bunch be zero ($r_{c0} = a_0$). Then $r_c = r_0 N$, and the motion of the center of the bunch is only produced by coherent errors although parametric errors also affect the velocity of this motion. The angular velocities of the vectors r_c and r_e are ν_0 and $\sqrt{\nu_0^2 - \nu_q^2}$. Because they are not the same, one should consider $r = r_e + r_c$,

$$\theta = r/r_0 = \theta_{par} + N. \tag{4}$$

According to [4], θ_{par} and θ^2_{par} have a log-normal distribution when a sufficiently large number n of periods have been traversed, and their mathematical expectation values (mean values) are, in accordance with Eqs. (19), (20), and (24),

$$\bar{\theta}_{par} = 1.39 \exp\left[\frac{7}{4} n(\Delta + \Delta_1)\right];$$
$$M(\theta^2_{par}) = \left(1 + \frac{1}{\sqrt{2}}\right) \exp[4n(\Delta + \Delta_1)]. \tag{5}$$

According to the results of [5], we obtain for $a_0 = 0$

$$M(N^2) = K_M \exp[4n(\Delta + \Delta_1)],\ M(N^4) = K_N \exp[4n(3\Delta + 4\Delta_1 - \Delta_2 \cos\tilde{\xi})],$$
$$K_M = \frac{\Delta\ \mathrm{coh}}{4(\Delta + \Delta_1)},\quad K_N = \frac{K_M \Delta\ \mathrm{coh}}{2(2\Delta + 3\Delta_1 - \Delta_2 \cos\tilde{\xi})}.$$

Here, $\tilde{\xi} = 2(\alpha - \beta) + \mathrm{const}$; α and β are the phases of the particle oscillations along the x and y axes. Expressions are given in [5] for the parameters Δ, Δ_1, Δ_2, and Δ_{coh} which characterize the effects of errors in a single period where one should read r_0 in place of a_0. In Eqs. (5), $\Delta + \Delta_1$ is written in place of Δ_1 in order to include all forms of parametric errors.

The final portion of the problem involves the determination of the distribution of the quantity θ (4). We limit ourselves to the case of a relatively small effect by coherent errors. Then the distribution of θ is approximately log-normal like the distribution of θ_{par}. Assuming the quantity N^2 also has a log-normal distribution, we obtain

$$M(N) = \frac{[M(N^2)]^{3/4}}{[M(N^4)]^{1/8}} = \frac{K_M^{3/4}}{K_N^{1/8}} \times \exp\left[n\left(\frac{3}{2}\Delta + \Delta_1 + \frac{\Delta_2}{2}\cos\tilde{\xi}\right)\right].$$

The mean values of θ and its square are

$$\bar{\theta} = \bar{\theta}_{par}\bar{\theta}_{coh}\quad \bar{\theta}_{coh} = 1 + \frac{K_M^{3/4}}{1.39 K_N^{1/8}} \exp\left[-\frac{n}{4}(\Delta + 3\Delta_1 - 2\Delta_2 \cos\tilde{\xi})\right],$$

$$M(\theta^2) = (1 + K_e) M(\theta^2_{par}),\quad K_e = \frac{K_M}{1.71} + \frac{2 \cdot 1.39 K_M^{3/4}}{1.71 K_N^{1/8}} \exp\left[-\frac{n}{4}(3\Delta + 5\Delta_1 - 2\Delta_2 \cos\tilde{\xi})\right].$$

Thus the relative contribution of coherent errors to the mean increase in beam radius slowly falls along the accelerator.

Setting $\theta = \sqrt{1 + 1/\sqrt{2}} \exp(U)$, we find

$$\bar{u} = 2 \ln\bar{\theta} - \frac{1}{2} \ln M(\theta^2),\quad \sigma^2 = M(U - \bar{u})^2 = -2 \ln\bar{\theta} + \ln M(\theta^2).$$

The confidence coefficient, i.e., the probability that the increase in beam radius θ does not exceed the confidence value

$$\theta_m = \sqrt{1 + \frac{1}{\sqrt{2}}} \exp(\bar{u} + m\sigma),$$

is

$$p_m = \frac{1}{2} + \frac{1}{\sqrt{2\pi}} \int_0^m \exp\left(-\frac{u^2}{2}\right) du = \frac{1}{2} + \Phi(m).$$

From tables of the function $\Phi(m)$, $p_m = 0.8413$, 0.9332, and 0.9800 for $m = 1$, 1.5, and 2.054.

Motion of the center of the bunch depends on $\tilde{\xi}$. Strictly speaking, therefore, $\bar{\theta}$ and p_m should be determined by averaging over all possible $\tilde{\xi}$ from 0 to 2π. However, one can roughly assume that $\cos\tilde{\xi} = 0$.

For example, let $\Delta = 0.006$, $\Delta_1 = 0.003$, and $\Delta_{coh} = 0.002$ in the main part of the accelerator. Then $K_M = 0.0556$ and $K_N = 0.00238$ when $\cos\tilde{\xi} = 0$. The initial values of $\bar{\theta}_{coh}$ and K_e will be 1.175 and 0.428. For $n = 100$, we obtain $\bar{\theta}_{coh} = 1.120$, $K_e = 0.206$, $\bar{\theta}_{par} = 6.72$, $M(\theta^2_{par}) = 62.5$, $\bar{u} = 1.874$, $\sigma = 0.536$, and finally, $\bar{\theta} = 7.52$, $\theta_1 = 14.81$.

LITERATURE CITED

1. L. Smith and R. Gluckstern, Rev. Sci. Instr., 26, 220 (1955).
2. B. I. Bondarev, A. P. Durkin, and Yu. L. Solov'ev, in: Proc. Radiotekhn. Inst., No. 9, Acceleration of Charged Particles. Experiments on Accelerators [in Russian], Moscow (1972), p. 3.
3. A. D. Vlasov, in: Proc. Radiotekhn. Inst., No. 14, Charged-Particle Accelerators [in Russian], Moscow (1973), p. 3.
4. A. D. Vlasov, in: Proc. Radiotekhn. Inst., No. 19, Accelerator Theory [in Russian], Moscow (1974), p. 32.
5. A. D. Vlasov, in: Proc. Radiotekhn., Inst., No. 22, Accelerator Engineering [in Russian], Moscow (1975), p. 162.

FLOWMETER WITH RADIATION DETECTOR FOR WELLS

I. G. Skovorodnikov

UDC 550.832.08

Tachometric flowmeters are presently widely used to measure both the velocity and the direction of fluid flow along the shafts of wells. These instruments usually consist of a detector-vane, a tachometric converter, and a measuring block on the earth's surface. The low sensitivity at small flow rates is the main disadvantage of these flowmeters; the low sensitivity results from the braking forces acting between the detector and the converter. A flowmeter with a tachometric radiation converter does not create a braking moment. The presently used surface flowmeters equipped with radiation detectors [1] do not allow the determination of the direction of the flow.

The V. V. Vakhrushev Mining Institute of Sverdlovsk has developed a well-type flowmeter with a radiation detector (Fig. 1) which is characterized by high sensitivity and allows the simultaneous determination of both velocity and direction of a flow. The characteristics of operation of the flowmeter are completely independent of the electrical and mechanical properties of the fluid in the flow to be examined.

The flowmeter (see Fig. 1a) comprises a vane 1 mounted in bearings in a frame 2, and a well-logging radiometer. A radioactive isotope 3 is mounted in an eccentric position relative to the axis of rotation on one of the blades of the vane. The frame is connected with a cup-like lead shield 4 which is attached with setting screws 5 to the lower end of the go-devil radiometer 6. The shield dimensions are such that the shield completely covers the radiometer detector 7 and shields it from the scattered radiation of the isotope. The bottom face of the lead shield is provided with a wedge-shaped (in a cross-section plane) cut 8 situated so that the source of the ionizing radiation passes exactly in front of the center of the cut when the vane rotates. This results in a narrow-beam geometry, i.e., only the direct radiation from the source is incident upon the detector. Centering springs 9 guarantee that the instrument is set to the well axis. The instrument in the well is connected via a well-logging cable 10 with the measuring panel 11 of the radiometer and its recorder 12.

Translated from Atomnaya Énergiya, Vol. 41, No. 2, pp. 146-147, August, 1976. Original article submitted December 17, 1975.

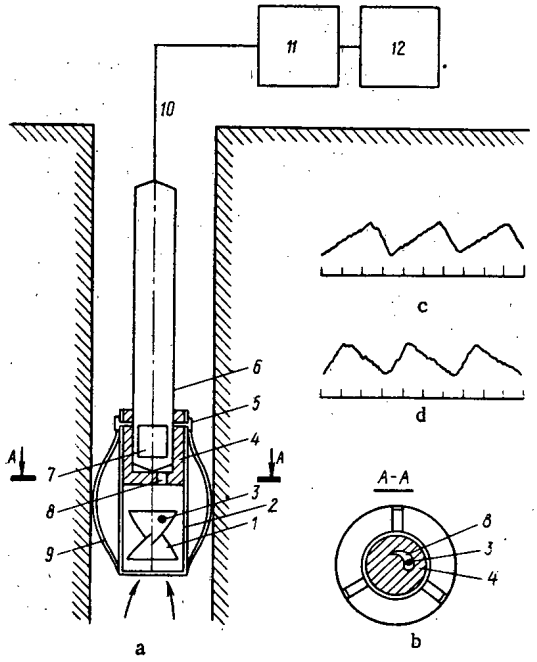

Fig. 1

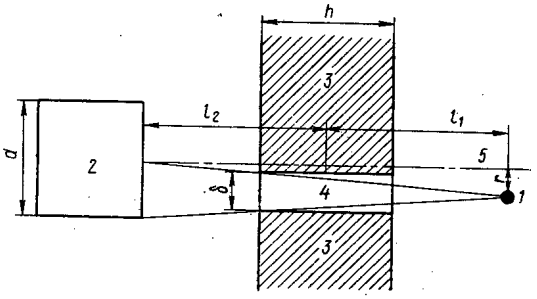

Fig. 2

Fig. 1. Well-type flowmeter with radiation detector: a) longitudinal cross section of the instrument; b) transverse cross section of the shield along the line A – A; c and d) recordings of the radiation intensity in ascending and descending flows, respectively.

Fig. 2. Calculation of the width of the cut in the shield: 1) radiation source; 2) detector of the radiometer; 3) lead shield; 4) cut in the shield; 5) axis of rotation of the source.

In the measurements the fluid flow sets the vane into rotation and the radioisotope is moved toward the cut in the shield. In the case of clockwise rotation, the configuration of the cut as shown in Fig. 1b implies that the radiation intensity recorded by the recorder first increases slowly in proportion to the increase in the width of the cut in the shield; then the radiation intensity increases sharply when the isotope goes beyond the limits of the cut. Figure 1c is a recording which was obtained in this case of the changes of the radiation intensity in the course of time. In the case of reversed direction of flow, the vane is rotated to the other side. In this case the radiation intensity first increases sharply and drops thereafter gradually, as indicated in Fig. 1d. Thus the direction of the flow can be easily determined from the form of the curve produced by the recorder of the radiometer. The velocity of vane rotation is calculated from the number of peaks appearing on the recording per unit time. Time marks are applied to the diagram with the aid of a special relay in the recorder. The dependence of the rate of vane rotation and the flow rate upon the well level is determined by calibration [2].

The flowmeter can be used as an attachment to serially produced well-type radiometers so that the instrument can be used at low cost and widely employed by producer organizations. The author has calculated the parameters of the main components of the flowmeter and has made additional tests for the determination of these parameters: amount of the radioisotope on the vane, thickness of the shielding, width of the cut in the shield, and optimum distance between the detector, the shield, and the radiation source.

The cobalt radioisotope ^{60}Co was used as the radiation source in the flowmeter. The source power should be such that the γ radiation generated at the point of the detector of the radiometer is at least by two orders of magnitude greater than the average radioactivity of the surrounding rocks. In this case the influence of the natural radiation from the well walls upon the results of the measurements can be ignored. Furthermore, a high radiation intensity reduces signal fluctuations at the radiometer output. Based on these requirements and with an assumed distance of 10 cm from the source to the scintillation detector, it was found that the required source intensity amounted to about 50 μCi. The distance from the radiation source to the detector was chosen on the basis of the optimum length of the collimating channel [3] and the design features of the well-instrument of the logging radiometer [4].

It was assumed in the calculation of the thickness of the bottom portion of the shield that the radiation from the source must be reduced at least tenfold to obtain a reliable determination of the radiation intensity differences when the isotope is in the position opposite the cut in the shield and beyond the cut behind the shield. The thickness of the shield was determined with the nomograms of [5] which indicate the attenuation of γ radiation of various energies in dependence of the thickness of a lead layer. In accordance with the above requirements, the bottom face of the shield must have a thickness of at least 3.5 cm. The absorbing effect of the fluid between the source and the detector of the radiometer can be disregarded. The thickness of the shielding side walls, which protect the detector from soft radiation scattered by the well walls, was assumed to be 1 cm.

The width of the cut in the shield at a given distance between the source, the shield, and the radiation detector is selected so that the entire radiation passing through the gap is fully incident upon the detector of the radiometer. It follows from the geometrical considerations outlined in Fig. 2 that the maximum width of the cut in the shield can be calculated with the formula

$$\delta = \frac{d\left(l_1 + \frac{h}{2}\right)}{2(l_1 + l_2)},$$

where d denotes the diameter of the radiation detector (scintillator); l_1 denotes the distance between the source and the center of the shield; l_2 denotes the distance between the detector and the center of the shield; and h denotes the thickness of the shield. The isotope must be attached to the vane at a distance r = d/2 from the axis of rotation.

When the distance between the source and the detector is 10 cm and the 3.5-cm-thick shield is placed in the center position between the source and the detector, the maximum width of the cut is 1 cm in the case of an NaI crystal used with an FÉU-35 photomultiplier as the detector.

These geometrical conditions of the measurements were reproduced in an experiment made with a PGOCh-1 (Agat) scintillation radiometer and an S-41 radiation standard containing 0.1 mg Ra. The standard was manually rotated with various rotation rates. A well-logging PASK-8 potentiometer was used as the recording instrument. The recording paper was wound off with maximum velocity by a special electric motor in the control panel of an AÉKS-900 logging station. The diagrams recorded were sawtooth-shaped and fully correspond to those shown in Fig. 1c and d; the sharp peaks indicate that the distance between the source, the shield, and the detector had been properly chosen.

We determined also the greatest admissible rate of vane rotation at which the radiometer can still determine changes in the intensity of the radioactive radiation passing through the cut in the shield. The calculation was based on the relation between the time constant τ of the radiometer, the velocity V of the motion, and the thickness b of the radioactive layer: $b/V \gg \tau$, which relation is well known from the theory of gamma logging [6]. When we assume that the length h of the cut in the shield is equal to half the length of the circle described by the isotope and when we switch from the velocity of the movement to the number n of rotations, the above relation assumes the form $1/n \gg \tau$.

In the serially produced logging radiometers [4], the minimum time constant is $\tau = 0.5$ sec. The maximum number of vane rotations for this τ value must not exceed 60 rpm. If necessary, the greatest admissible rate of vane rotation can be increased by decreasing the time constant of the radiometer.

As far as recordings made with the radiometer are concerned, there are no restrictions for the minimum rate of vane rotation. Therefore the lower sensitivity limit of the flowmeter depends only upon the frictional force experienced by the vane in its bearings.

At the present time the well-type flowmeter with the radiation detector is in the stage of the design development of a prototype.

LITERATURE CITED

1. D. I. Ageikin, E. N. Kostina, and N. I. Kuznetsova, Detectors of Automatic Control and Regulation Systems [in Russian], Mashgiz, Moscow (1959).
2. V. F. Preis, M. S. Rovenskii, and A. M. Derun, Time-Dependent Control of Hydrologging Work with the Flow-Metering Technique [in Russian], Sverdlovsk (1969).
3. V. A. Artsybashev, Nuclear-Geophysical Prospecting [in Russian], Atomizdat, Moscow (1972).
4. A. A. Zel'tsman, Construction of Apparatus for Geophysical Research in Wells [in Russian], Nedra, Moscow (1968).

5. N. G. Gusev, Shielding from the Gamma Radiation of Fission Products [in Russian], Atomizdat, Moscow (1968).
6. V. V. Larionov, Nuclear Geology and Geophysics [in Russian], Gostoptekhizdat, Moscow (1963).

RADIOACTIVITY OF THE WATER IN THE GROUND SHIELD OF ACCELERATORS

V. D. Balukova, V. S. Lukanin, B. S. Sychev, and S. I. Ushakov

UDC 551.510.72:614.876

The construction of the high-current proton accelerator Mezonnaya Fabrika (Meson Factory) [1] calls for research on the degree to which the subsurface water is contaminated by the accelerator. Radioactive isotopes which are formed in the ground shield of the accelerator and in the subsurface water may travel over substantial distances and create a potential hazard by contaminating water-supply sources.

In [2-5] the activation of soils by secondary particles generated in proton accelerators and the washing-out of the resulting isotopes by subsurface water were investigated. The induced radioactivity of the water was earlier considered in [6-8].

We consider in the present work the activation of the subsurface water taken from the premises of the Mezonnaya Fabrika in Krasnaya Pakhra, Moscow District; we studied the absorption of the isotopes formed in the water by the soil. The water had been irradiated for 35 days by secondary particles (with energies of up to 70 GeV) generated by the proton synchrotron of the Institute of High-Energy Physics (city of Serpukhov). The flux of particles with energies in excess of 20 MeV amounted to $(4.5 \pm 0.7) \cdot 10^7$ particles/cm^2 · sec at the point of irradiation; the flux of thermal neutrons was $(2.0 \pm 0.3) \cdot 10^7$ neutrons/cm^2 · sec.

The water was stored for one month after its irradiation. The short-lived isotopes ($T_{1/2} < 1$ week) had practically decayed after that time. The induced γ radioactivity was measured with a semiconductor spectrometer. The induced β radioactivity was determined with a UMF-1500 device with small background and with a Protok 4π-β-counter (for measuring the tritium). A ring counter was the radiation detector of the UMF equipment. The specific activities of the isotopes were determined with the method of measuring the β radiation of thick-layer sources [9]. The isotope composition of the source and the contribution of each isotope to the measured activity were determined by constructing the absorption curve of the β radiation in aluminum. The tritium concentration was measured in distilled water which had been irradiated along with the subsurface water. One month after the irradiation, only the β emitter, the tritium, remains in the distilled water (the tritium is formed only from oxygen, as in the case of the subsurface water); the tritium need not be separated from the other isotopes. The results are listed in Table 1.

The subsurface water which had been contaminated in the region of the accelerator comes into contact with the rocks of the water-bearing level which can cause purification of the water mainly by absorption of the isotopes by the soil. The absorbing capability of the ground for the radioactive isotopes is characterized by the distribution coefficient, which was determined as follows: 5 g of soil were placed into a receptacle to which 50 g of radioactive solution were added; the contents were mixed; then the solution was divided with a centrifuge and the residual radioactivity of the solution was determined. The distribution coefficient was calculated with the formula $K_d = A_s/A_f$, where A_s denotes the specific activity of the solid phase (soil), and A_f denotes the specific activity of the fluid phase (solution removed by centrifuging).

In order to determine the distribution coefficient of beryllium, irradiated subsurface water was the initial solution. When the absorption of the remaining isotopes was investigated, radioactive standard samples of NaCl, $(NH_4)_2HPO_4$, SO_4 ions, and $CaCl_2$ dissolved in nonirradiated subsurface water were employed. The results are listed in Table 2. It follows from Table 2 that the absorption depends upon both the isotope and the type of the soil (samples from the premises of the Mezonnaya Fabrika).

Translated from Atomnaya Énergiya, Vol. 41, No. 2, pp. 148-149, August, 1976. Original article submitted December 23, 1975.

TABLE 1. Measured Values of the Specific Isotope Activity

Isotope	$T_{1/2}$, day	Max. energy (keV) of β spectrum	Max. permissible conc. (decays/sec·g) in water of open water reservoirs	Activity (decays/sec·g at end of irradiation	
				γ-radiation	β-radiation
^{3}H	4550	18	120,0	No γ	500±300
^{7}Be	53	No β	67,0	4400±700	No β
^{22}Na	950	575	1,1	0,65±0,10	0,80±0,20
^{32}P	15	1700	0,7	No γ	2,0±0,4
^{33}P	25	250	No data	»	8,4±3,0
^{35}S	87	167	2,3	»	7,7±4,0
^{45}Ca	153	255	0,3	»	1,0

TABLE 2. Distribution Coefficients of the Isotopes ^{7}Be, ^{22}Na, ^{32}P, ^{35}S, and ^{45}Ca

Soil	K_d (error ~ 10%)				
	^{7}Be	^{22}Na	^{32}P	^{35}S	^{45}Ca
Loam:					
alluvial	1600	0,8	—	2,3	11
limnetic	360	0,5	18	0,6	5
morainic	1400	0,2	—	0,5	14
Sand:					
coarse	50	0,8	16	0,6	5
fine (powder)	350	1,2	—	0,4	4

The absorption of tritium was not investigated, because the tritium moves in the subsurface currents and is hardly retained by the soil [11].

Let us compare the contamination of a water-bearing layer by activation of the soil and the subsurface water. We assume that the water intake wells are located more than 1000 m from the accelerator. Since the real migration of the underground water changes from 1.5 m/year to 1.5 m/day [12], we assume that the velocity of the ground water at the site of the accelerator is 1 m/day. Only the isotopes T and ^{22}Na are still in the contaminated ground water when it arrives at the well. The concentration of the other isotopes is much lower, owing to absorption and natural decay. Thus, only T and ^{22}Na can cause contamination.

Soil samples, which had been picked at the building site of the accelerator, were irradiated in our work along with the subsurface water. After the irradiation, the concentration of the ^{22}Na isotope in the soil was measured. It was observed that the specific ^{22}Na activity in the soil is about 200 times greater than the experimentally obtained specific ^{22}Na activity in the subsurface water. Estimates show that the specific activities of tritium in water and soil irradiated under identical conditions are approximately the same.

The natural bedding of the water-bearing layers consists of a solid phase (85%) and water (15%). Therefore when the water-bearing layer is directly irradiated in the form of the solid phase, six times more tritium is formed than in the liquid phase, whereas 1200 times more ^{22}Na is formed.

The tritium which is formed in the ground is fully washed out by the underground water [4], whereas only 10-20% of the sodium are washed out [4, 5]. The amount of tritium which enters into the subsurface water after having been washed out from the soil is six times greater than the amount of tritium formed by the activation of the water proper; in the case of ^{22}Na, the amount is 100 times greater.

Thus, the risk of contaminating underground water depends upon the activation of the soil proper and the subsequent removal of the radioactive elements which are washed out by the subsurface water. The activation of the underground water can be practically disregarded.

The authors are indebted to V. N. Lebedev for supporting the present work.

LITERATURE CITED

1. B. P. Murin, in: Transactions of the Radiotechnical Institute [in Russian], No. 16, izd. Radiotekhn. In-ta, Moscow (1974), p. 4.
2. F. Hoyer, CERN 68-42 (1968).
3. T. Gabriel and R. Santoro, Trans. Amer. Nucl. Soc., 14, No. 2, 892 (1971).
4. M. Awshalom et al., IEEE Trans. Nucl. Sci., NS-18, No. 3, 739 (1971).
5. A. A. Aleksandrov et al., At. Énerg., 34, No. 3, 177 (1973).
6. W. Middelkoop, CERN BT/66-3 (1966).
7. R. Thomas, UCRL-20131 (1970), p. 21.
8. M. M. Komochkov and Yu. G. Teterev, Preprint OIYaI [in Russian], R16-6314, Dubna (1972).
9. N. G. Gusev, Dosimetric and Radiometric Techniques [in Russian], Atomizdat, Moscow (1966).
10. Standards of Radiation Safety [in Russian], NRB-69, Atomizdat, Moscow (1972).
11. N. V. Churaev and N. I. Il'in, Radioactive Indicator Methods in Research on the Movement of Subsurface Water [in Russian], Atomizdat, Moscow (1973).
12. G. Higgins, J. Geophys. Res., 64, No. 10, 1509 (1959).

EFFECT OF γ RADIATION OF PRESOWN SEEDS ON THE CROP YIELD AND PRODUCTIVITY OF OPEN-GROUND TOMATOES UNDER THE CONDITIONS OF THE MONGOLIAN PEOPLES REPUBLIC

D. Voloozh and D. Zhamyansurén

UDC 577.3:539.12.04

In recent years, many investigations have been carried out on the presowing irradiation of seeds of agricultural cereal crops by γ-quanta for increasing the crop yield. The case of the stimulating effect of small radiation doses and the investigation of the mechanism of the biological effect of ionizing radiations is interesting from the theoretical and practical points of view [1-9]. The effect of stimulation and the radiosensitivity of agricultural plants have been studied intensively by different authors [10-14].

The irradiation of seeds causes a change of the physiological and biochemical processes [8, 15-17, 18, 19]. It is well known that the effect of irradiation depends on a number of factors, in particular on the temperature, oxygen concentration during irradiation, and different geographical zones.

Because of this, experiments were initiated on the presowing irradiation of a number of plants under the conditions existing in Mongolia.

Materials and Procedure. The effect of presowing γ-irradiation on the crop yield and biochemical changes of fruits has been studied on early varieties of tomatoes. The experiments were carried out in the testing field of the Scientific-Research Institute of Plant-Growing and Agriculture in 1971-1973 at Dzun-Khara, in order to find the optimum dose of irradiation of tomato seeds for the purpose of increasing the crop yield and for improving their quality in the extreme climate of the Mongolian Peoples' Republic.

In the experiment, dried tomato seeds of the Nevskii variety were used, divided into districts of the main agricultural zones of Mongolia. The repeatability of the experiment was duplicated and the seeds were obtained from the 1970-1972 crop. The irradiation source was ^{137}Cs with a dose intensity of 56 R/h. The total exposed doses of radiation amounted to 0.1; 0.5; 2.5; 3.0; 4.0; 5.0; 6.0 and 7 kR. The seeds were screened seven days after irradiation by a procedure used for these crops. Plants from unirradiated tomato seeds were used as a control.

As the criterion for the stimulating effect of the γ-quanta, the germination of the seeds, the number of fruits produced from a single plant, the content of dry matter, and the total sugar were investigated. The germination of the seeds is expressed as a percentage, and the fruit yield in centners/ha. The amount of dry matter was determined by a gravimetric method and the total sugar by Bertran's method.

TABLE 1. Effect of γ-Irradiation of Seeds on the Average Weight and Number of Tomato Fruits

Irradiation dose, kR	No. of fruits per plant	Average weight of fruits, g	Irradiation dose kR	No. of fruits per plant	Average weight of fruits
Control	18,5±2,37	38,8±1,31			
0,1	19,4±1,8	38,6±2,24	4,0	19,6±3,5	39,2±1,98
0,5	16,9±3,0	41,3±2,20	5,0	17,5±2,9	38,9±2,80
2,5	20,9±7,4	43,1±2,10	6,0	17,9±3,1	38,2±2,08
3,0	21,3±5,3	44,2±1,10	7,0	15,0±0,1	36,3±3,01

Scientific-Research Institute of Plant-Growing and Agriculture, Dzun-Khara. Institute of Physics and Technology, Academy of Sciences of the Mongolian Peoples' Republic, Ulan-Bator. Translated from Atomnaya Énergiya, Vol. 41, No. 2, pp. 149-151, August, 1976. Original article submitted January 28, 1976.

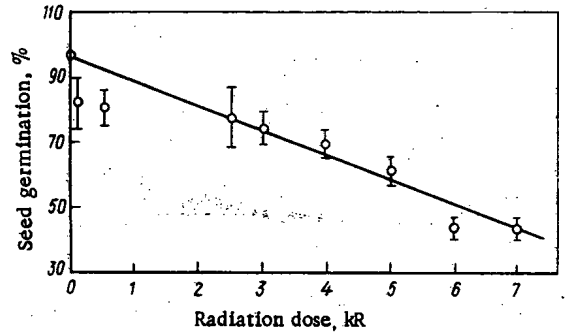

Fig. 1

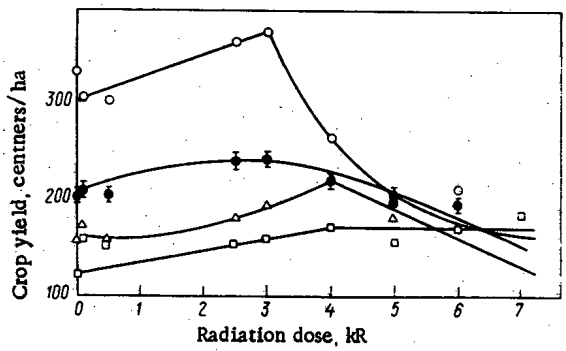

Fig. 2

Fig. 1. Dependence of tomato seed germination on radiation dose.

Fig. 2. Dependence of crop yield of tomatoes on irradiation dosage: ○) 1971; △) 1972; □) 1973; ●) average value for these years.

Preliminary Results and Discussion. Figure 1 shows the dependence of the seed germination on the radiation dosage. It can be seen that seed germination decreases with increase of the total exposed dose of radiation and at 7.0 kR it is reduced almost by 60%.

During the exposed dose of radiation (2.5 to 4.0 kR), a stimulating effect of the γ-quanta is observed on the number and average weight of the fruits (Table 1). In this same dose region, the crop yield is increased (Fig. 2). With all radiation doses it varies from year to year and this, obviously, is due to the difference in temperature during irradiation, the physiological state of the seeds, and the meteorological conditions during the vegetative development of the plants.

In the case of irradiation with a dose of 6-7 kR, the development of the plants is retarded and the crop yield is reduced by 23%. With a radiation dosage of 2.5 to 4.0 kR, the crop yield is increased by 16.8-18.6%, which coincides with the data of [4, 6]. In our experiment, with a stimulating dose of 2.5 kR, the ripening period of the fruits is shortened by 5-7 days, which is very important under Mongolian conditions. It is most interesting that the physical condition of the plants is improved in proportion with the increase of the radiation dose, but the ripening period of the fruits is delayed in comparison with the controls. This delay is observed at a radiation dose in excess of 4 kR. In the case of a high radiation dose, plants are produced with thickened stalks, rich leaves, and colors. An increase of yield is observed with increase of the average weight and number of fruits. These same data are derived in [6, 15].

The dry matter was determined in the middle of August — in the period of complete ripening of the fruit (the start of ripening comes on August 1, and the end of the last harvesting on September 1). Table 2 shows the dry matter content in the fruits, which increases with radiation doses of 0.1 to 4.0 kR and in the case of 5-7 kR it is found to be within the norm limits.

The total sugar content in the fruits (Table 3) for all radiation doses fluctuates within standard bounds, which also coincides with the data of [8].

The results of the investigation show that prolonged γ-irradiation of tomato seeds of the Nevskii variety with doses of 2.5 to 3.0 kR stimulate crop yield by 16.8-17.1% in consequence of the increase in number and

TABLE 2. Content of Dry Matter in Tomato Fruits

Radiation dose, kR	Dry matter content, %	Comparison with control, %	Radiation dose, kR	Dry matter content, %	Comparison with control, %
Control	5,44±0,32	100			
0,1	5,86±0,26	107,7	4,0	5,82±0,26	107,2
0,5	5,68±0,04	104,4	5,0	5,42±0,21	99,9
2,5	5,75±0,22	105,2	6,0	5,26±0,12	96,6
3,0	5,72±0,20	105,1	7,0	5,39±0,04	99,1

TABLE 3. Content of Sugar in Tomato Fruits

Radiation dose, kR	Sugar content, %	Comparison with control, %	Radiation dose, kR	Sugar content, %	Comparison with control, %
Control	2,50±0,01	100			
0,1	2,48±0,09	98,1	4,0	2,48±0,01	98,0
0,5	2,45±0,14	96,7	5,0	2,29±0,01	95,0
2,5	2,35±0,17	92,9	6,0	2,45±0,12	96,8
3,0	2,40±0,02	94,8	7,0	2,34±0,03	92,4

average weight of the fruits and the dry matter content. This irradiation only slightly affects the variation of the sugar content of tomato fruits.

LITERATURE CITED

1. A. A. Abdulaev and N. M. Berezina, in: All-Union Scientific Conference on the Application of Isotopes and Radiations in Agriculture [in Russian], izd. VASKhNIL, Moscow (1968), p. 12.
2. I. M. Akhund-Zade, in: All-Union Scientific Conference on the Application of Isotopes and Radiations in Agriculture [in Russian], izd. VASKhNIL, Moscow (1968), p. 13.
3. N. M. Berezina, Izotopy v SSSR, No. 21, 8 (1971).
4. N. M. Berezina, in: The Application of Isotopes and Nuclear Radiations in Agriculture [in Russian], Atomizdat, Moscow (1971), p. 60.
5. N. M. Berezina, A. M. Kuzin and D. A. Kaushanskii, At. Énerg., 37, No. 1, 43 (1974).
6. N. M. Berezina and D. A. Kaushanskii, Presowing Irradiation of Seeds of Agricultural Plants [in Russian], Atomizdat, Moscow (1975).
7. A. M. Kuzin, Radiobiologiya, 8, No. 5, 635 (1972).
8. I. G. Suleimanova, ibid, 21 (1972).
9. H. Glubrecht and E. Nieman, "Stimulating action of low doses of ionizing radiation in plants," Proc. of Atomic Energy Development Conf., Geneva (1970).
10. I. M. Vasil'ev et al., Biofizika, 5, No. 5, 570 (1960).
11. S. B. Gornovskii, in: Proceedings of the 4th Universal Biofizics Conference, pt. 4, Moscow (1972), p. 509.
12. D. M. Grozdinskii, et al., Radiobiologiya, 5, No. 4, 596 (1965).
13. A. I. Kuzin, N. M. Berezina, and O. N. Shlakova, Biofizika, 5, No. 5, 566 (1960).
14. L. I. Lebedeva, Radiobiologiya, 8, No. 2, 293 (1968).
15. E. V. Budnitskaya, V. N. Stoletov, and A. M. Chopyak, Radiobiologiya, 7, No. 1, 133 (1967).
16. E. V. Budnitskaya, Uspekhi Sovremennol Biologii, 43, No. 3, 280 (1957).
17. G. V. Il'ina, N. N. Kuznetsova, and S. G. Rydkii, Radiobiologiya, 5, No. 4, 3 (1965).
18. S. Kenneth, Rad. Res., 25, 470 (1965).
19. R. Romani, Rad. Res., 6, No. 2, 87 (1966).

INFORMATION

JUBILEE CELEBRATIONS AT DUBNA

A. I. Artemov

Twenty years ago, in March 1956, representatives of a number of socialist countries subscribed to the founding of an international scientific-research organization — the Joint Institute of Nuclear Research. To this event was devoted a week of jubilee celebrations, which took place on June 1-6, 1976 at Dubna.

On June 1, the Committee of plenipotentiaries of the member countries of the Joint Institute of Nuclear Research was set up. At this session, the Republic of Cuba was accepted into the constitution of the JINR by unanimous decision.

On the following day, in the presence of numerous guests and colleagues of the institute, a joint celebration session of the committee of plenipotentiaries and of the Scientific Council of the JINR was held. It was opened by the representative of the Soviet Union, A. M. Petros'yants, Chairman of the Committee for the Utilization of Nuclear Energy.

The society of scientists — physicists, formed in March 1956, he said, was the first scientific organization of the socialist countries. Whereas it was not yet a test of collaboration with an adequate experimental basis, it was not sufficient for the specialists. All this was created gradually by combined efforts. More important are the achievements of the JINR today — a universally acknowledged and authoritative scientific center, making its weighty contribution to the knowledge of the fundamental properties of matter.

The initial experimental basis of the Joint Institute comprised two accelerators — 680-MeV synchrocyclotrons and a 10-GeV synchrophasotron. Now this basis has been expanded considerably. The institute has available such unique facilities as a pulsed fast-neutron reactor, multicharged ion cyclotrons, large magnetic spectrometers, bubble chambers, and a powerful computer center. The scientific successes of the JINR mostly are determined in that here, groups of talented scientists from all the member countries work.

Fig. 1. Presentation of the Order of the Peoples' Friendship to the Joint Institute of Nuclear Research.

Translated from Atomnaya Énergiya, Vol. 41, No. 2, pp. 153-155, August, 1976.

Summing up the 20-year activity of the institute, it may be said with total justification, continued A. M. Petros'yants, that the experience of the society of the scientists of the various countries was very successful. The institute had become a source of physical ideas and fundamental data on the microworld. At the same time, it is a source of many technical inventions and scientific-technical experience, which are widely used in applied research and in solutions of national-economic problems.

Remarking on the important contribution of the institute in the training of scientific and engineering personnel, A. M. Petros'yants said further, "The Joint Institute of Nuclear Research is entering into a new decade of its activity with clear aims and great scientific problems. We wish all colleagues of the institute great creative success."

The speech cleared the floor for the President of the Academy of Sciences of the SSSR, A. P. Aleksandrov. He briefly touched upon the history of the formation of the Joint Institute of Nuclear Research and he mentioned the prominent successes of the Dubna physicists in the investigation of the elementary particles of the atomic nucleus, and also in the establishment and strengthening of international scientific collaboration. A. P. Aleksandrov warmly congratulated the international group of the JINR with the jubilee and the highest government award of the Soviet Union – the Order of Peoples' Friendship. On the instructions of the Presidium of the Supreme Soviet of the SSSR, A. P. Aleksandrov conferred the award on the representatives of the institute – the Director of the JINR, Academician N. N. Bogolyubov and the Vice-Director Academician K. Lanius (German Democratic Republic) and Professor Ch. Shiman (CzSSR).

In reply, Academician N. N. Bogolyubov warmly thanked the Central Kommissariat of the Communist Party of the Soviet Union and the Presidium of the Supreme Council of the SSSR for the inspiring assessment of the activities of the Joint Institute and for the high award.

Then N. N. Bogolyubov gave a report on the work results of the institute over 20 years.

The government of the Soviet Union, in replying to the pioneer of the formation of the JINR, in the introduction passed on to the two institutes found in Dubna. On this basis were created the laboratories of theoretical physics, high energy, nuclear problems, nuclear reactions, and neutron physics. Later, the laboratories of computer techniques and automation were set up and also the Division of New Methods of Acceleration.

Today, the Joint Institute of Nuclear Research is well known as a prominent scientific center, one of the most prominent in the world. The results of important investigations created authority in it and brought universal recognition. The scientific achievements of the JINR are due to the democratic principles of its organization and activities, its unique experimental basis, and its wide international connections. The success of the institute is decided by the people: talented scientists, experienced engineers and technicians, highly qualified workers and employees. Today in the JINR, among the 900 scientific workers are 5 academicians and 8 corresponding members of the Academy of Sciences, 90 doctors, and 380 candidates of science.

Theoreticians of Dubna made a fundamental contribution to the physics of elementary particles, the theory of the nucleus and quantum statistics. One of the principal results of the work on the quantum field theory consists in that for the first time an axiomatic physical thoery was constructed, which led to the appearance of a new language and a change of the very style of physical thinking. The advantage of the new approach was manifested most clearly in the proof of the dispersion relations, which have been at the foundation of numerous qualitative and quantitative theories for describing hadron interactions.

The region of superhigh energies occupies a special role in the physics of elementary particles and nuclear physics. Asymptotic mechanisms in hadron interactions, which have been studied intensively on the basis of the general principles of the quantum theory of fields, enabled abundant information to be obtained about the physical phenomena in the microworld.

During the last twenty years, theoretical nuclear physics has changed completely, having developed on the basis of the constantly growing experimental capabilities. Modern theoretical nuclear physics has enabled the diverse and, at first sight, contradictory properties of atomic nuclei to be described by the application of the many-body quantum theory.

Considerable achievements in physics at Dubna have been made in the theory of condensed media. This scientific trend is most closely affiliated to applied problems of modern science. A fundamental result was the establishment in 1958 of the microscopic theory of superconductivity.

An extensive program of investigations with nucleons and mesons in the energy region up to 10 GeV has been carried out on the synchrophasotron of the High-Energy Laboratory. The antisigma-minus hyperon was

discovered and a new series of resonances was detected. Interesting investigations of vector meason decays were undertaken and they led to the discovery of pi-zero meson decay into an electron — positron pair.

The construction of facilities with propane and hydrogen chambers enabled investigations in the field of resonance physics and the physics of multiple processes to be developed. Series of investigations in the study of scattering of protons and mesons by nucleons and nuclei received international recognition.

The addition to the synchrophasotron of unique qualities based on the relativistic acceleration of nuclei, the acceleration and extraction from the synchrophasotron of beams of deuterons, α particles, and carbon nuclei, have permitted the start of a new field of science — relativistic nuclear physics.

Throughout the 20 years, the Laboratory of Nuclear Problems group has successfully worked on problems of medium-energy physics, which contributed to the excellent performance of the 680-MeV synchrocyclotron.

Important data have been obtained on the physics of hadrons. Analysis of nucleon — nucleon interactions has enabled the law of charge dependence of nuclear forces to be carefully verified. Detailed data on meson creation have been obtained. The validity of the dispersion relations was demonstrated for the interaction of pions and nucleons and the coupling constant of the pion with the nucleon was determined experimentally.

The symmetry of the muon-electron in weak interactions was investigated and confirmed and for the first time recoil nuclei from a muon neutrino were observed. The beta-decay of pions was discovered. The law of conservation of lepton number was investigated and the conclusions of the theory of universally weak interactions were verified.

Based on experimental data about exclusions in different weak particle decays, an idea was expressed and verified concerning the existence of two types of neutrino.

A large work cycle has been carried out on the study of mesoatomic phenomena, and also a new physical phenomenon has been discovered — double charge exchange of ions by nuclei.

A broad program of investigations into nuclear spectroscopy has been accomplished successfully. More than 100 new isotopes have been discovered. These investigations have provided important results for verifying the superfluid model of the nucleus, developed by theoreticians of the institute.

On the synchrocyclotron, during the last 10 years, together with doctors and biologists of the Academy of Medical Sciences of the SSSR, medical — biological and oncologistic investigations have been carried out using protons and pions.

At present the synchrocyclotron is undergoing reconstruction to a high-powered phasotron.

N. N. Bogolyubov spoke in detail about the joint work of the physicists at Dubna, Serpukhov, and Batavia. Large-scale physics facilities were constructed for investigations on the Serpukhov accelerator by specialists of the JINR: 2-m hydrogen and propane chambers, spark spectrometry, a complex for searching for new particles, and other instruments. In these joint experiments, data were obtained which are of great value for the theory of elementary particles, and a new step was taken in the investigation of antimatter. Now the Dubna physicists are participating in the development of an accelerator–storage device complex in the Institute of High-Energy Physics. A series of first-class experiments on the study of nucleon interactions has been carried out in Batavia with the aid of a unique instrument constructed in the JINR — a jet hydrogen target.

Later N. N. Bogolyubov summed up the activities of the Laboratory of Nuclear Reactions, where outstanding work on the synthesis of the transuranic elements has been achieved on the multicharged-ion cyclotron.

Long-duration experiments with heavy ions have led the scientists of the JINR to the discovery of new physical phenomena: spontaneous fission of nuclei with anomalously short periods of the isomeric state of a new type of radioactive decay of the nucleus — the emission of delayed protons. In heavy ion-transfer reactions, more than 30 new isotopes of light elements with a large surplus of neutrons have been synthesized.

Interesting investigations have been carried out on the structure of neutron-deficient isotopes. Unique data have been obtained on heavy quasimolecules.

At present, a group from the laboratory is assisting Polish physicists to install a 2-m cyclotron for the acceleration of multicharged ions. Work is being carried out successfully on the building of the largest cyclotron with a pole diameter of 4 m.

Future applied projects are being worked on successfully in the laboratory — and construction of nuclear filters, the development of methods of activation analysis, etc.

Having described the work of the Laboratory of Computer Techniques and Automation, the speaker talked about the search for new methods of acceleration of particles and nuclei, with which the Division of New Methods of Acceleration of the JINR is occupied. One of the most important trends of its activities is the development of the collective method of acceleration. Preparation is now going on for the startup of a prototype heavy-ion accelerator.

Scientists of the JINR have unique possibilities for experiments on the pulsed fast reactor, constructed by the physicists and engineers of the Neutron Physics Laboratory and with considerable assistance from the FÉI in Obninsk. In the spectrometric investigations carried out on this reactor, extensive data have been obtained about neutron resonances of nuclei. An original procedure has enabled polarized neutron beams to be obtained, and the magnetic moments of highly excited states of nuclei to be measured, a large program of investigations of the alpha-decay of neutron resonances has been carried out, and also gamma-spectra in the resonance capture of neutrons has been studied. For the first time, experiments have been carried out on the detection and storage of ultracold neutrons in a closed cavity.

At present, a new and more powerful pulsed reactor, IBR-2, is being constructed. This will be a unique facility and physicists of the member countries will be provided with first-class conditions for investigations of the structure of the nucleus and studies of condensed media.

At the end of his report, N. N. Bogolyubov said; "Permit me in the name of all the workers of the Joint Institute of Nuclear Research to express our thanks to the Communist and Working Parties and to the governments of the member countries of the institute for constant and generous support in all stages of development of the JINR during these 20 years. We express our appreciation to the plenipotentiaries of the governments of member countries for their efficient supervision. We consider it our duty to mention the exceptional fruitful work of all the members of the Scientific Council of the institute for having shown a great interest in the choice of the main trends of research in the Joint Institute of Nuclear Research ... .

Concluding this report, I want to mention that our institute has outstanding achievements and traditions. But the most important is that we see the institute has excellent prospects. I am in no doubt that this will enable the scientists of socialist countries to achieve new boundaries in knowledge of the secrets of the microworld of elementary particles and of the atomic nucleus."

After the report, salutory speeches were made by the plenipotentiaries of the member countries of the JINR, Kh. Kristov (Bulgaria), L. Pal (Hungary), Le Van Tkhiem (Democratic Republic of Vietnam), F. Hilbert (German Democratic Republic), Kim Gen Chun (Chinese Peoples' Republic), T. Saéns (Cuba), D. Tsévégmid (Mongolia), Ya. Felitski (Poland), I. Ursu (Romania), and Ya. Kozheshnik, (Czechoslovakia), and also the Ambassador Extraordinary and Plenipotentiary of Czechoslovakia in the SSSR, Jan Gavelka and the representative of the Council for Economic and Mutual Aid A. F. Panasenkov. In their salutory addresses they mentioned the decisive contribution of the Soviet Union in the creation of the JINR and stressed that the institute is a large-scale international scientific-research organization, an excellent example of socialist scientific integration. The Joint Institute of Nuclear Research has rendered inestimable assistance to the scientists of the socialist countries in the development of nuclear physics, the training of national research personnel, the creation and establishment of national scientific centers. The 20-year activity of the JINR gives every justification to suppose that joint scientific research will play a major role in integrated processes of socialist collaboration.

The plenipotentiaries communicated to the international group of the JINR the congratulations of their governments on the occasion of the 20th anniversary of the institute.

The jubilee celebrations at Dubna concluded the 40th session of the Scientific Council of the Joint Institute of Nuclear Research "Twenty years of the JINR and the development of the physics of elementary particles and of the atomic nucleus." At the session, distinguished scientists of the socialist countries presented their reports: the Vice-President of the Academy of Sciences of the SSSR, Academician A. A. Logunov (report "High-energy physics"), Academician I. Todorov (Bulgarian Peoples' Republic) and Vietnam Professor Nguen Van Kh'eu ("Theoretical investigations in the field of physics of elementary particles"), Vice-Director of the JINR Academician K. Lanius and Professor R. Poze from the German Democratic Republic ("Automation of a physical experiment and the application of computers"), Corresponding Member of the Polish Academy of Sciences A. Khrynkevich ("Nuclear physics and investigations with multicharged ions"), Chancellor of the Mongolian State University N. Sodnom ("Medium energy nuclear physics") and the Hungarian Academician L. Pal ("Solid-state physics and investigations with neutrons").

The Scientific Council approved the problem-thematic plans of scientific-research work and the international cooperation of the laboratories, and the decision of the judge of a competition for JINR awards.

STANDARDS OF THE INTERNATIONAL ELECTROTECHNICAL COMMISSION IN NUCLEAR INSTRUMENT MANUFACTURE

V. V. Matveev and L. G. Kiselev

Fifteen years have passed since the first meeting of the Technical Committee 45 of the International Electrotechnical Commission (TK 45 MÉK). During this period, TK 45 has worked on 40 publications on standardization in nuclear instrument manufacture. TK 45 is the most active technical committee of the MÉK, Several tens of governments have participated in its work, directing through its national committees comments on the documents processed. About 15 governments, including the Soviet Union, USA, France, Great Britain, Poland, Italy, Japan, etc., have participated in its documents and working groups directly at the sessions of the technical committee.

The earlier publications of the MÉK were called recommendations, but since 1975 they have been issued as standards and are intended for international usage. For the purpose of cooperation of the international unification of the MÉK, the wish has been expressed that for the national committees in its constitution the text of the national standards should be as close as possible to the text of the publications.

The standards of TK 45 MÉK express agreement from the international point of view on a wide circle of problems in various applications of nuclear instrument manufacture. They are the reflections of the latest achievements concerned with the design principles, characteristics, the methods of testing equipment for nuclear instrument manufacture.

The regular meeting of TK 45, its subcommittees, and its working groups was held in San Diego (California, USA) from December 4-13, 1975. At the sessions, where more than 65 delegates from 12 governments of Europe, America, and Asia participated, the activities during the past year were summed up.

In 1976, 391 chapters came off the press of The Detection and Measurement of Ionizing Radiations by Electrical Methods of the International Electrotechnical Dictionary. The terms and their definitions in this dictionary are given in three languages, including Russian for the first time. It is advantageous in domestic scientific-technical literature and standard-technical documentation to use standard terminology. Publication 516 of the MÉK, A Modular System of Data Collection — the CAMAC System, has been issued. This publication fixes in the international standard the principles of organization and the constructional features of the CAMAC system, worked out initially by the ESONE committee. In Publication 515, the characteristics and methods of testing radiation detectors for use in nuclear reactors are given. Publication 231D has been issued, which specifies the general principles of design of equipment in pressurized water reactors.

The characteristics and methods of testing dc amplifiers, which are widely used in nuclear-instrument manufacturing equipment, are laid down in Publication 527. This publication also contains the definition of terms which find a wider application in various measurement devices, as well as methods of verifying the metrological characteristics of the latter.

Publication 504 is devoted to the technical characteristics and methods of testing dosimeters for determining hand and foot contamination. Publication 463 has been issued with an account of the technical characteristics of portable dosimeters and monitors for x-ray and γ radiation for the determination of radiation safety.

In addition, TK 3, which is concerned with the standardization of symbols and markings, has issued Publication 117/4A, where symbols are laid down for the marking of radiactive radiation detectors. This publication has been developed on the basis of the initial proposals of experts of the SSSR in TK 45.

Translated from Atomnaya Énergiya, Vol. 41, No. 2, pp. 156-157, August, 1976.

In 1976, two further publications will be issued, relating to the CAMAC interface system. It should be noted that, together with the standardization of the CAMAC interface TK 45, TK 66 forms the standard "Interface system for programmed measuring instruments," on which is based the Hewlett — Packard System (USA). At the TK 45 meetings, on the proposal of Soviet experts concerning the coordination of work on interface systems in MÉK, it was decided to exchange information between TK 45, TK 66, and TK 65, and also PK 3, TK 85, ISO. At present, there are no documents on interface systems in the last two committees.

On the results of consideration of the comments of the national committees, of five documents from the TK 45 Secretariat, it was decided to transfer to the category of documents of the Central Bureau and to distribute them for voting according to rule in six months. Among them is document 45A (Secretariat) 37, where the general principles are proposed for the use of digital computers in nuclear reactors, document 45A (Secretariat) 38 which is supplementary to Publication 231 and defines the general principles of equipment design for liquid-metal fast reactors. In document 45A (Secretariat) 44, the order of carrying out periodic tests and inspection of the safety systems of reactors is stated. In documents 45 (Secretariat) 184 and 187, the dimensions of measuring glasses for liquid scintillators and test tubes for radioactive samples are laid down.

A number of documents will be exploited as documents from the Secretariat and the Working Groups. Document 45A, Reactor Equipment, continues the elaboration of the documents: General Principles for Communication Lines of Reactor Safety Systems — 45A (Secretariat) 45, The Collection and Assessment of Data on the Reliability of Plants for Reactor Safety Systems — 45 (Secretariat) 34. At the meetings of PK 45A, proposals were considered for the improvement and revision of Publication 232, The General Characteristics of Reactor Equipment. Many situations of this document, in particular mechanical characteristics, are obsolete and therefore it was decided to include a number of the statutes of this publication in Publication 231 which is planned for reissue, and discontinuing action on Publication 232. The chairman of the IAEA, A. Grabov, participated in the work of PK 45A, which proposed to exchange information in the field of standardization of reactor equipment between both organizations.

PK 45B, Dosimetric Instruments and Radiation Safety Instruments, undertook the preparation of the document RG B3 (Secretariat) 23 on absorbed dose meters and monitors for β- and γ-radiations, and also several documents related to the characteristics of meters and monitors for radioactive gases, in particular, iodine and tritium in the vapor phase. The document Portable Meters and Monitors for Equivalent Neutron Dose — 45 B (Secretariat) 25 was prepared, and also a new edition of Publication 325, relating to meters and monitors for surface contamination by α and β radiations.

The Working Group RG I, Terminology, continues work on refining terms and their definition, used in the PK 45B documents. RG 3, Interchangeability, has prepared as a Secretariat document a plan for a standard on a consistent interframe organization of the CAMAC system. RG 5, Geological Survey Equipment, has prepared a document concerning the plant used for the sorting and high-speed analysis of radioactive ores. RG 6, Radioisotope Instruments, is preparing a document on the characteristics and methods of testing density meters. RG 9, Detectors, has prepared a new issue of Publication 340, which lays down the methods of testing amplifiers and preamplifiers for semiconductor detectors, and also documents on the definition of the terms used here. RG 10, Multichannel Analyzers, has prepared a document on the determination of the measurement error of the "live" time of analyzers for inclusion as a subchapter in document 45 (Secretariat) 189, Methods of Testing Multichannel Amplitude Analyzers. Preparation of a document is continuing which establishes the technical requirements and methods of testing devices used with analyzers at high loads.

Other documents will be prepared by the working groups.

At the next sessions of TK 45, its subcommittees and working groups, the Soviet delegation participating will consist of V. V. Matveev, L. G. Kiselev, L. M. Isakov, and Yu. K. Kulikov.

CONFERENCES AND MEETINGS

NEW MATERIALS AND PROGRESSIVE TECHNOLOGY IN THE PRODUCTION OF PLANTS FOR NUCLEAR POWER STATIONS

Z. G. Usubov

On January 5-8, 1976, at the Exhibition of Achievements of the National Economy of the USSR in Moscow, a conference took place on Experience of Introduction and Prospects for the Development of New Materials and Progressive Technology in the Production of Equipment for Nuclear and Thermal Power Stations, which was heard and discussed at sessions of three sections of 135 reports by scientists and eminent specialists from power engineering construction factories, metallurgical, power generation, aviation, chemical, and other branches of industry.

The conference was opened and a report was presented on the problems of power engineering construction in the 10th Five-Year Plan by the Minister for Power Engineering Construction, V. V. Krotov.

At the plenary session, reports were heard on the present-day situation and the prospects for development of new materials and progressive technology in the production of plants for nuclear power stations (N. N. Zorev), materials for the main units of power generating equipment for thermal power stations (I. R. Kryanin), and the demands for materials for power generating facilities (V. N. Zemzin).

Great attention was paid at the conference to the achievements of Soviet power-engineering construction and to the future development of materials and production technology for nuclear and thermal power station plants.

The principal reports of the first section were devoted to the creation of new materials for nuclear power facilities, progressive technological processes, control methods, and also to the introduction of automated technological plants. New steels were analyzed for the manufacture of reactor vessels, steam generators, volume compensators, hydroreservoirs, and other units of the primary circuit of the VVÉR-1000.* The new steels have higher technological and strength properties, they are more resilient, and in radiation stability they surpass those used abroad.

New materials were proposed not only for VVÉR facilities but also for RBMK† facilities, with dissociating coolant for fast and gas-cooled reactors.

New materials were recommended for cladding, the use of which prevents sticking in the screw threads of joints in nuclear facilities in the case of prolonged operation in a coolant medium with high parameters.

The results of work, where efficient methods of increasing the radiation stability of reactor vessels were proposed, are of considerable interest.

Reports concerning the development of new technological processes for the manufacture of plants for nuclear power stations occupied a high place in the conference, starting with extraction of the metal, forging, welding, thermal treatment and final mechanical treatment, assembly, and testing.

Urgent problems of development of metallurgical processes for increasing the quality of metals were highlighted in the reports. A new technological process was proposed for the manufacture of large-scale steel castings in shapes with differential cooling with respect to height. A technology has been developed and a one-piece shell with spurs has been manufactured for the PGV-1000 steam generator, corresponding in mechanical properties to the requirements of the technical conditions. A new stainless steel of the martensite class with a small amount of stable residual austenite has been studied comprehensively, as applicable to the operating

* Water-cooled/water-moderated reactor.

† High-power boiling reactor.

Translated from Atomnaya Énergiya, Vol. 41, No. 2, pp. 157-158, August, 1976.

conditions of the GTsN-195 vessels and the slide valves of the Du-850, A new technology and plant was proposed for drop-forging unique fittings for nuclear power station plants, and also the manufacture of large-scale and single-piece drop-forged profiled units of manifolds. Problems were discussed for the modernization of forge-pressed plants for the production of large-scale blanks, and a new technology was recommended for the manufacture of forgings from blanks, enlarged by electroslag welding.

The greatest number of reports was devoted to the development of materials, technology, and automated plants for welding and filling during the production of units. New welding materials and technology for electric arc welding of case units of nuclear power station plants were proposed, which will provide, in addition to high mechanical properties, stability of the welded joints against the formation of cracks during welding and thermal treatment. There was interest in the new technology of gas-electric welding in the slit separation of thin-walled vessels, which is extremely promising for use instead of flux-welding. One of the most promising is the electron-beam weld. The successful introduction into turbine-producing factories has permitted the necessary experience to be built up for the start of industrial operations associated with its acceptance in the manufacture of nuclear power station plants. The industrial application of the process will permit the output of welded thin-walled units to be increased by a factor of 10-15, and the consumption of welding and structural materials and electric power to be reduced, and will permit the process to be mechanized and automated, as well as improving the working conditions of the welders.

An austenitic steel has been developed for electrode tapes, intended for single-traverse filling or for making the first layer of a two-layered anticorrosion lining of the inside surfaces of VVÉR pressure vessels, and alternatives of single- and double-traverse filling have been studied, which will ensure the required aggregate of properties during filling of the vessel units. In order to increase the output of the process of anticorrosion filling, an experimental-industrial testing of a sample of the new filling plant has been developed and has taken place.

There is considerable interest in the use in nuclear engineering of steel plated by an explosion. A technology has been developed and introduced for the direct explosion plating of forgings, castings, and thick plates (without subsequent rolling). The technique has undergone experimental-industrial testing. At present, a workshop plating technique is under development, which includes the construction and extensive investigation of an experimental explosion chamber.

Problems of the surface protection of nuclear power station plants by a chemicothermal treatment method of fast reactor units from scoring and self-welding, tempering of large-scale forgings for power-generating plants, the formation of cracks during thermal treatment after welding and filling of casings, prospects for the use of special coatings for preventing oxidation of nuclear and thermal power plant units during heat treatment also have been reflected in the addresses of the conference participants.

Reports were extremely interesting, in which detailed data were cited about the materials, technology, and equipment in the production of nuclear power station pipelines, zonal electrical heating for welding and the heat treatment of welded joints, and mechanical treatment of large-scale plants.

A part of the reports was devoted to the development of a technology of manufacture of thin-walled precision tubing. A large group of reports highlighted the problems connected with automation of nondestructive testing of blanks and welded joints and with strength tests of materials used for the manufacture of nuclear power station plants. Reports were also presented which were devoted to the theoretical and experimental investigation of the stressed state of nuclear power installation structures.

The resolutions of the conference reflect paths for the development of new materials and progressive technology in the production of nuclear and thermal power station plants, the mechanization and automation of production processes, increasing the quality of production and output of work, and measures for metal economy.

The completion of the problems posed will require great creative efforts by the factory workers, scientific-research institutes, design bureaux, and other organizations of the various ministries and departments, and will promote further accelerated development of the country's power generation and modernization of its power-engineering basis.

Theses of the reports were issued at the start of work of the conference. It is proposed to issue the reports.

SEMINAR ON WATER-COOLED/WATER-MODERATED REACTORS IN FRANCE

A. D. Amaev and V. N. Filippov

Three two-sided seminars were held in 1974-1976 on water-cooled/water-moderated power reactors (VVÉR) within the framework of the agreement between the Soviet State Commission for Atomic Energy and the French Commisariat a l'Énergie Atomique (CEA). The last of these, on fuel composition and fuel element structural materials, took place at the Saclay Nuclear Research Center from February 18-24, 1976.

The program of the seminar included, in addition to the theoretical part, a visit to the laboratories, research reactors, and workshops. Five reports were presented by the Soviet Union on test-rig and reactor tests of VVÉR and AMB reactor fuel elements, and also fuel assemblies for RBM-K reactors.* The French specialists read eight reports and gave the Soviet delegation a large number of leaflets on intrareactor measurement techniques and "hot" laboratory equipment.

The leader of the French delegation, J. Delafosse, recounted in his report the development program of nuclear power stations in France. In recent years, the French program for the construction of nuclear power generating plants has undergone significant changes. Instead of the gas — graphite reactors, which are traditional for France, it is planned in the future to install nuclear power stations with light water reactors (LWR) of the pressure-vessel type. This decision is explained mostly by the complicated fuel — power balance of the country, due to the limitation of mineral fuel resources and the power generation crisis. This situation compels France to increase the quota of electric power produced by nuclear power stations from 22% in 1973 to 40% in 1985, with an annual increase of power generating capacity of $5\text{-}7 \cdot 10^3$ MW(el). In order to ensure the required rate of construction of nuclear power stations, it has been recognized as advantageous to purchase a license on a reactor with a capacity of 925 MW(el) by Westinghouse (USA). France intends to construct 17 of these reactors up to 1980. From 1980 to 1985, it is proposed to construct a further 30 reactors, of which six will be of 1300 MW(el) capacity. The latter are being developed by French specialists and after 1985 it is proposed to construct nuclear power stations with reactors only of this type.

The first charges of the 925 MW(el) reactors will be produced with a fuel element design of Westinghouse, but subsequent charges will be with improved assemblies of French design. In connection with this, the French CEA is working on a broad complex program of numerical and experimental investigations of fuel, structural materials, and the construction and means of testing fuel elements and fuel element assemblies.

Reactor testing of materials and fuel elements is carried out in the reactors OSIRIS at Saclay, SILOÉ at Grenoble, BR at Moll, and the prototype of the portable facility PAT at Caderache. The characteristic feature of the OSIRIS and SILOÉ pool-type reactors is their saturation with experimental devices. Thus, in the OSIRIS reactor, with a capacity of 70 MW, there are five loops in which several channels can be tested independently (coolant — water, sodium and gas). In the same tank is installed a mockup of the ISIS reactor with a capacity of 1 MW, which is used for translucent neutronography. In OSIRIS, a procedure has been developed for the gamma-spectrometry of fuel elements directly in the tank, which together with the neutronography method permits the fuel burnup in the fuel element to be monitored nondestructively at various stages of testing. Beside the loop facilities, individual channel-probes are used extensively. Four types of standard channel-probes, which have been developed and have been used for many years, are for repeated use in the irradiation of materials and fuel element rods in research reactors. They are single-type for the French CEA research centers. Tests and subsequent investigations are carried out by a single procedure, which enables the results obtained to be compared. For different testing programs, numerous structural devices and accessories have been developed. Reliable multisectional heaters are worthy of mention, which are installed in

* High-power boiling reactor.

Translated from Atomnaya Énergiya, Vol. 41, No. 2, pp. 158-159, August, 1976.

experimental channels in order to ensure the required temperature for testing of the samples. The channels are equipped with thermocouples for measuring temperatures up to 2600°C, tensometric sensors, membrane sensors for measuring the pressure inside the fuel elements, movement sensors with signal transmission by means of waveguides, and other devices. Data from the experimental devices are collected and processed by means of portable computers, and automation is used extensively. All this makes it possible to economize in time and to carry out different experiments simultaneously. The following figures were given for the scale of investigations in the SILOÉ reactor with a capacity of 32 MW: total number of channel-probes tested in the reactor over 10 years of its operation exceeds 1000; total time of operation of all experimental facilities — in excess of 1 million hours. The saturation of the "hot" chambers of the Saclay laboratory should be mentioned, with its modern facilities and instruments. In addition to the standard complex of testing machines and microscopes in the chambers, there are facilities for the continuous measurement of the dimensions of fuel elements by means of sliding induction sensors, equipment for x-ray spectral analysis of the KAMEKA type, facilities for autoradiography, etc. Particular attention should be paid to the saturation of the "hot" laboratory with various lift-portable intralaboratory mechanisms, and also the reliable systems of manipulators of American and French production.

Within the framework of the LWR program, the French CEA has extensively extended work on an investigation of the alloy Zircalloy-4, which is used as a cladding material for fuel elements. Although this alloy is considered to have been thoroughly studied, data on creep in a diametral direction, plasticity and strength after irradiation are very few, which makes it difficult to choose the optimum scientifically based conditions of heat treatment and chemical composition of the alloy. The effect was investigated of the content of oxygen, tin, and also the annealing temperature of cold-deformed fuel element tubes in an assembly of short- and long-duration mechanical features before and after irradiation. Samples of almost every variation of alloy composition were subjected to irradiation, and also different conditions of heat treatment. Starting from 1970, more than 20,000 measurements have been made on irradiated tubes. It has been established that an increase in the alloy of the content of oxygen to 0.16% and tin to 2.6% considerably improves the resistance to creep in the diametral direction. Complete recrystallization annealing at 600°C is recognized as the optimum heat treatment. Because of the results obtained, new requirements have been introduced into the French technical requirements for the content of tin and oxygen in the alloy, intended for fuel element cladding, and also testing of the tubes has been introduced at an internal pressure with a specified uniform and nonuniform increase of diameter. In addition to Zircalloy-4, investigations have been carried out of a zirconium alloy with 1% niobium. It has been established that an oxygen content of not less than 0.1% in the alloy and annealing at 700°C improves the creep resistance of the alloy under reactor irradiation conditions. At higher temperatures of annealing, the strength characteristics are improved but the creep resistance is worsened. It is found that fuel element claddings of the zirconium — niobium alloy with oxygen have a lower diametral creep by a factor of 1.5 than those of Zircalloy-4 alloy, heat-treated at optimum conditions.

Work has been carried out in the following directions for uranium dioxide reactor fuel and for the fuel element as a whole: establishment of the limiting thermal loadings; study of the yield of gaseous fission products as a function of the working conditions of the fuel elements; determination of the boundary transitional power cycles in the case of a cyclic type of operation of the fuel elements; determination of the effect of fuel contamination on the efficiency of the cladding; investigation of fuel compaction and fuel pellet shrinkage in the longitudinal and transverse directions; study of the mechanical interaction between the fuel and the fuel element cladding; investigation of the thermal conductivity of fuel and the diffusivity of the gap between the fuel and the cladding, etc.

Considerable successes have been achieved by the French specialists in the creation of a technology for the manufacture of fuel pellets with a size stability on irradiation. The results obtained in the investigations of fuel and claddings have enabled the French to recommend the manufacture of fuel pellets without the introduction under the cladding of helium under pressure, as was forseen in the Westinghouse plan. In other requirements on the fuel and fuel elements, there are no differences from international requirements.

Tests of the fuel elements at increased loadings have led French specialists to the conclusion that, from the point of view of long-term efficiency, the permitted linear capacity may exceed 600 W/cm. Consideration of this problem from the position of possible emergency situations, for example by the dehydration of the active zone due to rupture of the large diameter pipelines, indicates the necessity for limiting it to 370-400 W/cm for the accepted reactor emergency cooling systems. Exceptional importance is attached to safety problems of nuclear power stations with LWR reactors by the French CEA and large funds are assigned for carrying out experimental work.

INTERNATIONAL CONGRESS ON REACTORS

V. I. Mikhan

The congress took place from March 30 to April 2, 1976 in Düsseldorf (Federal German Republic). These congresses have been held annually by the Society of West German Scientists — specialists in the field of nuclear energy. Its principal participants are representatives of the various research and industrial organizations in the Federal German Republic. Specialists from other countries, mainly Western Europe, also participated in the meetings of the Congress. About 1900 people were present at the 1976 congress, of which about 1700 were from the Federal German Republic.

The meetings of the congress were divided into plenary and sectional. At the plenary (morning) sessions summary reports were read, associated with the development of nuclear power generation: the utilization of low-grade uranium ores, methods of uranium enrichment, the effect of meteorological conditions on the spread of fallout from nuclear power stations, experience in the development, construction, and operation of nuclear power stations with pressurized light-water reactors (Biblis-A) and high-temperature gas-cooled reactors (TNTR-300). The construction of thermonuclear reactors was also considered, the consequences of possible emergency situations at nuclear power stations, the results of investigations of reactor safety, and the effect of irradiation on the vital activity of cells, etc. Thirteen of these reports were read.

In the summary reports, well-known data were contained in the majority of cases. The purpose of these reports was to convince a wide circle of the scientific-technical community and directors of various industrial firms in the necessity and advantages of nuclear power development and the safety of nuclear power stations both for their staff and for the surrounding population.

The afternoon sessions were held in four sections, so that at some of them two or even three meetings were sometimes held simultaneously. Thus, on one day of the congress, reports were heard simultaneously at six meetings. In all, 228 reports were read.

The theme of the first section concerned the characteristics of reactors and reactor experiments. The main attention was paid to an investigation of the various aspects of safety of nuclear power stations. The program of work for this section included 78 reports.

The main development of nuclear power generation in the Federal German Republic at the present time consists in nuclear power stations with pressure vessel light-water reactors with boiling and nonboiling water. Therefore, about half of the reports of the first section was devoted to the safety of light-water reactors. In the majority of them, the behavior of the various units of the reactor facilities in emergency situations was considered theoretically, mainly in the case of rupture of plant housings and pipelines, causing the loss of coolant. The dynamics of change of the coolant parameters under such emergencies, and the behavior of the plant units and fuel elements were determined by calculations.

The greatest interest was in the experimental investigations of the safety of light-water reactors. Among these should be mentioned a study of the behavior of fuel cassettes in the case of rupture of the circuit of a boiling-water reactor, an investigation of the swelling of fuel element claddings with the loss of pressure and a change of coolant pressure, and stresses in the pressure vessel as a result of ruptures, on models.

Some reports touched upon investigations of the safety of high-temperature gas-cooled and fast reactors with liquid-metal coolant, which are assessed in the Federal German Republic as the most promising for the future development of nuclear power generation. At the meetings of this same section, problems associated with melting of the active zone were considered. It was stressed that the monitoring and control systems developed for reactors, make such an emergency extremely low probability. Nevertheless, the properties of the alloy formed, the scale and consequences of melting under different conditions, etc., are being studied carefully.

Translated from Atomnaya Énergiya, Vol. 41, No. 2, p. 160, August, 1976.

The second section (62 reports) was devoted to fuel elements and the fuel cycle. It should be noted that the design of the fuel elements, fuel cassettes, and their characteristics were almost undiscussed. The main attention was paid to reprocessing of irradiated fuel, its technology, trapping the gases released, removal of radioactive waste, and safety.

As concerns the fuel elements themselves for light-water, high-temperature, and fast sodium reactors, only certain specific problems were considered for them, such as, for example, new ideas about creep of zirconium alloys, the results of the latest investigations of fuel elements in the case of a rapid loading, etc.

The theme of the third section was the planning, construction, and operation of reactor facilities and their plants. In the 60 reports, the results of developments, investigations, and experience in the operation of the various monitoring sensors for reactors, methods of measuring the characteristic parameters of reactors, were presented. The design and operating conditions of primary circuit plants were considered.

In this section, great attention was paid also to the reliability and safety of reactors. The necessity for careful monitoring of the reactor plant in production and in operation was stressed. In a number of reports, statistical operating data of the reactor and various plants were analyzed.

At the meetings of the fourth section (28 reports), reactor concepts were considered and problems of economics. Prospects for the development of high-temperature gas-cooled and fast reactors, with both sodium and gas coolant, were discussed mainly. Several reports were devoted to thermonuclear facilities and also to the possibility of using the high-temperature heat produced in gas-cooled reactors for technological purposes.

The congress was excellently organized. Before the start of the meetings, each participant was given a detailed program and a collection of short accounts of all the reports of the sectional meetings. During working of the congress, several interesting excursions to research centers and to stations with reactor facilities were organized for the participants.

AMERICAN—JAPANESE SEMINAR ON THE PLANNING, OPERATION, AND USE OF PULSED FAST REACTORS

E. P. Shabalin

The seminar was organized by the Americal National Council for Science and the Japanese Society for the Promotion of Science, and took place from January 19-23, 1976 in the nuclear research laboratory of Tokyo University at Tokai-Mura (approximately 100 km from Tokyo). Japan was represented by 11 participants and 18 observers, the USA by seven participants; scientists from other countries were also invited: two participants from France and the Soviet Union and one participant from Great Britain.

Reports (35 in all) were presented at the seminar devoted to the planning, calculation, and investigations of pulsed fast reactors with both self-quenching (Godiva-type reactor) and periodic action with external quenching of the pulse. To the latter type, besides the IBR-30 and IBR-2 reactors at Dubna, the Japanese reactor YAYOI which has been recently brought into operation (at the end of 1975) also belongs. The participants of the seminar were able to familiarize themselves thoroughly with this unique reactor, through the numerous reports of Japanese scientists (Kh. Vakabayashi, Sh. An, etc.) and directly during its inspection. The YAYOI reactor has a compact active zone of metallic highly enriched uranium (critical mass about 28 kg) and a thick reflector of enriched uranium and lead. Equipped with five systems of fast and slow reactivity changes and with a complex control and interlocking system, the reactor can operate in several cycles: pulsed and periodically repeated power pulses, single-burst cycle, power pulses according to a sinusoidal law, in the constant power cycle and in the booster cycle (i.e., as a neutron multiplier with an externally pulsed source). It is interesting that in the YAYOI reactor, the previously used methods of reactivity modulation are not being used; instead, circulation of the active element, affecting the reactivity, through a closed pneumatic loop and "shooting through" of

Translated from Atomnaya Énergiya, Vol. 41, No. 2, p. 161, August, 1976.

the active element (a nylon "bullet") through the reactor by means of an explosive device with a periodic action (machine-gun type) is used. The minimum power pulse duration of the reactor is 58 μsec. The maximum power of the reactor per single pulse is 1 MW and the average power in continuous operation is 2 kW (reactor cooled by air).

Another interesting feature of the YAYOI consists in that it is installed on rails and can be moved to any of four positions for operating with one of the experimental facilities — thermal column, time of flight spectrometers and time of retardation in lead, a cryostat for irradiation at low temperatures, etc. The purpose of the reactor is: fundamental investigations in nuclear physics and the physics of the condensed state, applied work on biological shielding and fast neutron dosimetry, and boron therapy.

The report by D. Rosher (USA) on the startup tests of a new American pulsed reactor of the self-quenching type SPRIII was interesting. It is intended for the intrazone irradiation of samples by neutrons with a fluence of up to $6 \cdot 10^{14}$ n/cm^2; the diameter of the cavity for irradiation is 18 cm. In one of the reports, D. Rosher suggested a method of determining the integrity of the fuel elements by the nature of the fluctuations after the power pulse.

Dr. R. Long (USA) gave a summary report on the six fast-pulsed reactors currently in operation in the USA, and dwelt on the special features of the design, parameters and thematics of utilization. In particular, R. Long reported that investigations into the generation of coherent light by "nuclear pumping" occupy 20% of the operating time of American pulsed reactors. Dr. K. Tom (NASA, USA), reported on the program of investigations into the creation of a reactor-laser in the USA.

In the report presented by the Joint Institute of Nuclear Research (Dubna, USSR), D. I. Blokhintsev spoke of the principles of the scram system of the IBR-2 reactor, the startup of which is expected at the end of 1976, and of the experimental work on verifying the nuclear safety of the reactor. The report created great interest.

Several reports were given by the Japanese scientists concerning a plan for a pulsed neutron source — a booster based on a linear electron accelerator. The characteristics of the source are similar to the characteristics of the IBR-2, with an average power of 2 MW.

Individual sessions of the seminar were devoted to equipment and methods of monitoring pulsed reactors, nuclear safety, the use of pulsed reactors; the latter theme, however, had little representation.

Of the resolutions accepted, the decision for a biannual seminar on the theme of pulsed reactors may be noted with a wider representation of reports on the use of pulsed reactors. The proceedings of the seminar will be published in the first half of 1976.

SYMPOSIUM ON THE TREATMENT OF RADIOACTIVE WASTE FROM THE NUCLEAR FUEL CYCLE

N. V. Krylova and Yu. P. Martynov

An international symposium was held on March 22-26, 1976 in Vienna, on the treatment of radioactive waste from the nuclear fuel cycle, organized by the IAEA and the Nuclear Energy Agency (NEA) of the Organization for Economic Cooperation and Development (OECD). More than 350 specialists from 32 countries and six international organizations participated.

Close attention is being paid to radioactive waste. This is confirmed by the expanding list of waste materials everywhere, which will be subjected to reprocessing, and also by the increase of budgets for research and reprocessing.

The reports of the symposium covered almost all the problems associated with the waste from the nuclear fuel cycle, but the greatest attention was paid, both in the number of readings (21) and in the reaction of the participants, to the treatment of highly active waste and particularly to the technological schemes presented for their consolidation. It was emphasized in the reports that, although at present the removal of gaseous radionuclides (krypton, iodine, etc.) does not present a serious hazard, it is advantageous to develop methods of discharge and storage, because of the possibility of exceeding the permissible radiation dosages in the vicinity of reprocessing plants. The processes developed for the purification of atmospheric effluents are designed for the separation of iodine by absorbing it on silica gel, impregnated with layers of silver, or on molecular sieves after oxidation. Later, cryogenic separation of krypton and xenon is carried out, which it is proposed to store under pressure in stainless steel vessels.

The main trend in the treatment of highly active waste is reprocessing into borosilicate glass. Because of this, countries in future will be developing the technology of vitrification of waste for use on an industrial scale in 1977-1987. In the reports presented by the USA, Great Britain, France and the Federal German Republic, the results were given of work on experimental and pilot-scale plants, and also plans for future vitrefication plants for highly active waste. Thus, in France a continuous two-stage process of vitrefication has been designed, consisting of calcination in a rotating drum furnace and fusion in Inconel crucibles with induction heating. The process has been tested on an experimental plant, operating since 1972 to 1975. A new facility for working on actual waste will be introduced in 1977.

It should be emphasized that there is a change of opinion in Great Britain and USA concerning the vitrefication of highly active waste. Thus, specialists from Great Britain, having been convinced of the advantages of this method, after 1972 reconsidered their opinion and at present are working intensely on a single-stage crucible process, Harvest. Research operations are planned to be completed in 1977. It is proposed to start construction of a plant for waste reprocessing in 1979 and be in operation by 1986. The American specialists, formerly supporters of the calcination of highly active waste and their storage in this form, now believe that because of the great achievements in vitrefication, it is possible to speak about the competitive efficiency of this method. In the USA, the search is being continued for an optimized scheme for the reprocessing of highly active waste. For this purpose, in the Pacific Northwest Laboratory in an assignment from the Directorate for Research and Development of Power Generation of the USA, the WFP program — which is a continuation of the previous WSEP — is being carried out, which is directed at the development of technological processes and their demonstration in a large-scale scheme for the consolidation of waste. The schemes presented provide for a two-stage process of calcination — fusion. In order to carry out the calcination, an atomizing — drying chamber was tested, a drying and calcination apparatus in a boiling bed and a horizontal thin-film evaporator. The fusion stages were verified in three variants of the apparatus — fusion in a container, in a continuous metal smelter and in a ceramic directly heated smelter (heat generated by the passage of a current in the glass melt). Based on the work carried out, a facility is being developed and designed for the

Translated from Atomnaya Énergiya, Vol. 41, No. 2, pp. 161-162, August, 1976.

consolidation of the waste formed during reprocessing of fuel elements, in a factory with an output of 5 tons per day. The plant for consolidation is provided with remote control of the process, the possibility of its replacement, a complete system of purification of the effluent gases, and a decontamination chamber for withdrawn plant.

The integrated system currently planned for waste consolidation includes calcination in a boiling bed or an atomizing—drying chamber and fusion in a container. However, in the future a change is possible of fusion in the container to fusion in a ceramic smelter or it is possible that the vitrefication process will be undertaken in a single stage in the smelter.

A facility for boiling-bed calcination, operating in Idaho (USA) since 1963, is shut down at present because of corrosion of the equipment, difficulty in decontaminating it, and irradiation of operating staff. A new facility is being developed now, with a higher output (11.4 instead of 0.8 m^3 per day) with shielding and manipulators for the decontamination and replacement of plant which is frequently taken out of service. It is proposed to start waste consolidation on the new plant in July, 1980.

Work is continuing on the modernization of the design for an experimental two-stage facility VERA in the Federal German Republic, the startup of which was planned for early in 1976 for actual waste, but has been delayed because of licensing difficulties in the Federal German Republic.

Great interest and lively discussion were created by the reports of the Soviet representatives on the technological developments of a vitrefication process (two-stage "KS-KT" and a single-stage "electrocooking"). They showed that the Soviet Union is in the forefront in the field of originating a high-output continuous vitrefication process.

The discussion of storage methods of highly active waste showed that at the present time, the majority of countries intend to store consolidated waste for 30-50 years in controlled surface storage facilities with air or water cooling. The appearance in different countries of broad programs for investigating the possibilities of storage of consolidated waste in geological formations (stratified salt, salt domes, limestone, granite, and other crystalline and volcanic rocks) should be mentioned.

In parallel with the technological development of waste consolidation processes work is being carried out on studying the properties of vitrefied highly active waste (thermal stability, effect of α-, β- and γ-radiations) and the feasibility of producing durable ceramic materials from them.

A number of reports was devoted to the treatment of α-emitting waste, and waste of low and average level of activity.

The symposium showed, on the whole, that in the treatment of waste from the nuclear fuel cycle, a tendency is observed toward reduction of their volumes both at the formation stage and during further reprocessing, and also toward a clear distinction between activity and chemical composition. The problem of reprocessing, storage, and burial for each category of waste will be decided separately, and the mixing of various categories is considered to be undesirable.

It is intended to publish the data of the symposium in September, 1976.

THE SEVENTH SPRING SEMINAR ON HIGH-ENERGY PHYSICS

S. G. Matinyan

This already-traditional seminar, organized annually by the high-energy physics group of the Karl Marx University, Leipzig, took place in Bermsgrün, near Schwartzenberg, from March 15-19, 1976. Colleagues from the Institute of High-Energy Physics, Tseiten, also participated actively in its work. As a rule, at this seminar for delivering lectures on the most urgent problems of the physics of elementary particles, physicists from other countries are invited. On this occasion, among those invited were Prof. J. Polkinghorn (Great Britain), who read a cycle of lectures on the scattering and formation of particles with large transverse impulses, and Prof. M. Le Bellak (CERN, Geneva), who reported on the theoretical work of CERN on Regge diagram technique with intercept of the Pomeron, with larger units, and on the analysis of local conservation of quantum numbers of the charge type and of a transverse pulse in the multiperipheral formation of particles. The representative of the Soviet Union, S. G. Matinyan delivered a lecture on the Parton—Regge description of inelastic interactions of high-energy particles with atomic nuclei. Reports of physicists from the German Democratic Republic were also heard at the seminar (the organizers of the seminar) on the creation of ψ particles in different high-energy beams, on correlation phenomena in quark models, on jet models in the formation of hadrons in e^+e^-, νp and ep collisions (I. Ranft), and on the creation of heavy lepton pairs in pp collisions (G. Ranft). In these reports, the discussion took place on the basis of models developed by the Leipzig physicists.

A number of original reports were also given: experimental study of K^-p interaction at high energies (I. Kaltwasser, GDR), thermodynamic model of the formation of strange particles (K. Hengsgen, GDR), multiple creation in the quark model (Likhard, CzSSR), transverse angular correlations (I. Kripfranz, GDR), cluster model of particle creation (R. Kirscher, GDR) and determination of fireball dimensions and angular correlations (A. Bara, Romanian Peoples' Republic), et al.

Some experimental work of physicists of the GDR, which was mentioned at the seminar, was carried out in collaboration with physicists of the Soviet Union and other socialist countries.

The seminar took place in a friendly atmosphere and was well organized.

Translated from Atomnaya Énergiya, Vol. 41, No. 2, p. 163, August, 1976.

NEW INSTRUMENTS

THE GUPS-1 IMMERSION FOLLOWER γ-LEVEL GAUGE

I. I. Kreindlin, Yu. I. Pakhunkov
and I. R. Rubashevskii

The GUPS-1 immersion follower γ-level gauge has been developed in the All-Union Scientific-Research Institute of Radiation Technology (VNIIRT), designed for the continous, automatic, remote-controlled measurement of the position of the interface between two liquid media, which have similar densities, in open and closed reservoirs (condensers, settling tanks, etc). The GUPS-1 can be used also to control the level of liquids which are in contact with an air medium. The availability of a standard output signal in the form of a frequency-changing voltage (GSP GOST 14853-69) enables the instrument to be used in an automatic regulation and control system.

The GUPS-1 consists of six units, shown in Fig. 1. The instrument functions in the following way. On entering the transceiver (Fig. 2) and being scattered by the medium being monitored, γ-quanta from the 241 Am radiation source act on the detector placed there. The stream of scattered radiation depends on the density of the surrounding medium (with increasing density, the stream of scattered radiation decreases).

The radiation quanta in the transceiver are converted into electrical pulses, the average frequency of which depends on the radiation flux being recorded. The pulsed signal from the transceiver unit enters the three-position electronic relay regulator. Depending on the position of the transceiver relative to the level of the interface between the two phases, a control signal appears at the corresponding output of the regulator, enters the power amplifier where it is converted to a 50-Hz ac voltage with an amplitude of 220V. This voltage is fed to the electric wiring slave mechanism unit, by means of which the transceiver is positioned at the interface.

TECHNICAL CHARACTERISTICS OF THE INSTRUMENT

Range of measurement, m 0-1.0; 0-1.6; 0-2.5
Basic measurement error for the surface layer between upper and lower media, mm:

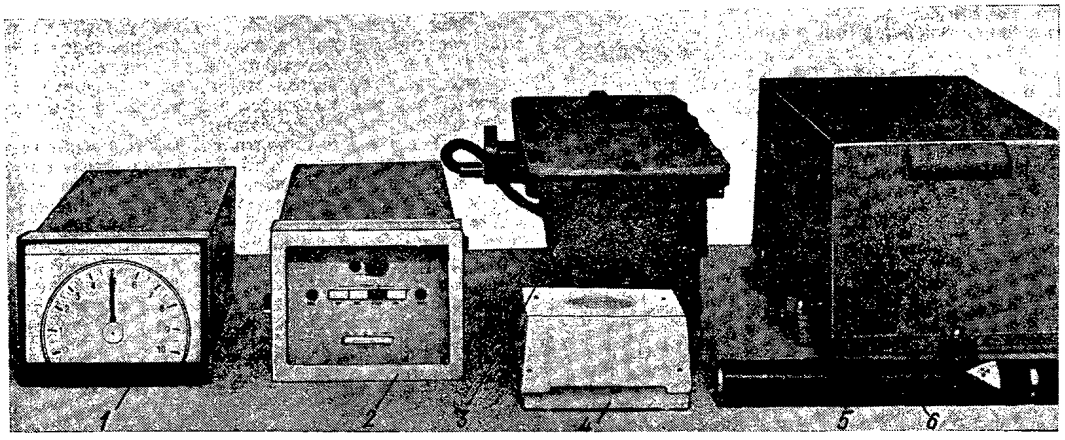

Fig. 1. GUPS-1 Immersion follower γ-level gauge: 1) VChP secondary instrument; 2) relay regulator; 3) power supply unit; 4) UITB-20 standard thyristor amplifier; 5) electric wiring unit; 6) transceiver.

Translated from Atomnaya Énergiya, Vol. 41, No. 2, pp. 163-164, August, 1976.

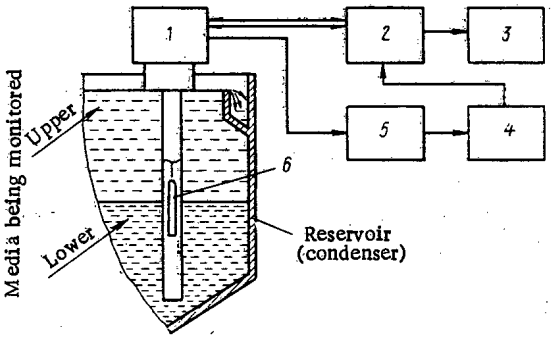

Fig. 2. Circuit diagram of GUPS-1 level gauge: 1) transceiver unit; 2) electric wiring slave mechanism; 3) VChP secondary instrument; 4) power amplifier; 5) electronic relay regulator; 6) transceiver.

for a density of the upper medium 1-1.05 g/cm^3, difference between density of media not less than 0.05 g/cm^3, thickness of transition layer not more than 200 mm; for a density of the upper medium 1.5-1.20 g/cm^3, difference between density of media not less than 0.10 g/cm^3, thickness of transition layer no more than 150 mm.	not more than ±40
Maximum tracking speed, mm/sec	6.3 ± 20%
Range of operating temperature, °C	
for transceiver unit (installed in the reservoir) and the electric wiring unit (installed near the reservoir)	from —30 to +50
for the regulator, power amplifier and secondary instrument (installed on operator's panel)	from —30 to +35
Temperature of medium being monitored in reservoir, °C	5-50
ac mains supply:	
voltage, V	$220^{+10\%}_{-15\%}$
frequency, Hz	50 ± 1
Power requirement, VA	not less than 150

In the electrical wiring unit, there is a standard frequency pickup and its output signals carry the data on the position of the interface. One of these signals is recorded by a secondary instrument and the other is intended for bringing in the automatic regulation and control system.

The transceiver unit, in order to protect it from the action of the surrounding medium, has a hermetic finish, the electric wiring unit has a dust and splash-proof finish, and the power amplifier and secondary instrument have a conventional finish.

The construction of the transceiver unit ensures operating safety for the servicing personnel, which allows it to be installed in any reservoir.

The special features of the GUPS-1 instrument in comparison with the well-known radioisotope level gauges are: the capability of measuring the position of the interface between two liquid media, which differ only very slightly in density; a high sensitivity of the detecting part (due to the use of the isotope 241 Am in the transceiver and a scintillation detector); the capability of carrying out measurements in reservoirs inside of which are rotating scraper mechanisms or stirrers; the availibility of a secondary control action.

Experimental models of the GUPS-1 instrument have passed the State warranty tests and the instrument has been recommended for series production. It can find a wide application in hydro- and nonferrous metallurgy for determining the height of a clarified layer during thickening of different ore pulps, in the annealing branch of industry for obtaining information about the position of the settled solid phase in suspensions, and also in situations where operating control of cleaning installations is required.

REVIEWS

S. V. Mamikonyan

EQUIPMENT AND METHODS OF FLUORESCENT X-RAY RADIOMETRIC ANALYSIS*

Reviewed by E. M. Filippov

The book reviewed is devoted to a current method for the high-speed analysis of a substance — a description of the procedure and instruments for an x-ray radiometric method (XRM).

It consists of four chapters, three appendixes and a bibliography.

In the first chapter, the main processes are described of the interaction of atomic and nuclear radiation with a substance. The procedural principles of analysis of saturated layers of a substance are stated, as well as methods of eliminating the matrix effect of the media being analyzed and an estimate of the measurement errors.

Radioisotope sources and detectors of characteristic radiation are considered in the second chapter. Together with scintillation and proportional counters, semiconductor detectors are discussed thoroughly.

In the third chapter, the principles and special features of construction of XRM equipment are considered: device circuits of various XRM sensors, electronic circuits of preliminary and main amplifiers, amplitude discriminators, autostabilization systems of spectrometric channels, recording devices and power supply sources. The possible sources of interference, which affect the measurement results, and methods for their elimination are discussed here.

In the concluding chapter, industrial XRM instruments are described, which are used under laboratory conditions for surveying the walls of mine workings and boreholes. Some foreign instruments are considered in addition to Soviet instruments.

In the appendixes, the mass-absorption coefficients are given for the characteristic emission of the chemical elements, atomic differential and integral cross sections of noncoherent and coherent scattering, the energies of the principal lines and the absorption edges of the emission by the elements.

Unfortunately, there are some faults in the book. In addition to considering methods of estimating the measurement errors, a procedure should be given for estimating the sensitivity thresholds of XRM. This is an extremely important parameter when assessing the procedure for the analysis of a substance, and it should be given serious consideration.

On p. 146 the author shows the threshold spectrum and calls it the integral spectrum. The integral curve of the spectrum should tend to a certain constant value and not to zero with increase of energy.

However, these remarks do not reduce the excellent impression of the book, in which the x-ray radiometric method is considered in a concise and lucid form.

The book will be extremely useful for practice and for scientific workers.

* Atomizdat, Moscow (1976); 15 author's folio, 1 ruble 66 kopecks.

Translated from Atomnaya Énergiya, Vol. 41, No. 2, pp. 165-166, August, 1976.

I. K. Morozova, A. I. Gromova,
V. V. Gerasimov, V. A. Kucheryaev,
and V. V. Demidova

THE LOSS AND DEPOSITION OF CORROSION PRODUCTS OF REACTOR MATERIALS*

Reviewed by N. V. Potekhin

The book being reviewed is devoted to one of the most pressing problems of nuclear power generation — the operation of nuclear power-generating plants. It presents a full investigation of the formation of corrosion products of reactor materials, loss into the coolant and deposition inside the circuit. The presence of corrosion products in the system of the primary circuit and their uncontrolled behavior can significantly reduce the reliability of a nuclear installation. Therefore, a knowledge of the mechanism of formation of corrosion products and the rules of behavior inside the circuit will assist in increasing significantly the reliability of power-generating facilities and in improving their operating safety. Published papers in this field prior to 1970 are used in the book and also the authors' own investigations; it contains much bibliographical information.

In the first chapter, the general mechanisms of formation of corrosion products of steel are considered, for different temperatures, aluminum alloys, zirconium and titanium alloys, and also the conditions of formation on metal of passive films. The Purbé diagram is given for the system iron — water at a different temperature. The material of the first chapter is of a general educational nature and assists in understanding the mechanism of formation of corrosion products, their specific form and chemical composition. At the end of the chapter, the composition of the corrosion products is considered, its dependence on the chemical composition of the corrosive medium and the temperature.

The second chapter is devoted to the loss of structural material corrosion products into the coolant. In volume and importance of the information given in it, this chapter is the main one. In it are described the kinetics of the loss of corrosion products from steel of the perlite class as a function of the chemical composition of the corrosive medium, the surface condition, temperature of the medium, rate of movement of the coolant and irradiation. The transfer to the coolant of the corrosion products of stainless steel, high-nickel, copper — nickel, zirconium, aluminum, and titanium alloys is also considered. Extensive data are given on the corrosion rates of all the principal structural materials and the loss of corrosion products into the coolant up to critical and supercritical parameters.

In the third chapter, the relation between the loss of corrosion products into the coolant is described and also their deposition on the inside surfaces of the primary circuit, as a function of the nature of the material on which the corrosion products are deposited, the chemical composition of the deposited corrosion products, the disperse composition of the deposits, irradiation, etc. These data can be used as reference data on corrosion, loss of corrosion products into the coolant and their deposition on the plant of the primary circuit, and also for the choice of the optimum water — chemical cycle.

The fourth chapter is devoted to activation of the corrosion products and transfer of the induced radioactivity in the circuit of water-cooled reactors. A simplified mathematical model is derived for the transfer of radioactivity and also a mathematical device for calculating the mass transfer of radioactivity through the circuit.

In remarking on the theoretical and especially the practical value of the book, certain critical comments must also be made.

The authors do not analyze the data on corrosion and loss of corrosion products into the coolant. Tables 34, 42 and 43 confirm this. The rate of corrosion and loss of corrosion products into the coolant under one and the same conditions differ by a certain factor.

The experimental data listed, without adequate critical analysis makes reading of the book difficult.

In the introduction it would be advantageous to indicate which sections are written by whom.

The critical comments mentioned do not reduce the practical value of the book. It is a notable contribution to the study of one of the most important problems of nuclear power generation. The authors' research

* Atomizdat, Moscow (1975); 15.26 author's folio, 1 ruble 77 kopecks.

significantly supplements the literature on this important problem. Undoubtedly, it will be met with great interest by a wide circle of specialists and workers in the fields of thermal and nuclear power generation.

N. D. Tyufyakov and A. S. Shtan'

PRINCIPLES OF NEUTRON RADIOGRAPHY*

Reviewed by Yu. V. Sivintsev

Neutron radiography — one of the extremely promising trends of radiation defectoscopy — is exceptionally young. The first serious work in this field of science appeared in the 1960's. Since then, a large number of papers have been published in the periodical literature; however, there was as yet no monograph in Russian devoted to their generalization.

The authors of the book being reviewed are well-known Soviet specialists in the field of radiation techniques and have set before themselves the problem of filling this void in Soviet scientific literature.

The monograph consists of a small foreword, seven chapters, and a bibliography of 46 references (16 foreign publications). The text of the book is illustrated with a large number of tables (21) and figures (68). Undoubtedly, the attention of the readers will be attracted to the excellent photography of the neutronograms given in the last chapter.

Structurally, the publication being reviewed breaks down into two parts: The first four chapters and a considerable part of the fifth chapter are devoted to an account of the principal theorems of neutron physics, and the remaining part (unfortunately, the lesser) contains a description of investigations on the principal theme of the monograph. From the point of view of the reviewer, this distribution of information in the book is uneconomical.

The principles of neutron physics are recounted in detail and clearly. Readers, specialists of industry and scientific-research organizations occupied with nondestructive monitoring, will obtain a clear representation of the principal concepts and theorems of neutron physics, sources, beams and neutron detectors. At the high scientific level of explanation in this section of the book stylistic, terminological and even semantic flaws are encountered. An unfortunate order of words in phrases is used frequently in the text, which obscures their meaning.

In the monograph being reviewed, it is doubtful whether it is worth reporting data on the radioactivity of the neutron (p. 8) or whether to derive the formula (3.1) for calculating the specific yield of neutrons, in order to conclude it with the words "as a rule the yield is estimated by empirical relations or is determined experimentally" (pp. 53-54).

In Table 3.4, the numerical values of the coefficients are given with exaggerated accuracy. On pp. 107-108, formulas are written unsuccessfully with the use of literal symbols. When describing the methods of recording neutrons (p. 115), the authors do not consider the inelastic scattering reaction on which, in particular, is based the use of threshold rhodium detectors. In Table 5.1, data are given about the sensitivity of photographic materials, but the interpretation of the physical meaning of this characteristic is not given.

The fifth and sixth chapters occupy the middle part of the monograph and are devoted strictly to neutron radiography — with neutron image detectors and the defectoscopic characteristics of the method. The efficiency of screen-converters, detectors with metallic screens, is characterized thoroughly here (nonphotographic methods are described in less detail), problems of contrast and poor definition of the neutronograms, and also factors which limit the sensitivity to defects. Together with the literature data, the authors widely cite the results of their own original investigations.

Unfortunately, by separating the data of this section from the last and seventh chapter "Practical Problems of Neutron Radiography," one is prevented from obtaining generalized data about the possibilities and limits of applicability of the method to a considerable degree.

*Atomizdat, Moscow (1975); 13.73 author's folio, 1 ruble 53 kopecks.

Other inadequacies of the book are the absence of clear conclusions, the use of such jargon expressions as "poor definition of a detector" (p. 193), "detailed sensitivity" (p. 208) and a considerable number of inaccurate misprints.

In assessing the monograph as a whole, it should be mentioned that Atomizdat has published a useful resumé of data on the principles of neutron radiography.

CHANGING YOUR ADDRESS?

In order to receive your journal without interruption, please complete this Change of Address notice and forward to the Publisher, 60 days in advance, if possible.

Old Address: (PLEASE PRINT)

NAME _____

STREET _____

CITY _____

STATE (or Country) _____

ZIP CODE _____

New Address: (PLEASE PRINT)

NAME _____

STREET _____

CITY _____

STATE (or Country) _____

ZIP CODE _____

Date New Address Effective: _____

Name of Journal: _____

Plenum Publishing Corporation
227 West 17 Street
New York, New York 10011

breaking the language barrier

WITH COVER-TO-COVER ENGLISH TRANSLATIONS OF SOVIET JOURNALS

in physics

Title	# of Issues	Subscription Price
Astrophysics *Astrofizika*	4	$175.00
Fluid Dynamics *Izvestiya Akademii Nauk SSSR mekhanika zhidkosti i gaza*	6	$225.00
High-Energy Chemistry *Khimiya vysokikh énergii*	6	$215.00
High Temperature *Teplofizika vysokikh temperatur*	6	$195.00
Journal of Applied Mechanics and Technical Physics *Zhurnal prikladnoi mekhaniki i tekhnicheskoi fiziki*	6	$225.00
Journal of Engineering Physics *Inzhenerno-fizicheskii zhurnal*	12 (2 vols./yr. 6 issues ea.)	$225.00
Magnetohydrodynamics *Magnitnaya gidrodinamika*	4	$175.00
Mathematical Notes *Matematicheskie zametki*	12 (2 vols./yr. 6 issues ea.)	$225.00
Polymer Mechanics *Mekhanika polimerov*	6	$195.00
Radiophysics and Quantum Electronics (Formerly Soviet Radiophysics) *Izvestiya VUZ. radiofizika*	12	$225.00
Solar System Research *Astronomicheskii vestnik*	4	$125.00
Soviet Applied Mechanics *Prikladnaya mekhanika*	12	$225.00
Soviet Atomic Energy *Atomnaya énergiya*	12 (2 vols./yr. 6 issues ea.)	$235.00
Soviet Journal of Glass Physics and Chemistry *Fizika i khimiya stekla*	6	$95.00
Soviet Microelectronics *Mikroélektronika*	6	$135.00
Soviet Physics Journal *Izvestiya VUZ. fizika*	12	$225.00
Soviet Radiochemistry *Radiokhimiya*	6	$215.00
Theoretical and Mathematical Physics *Teoreticheskaya i matematicheskaya fizika*	12 (4 vols./yr. 3 issues ea.)	$225.00

Back volumes are available. For further information, please contact the Publishers.

SEND FOR YOUR FREE EXAMINATION COPIES

PLENUM PUBLISHING CORPORATION
227 WEST 17th STREET
NEW YORK, N. Y. 10011
Plenum Press • Consultants Bureau
• IFI/Plenum Data Corporation

United Kingdom: Black Arrow House
2 Chandos Road, London NW10 6NR England

Declassified and Approved For Release 2013/09/23 : CIA-RDP10-02196R000700080002-8

breaking the language barrier

WITH COVER-TO-COVER
ENGLISH TRANSLATIONS
OF SOVIET JOURNALS

in geoscience

Title	# of Issues	Subscription Price
Chemical and Petroleum Engineering *Khimicheskoe i neftyanoe mashinostroenie*	12	$275.00
Chemistry and Technology of Fuels and Oils *Khimiya i tekhnologiya topliv i masel*	12	$275.00
Colloid Journal of the USSR *Kolloidnyi zhurnal*	6	$225.00
Cosmic Research (Formerly Artificial Earth Satellites) *Kosmicheskie issledovaniya*	6	$215.00
Lithology and Mineral Resources *Litologiya i poleznye iskopaemye*	6	$225.00
Soil Mechanics and Foundation Engineering *Osnovaniya, fundamenty i mekhanika gruntov*	6	$195.00
Solar System Research *Astronomicheskii vestnik*	4	$125.00
The Soviet Journal of Ecology *Ékologiya*	6	$145.00
Soviet Mining Science *Fiziko-tekhnicheskie problemy razrabotki poleznykh iskopaemykh*	6	$225.00
Water Resources *Vodnye Resursy*	6	$190.00

Back volumes are available.
For further information, please contact the Publishers.

SEND FOR YOUR FREE EXAMINATION COPIES

PLENUM PUBLISHING CORPORATION
Plenum Press • Consultants Bureau
• IFI/Plenum Data Corporation
227 WEST 17th STREET
NEW YORK, N. Y. 10011

United Kingdom: Black Arrow House
2 Chandos Road, London NW10 6NR England